ABSTRACT

Title of Document: IDENTIFICATION OF THE MOLECULAR MECHANISMS OF ZEBRAFISH INNER EAR HAIR CELL REGENERATION USING HIGH-THROUGHPUT GENE EXPRESSION PROFILING

Jin Liang, Doctor of Philosophy, 2010

Directed By: Dr. Arthur N. Popper, Department of Biology

All nonmammalian vertebrates studied can regenerate inner ear mechanosensory receptors, i.e. hair cells, but mammals only possess a very limited capacity for regeneration after birth. As a result, mammals suffer from permanent deficiencies in hearing and balance once their inner ear hair cells are lost. The mechanisms of hair cell regeneration are poorly understood. Because the inner ear sensory epithelium is highly conserved in all vertebrates, we chose to study the hair cell regeneration mechanism in adult zebrafish, hoping the results would be transferrable to inducing hair cell regeneration in mammals. We defined the comprehensive network of genes involved in hair cell regeneration in the inner ear of adult zebrafish with the powerful transcriptional profiling technique, Digital Gene Expression (DGE), which leverages the power of next-generation sequencing. We also identified a key pathway, stat3/socs3, and demonstrated its role in promoting hair cell regeneration through stem cell activation, cell division, and differentiation. In addition, transient

pharmacological up-regulation of stat3 signaling accelerated hair cell regeneration without over-producing cells. Taking other published datasets into account, we propose that the stat3/socs3 pathway is a key response in all tissue regeneration and thus an important therapeutic target not only for hair cell regeneration, but also for a much broader application in tissue repair and injury healing.

IDENTIFICATION OF THE MOLECULAR MECHANISMS OF ZEBRAFISH INNER EAR HAIR CELL REGENERATION USING HIGH-THROUGHPUT GENE EXPRESSION PROFILING

By

Jin Liang

Dissertation submitted to the Faculty of the Graduate School of the
University of Maryland, College Park, in partial fulfillment
of the requirements for the degree of
Doctor of Philosophy
2010

Advisory Committee:
Professor Arthur N. Popper, Chair
Dr. Shawn M. Burgess
Professor Jens Herberholz
Dr. Matthew W. Kelley
Professor Luisa P. Wu

Dedication

I dedicate this dissertation to my mother Ms. Zhihua Sun and my late father Professor Zhongchao Liang for their love and inspiration.

Acknowledgements

My dissertation would not have been possible without the help of many people. My deepest gratitude goes to my advisors, Dr. Shawn Burgess and Dr. Arthur Popper, for their guidance, inspiration, support, and encouragement throughout my PhD training. I would like to express my special thanks to Dr. Burgess who not only advised my project, but also taught me how to be a scientist. My thanks also go to my committee members for their advice and help. I would also like to thank Mr. Gabriel Renaud and Dr. Tyra Wolfsberg for their help with the programming and Dr. Alexander Wilson for his expertise in biostatistics. Many thanks to previous and present members in Burgess lab and Popper lab for their help and support.

I would like to thank the Neuroscience and Cognitive Science program (NACS) at the University of Maryland, College Park and Graduate Partnership Program (GPP) at National Institutes of Health for providing excellent training opportunities for PhD students. This research was supported by the Intramural Research Program of the National Human Genome Research Institute, National Institutes of Health

Last but not least, I would like to thank my parents, especially my mother, for the love and support that help me through the ups and downs in my life.

Table of Contents

List of Tables

List of Figures

Chapter 1 Introduction

The sensory epithelium is the major functional structure of the inner ear. It is mainly composed of two basic cell types: hair cells and supporting cells (Fritzsch, Pauley, & Beisel, 2006). Inner ear hair cells are the basic mechanosensory unit for hearing and balancing (Vollrath, Kwan, & Corey, 2007). Loss of inner ear hair cells is the major cause of permanent auditory and vestibular deficiencies in mammals because they are not able to regenerate hair cells (Roberson & Rubel, 1994). In the US, approximately 15% (26 million) of people aged 20-69 have high frequency hearing loss resulted from overexposure to noise (NIDCD/NIH). In most cases, the functional deficits resulted from the loss of the inner ear hair cells in the cochlea.

All nonmammalian vertebrates studied show the ability to regenerate their inner ear hair cells, including birds (Corwin & Cotanche, 1988; Cruz, Lambert, & Rubel, 1987; Ryals & Rubel, 1988), lizards (Avallone, Fascio, Balsamo, & Marmo, 2008; Avallone et al., 2003), frogs (Baird, Steyger, & Schuff, 1996), and fish (Lombarte, Yan, Popper, Chang, & Platt, 1993; Schuck & Smith, 2009; Smith, Coffin, Miller, & Popper, 2006). Among all the animals used for hair cell regeneration studies, zebrafish (*Danio rerio*) is particularly amenable to genetic and genomic approaches because of high-quality genomic sequence data and the opportunities for mutational analysis.

The inner ear sensory epithelium is highly conserved across all vertebrates (Fritzsch, Beisel, Pauley, & Soukup, 2007; Fritzsch et al., 2006), so many studies can be done in nonmammalian vertebrates that will identify genes and pathways that

might be needed for inducing hair cell regeneration in mammals. To date, however, such studies have only achieved limited success because they mainly focused on a small number of genes already known to be important for inner ear development.

Understanding the mechanism of hair cell regeneration in nonmammalian animals will help design strategies to potentially induce similar regeneration events in humans in order to treat hair cell loss-induced hearing and balance disorders. It is not only of scientific but also of clinical interest to understand the molecular mechanism involved in hair cell regeneration.

For over 20 years, studies on hair cell regeneration in nonmammalian vertebrates have yielded limited progress. Most of studies were carried out in the "one-gene-at-a-time" fashion, thereby limiting understanding of the larger, gene network interactions. There were a few studies aimed at large-scale candidate gene screening in chickens, but they were limited by the techniques used (Hawkins et al., 2003, 2007), and by the lack of efficient follow-up approaches. The previous studies suggest that: 1) large-scale studies are a more efficient way to define a process as complicated as hair cell regeneration; 2) using chickens as a model organism for hair cell regeneration studies has major limitations, particularly the lack of genetic tools for follow-up studies.

The goal of my PhD project was to achieve a comprehensive understanding of the hair cell regeneration mechanisms at the molecular level. To achieve this goal, we used zebrafish as the model system because the animal allowed me to study the hair cell regeneration mechanism with high-throughput techniques as well as testing the functions of genes of interest *in vivo*.

In my PhD project, the cellular features in inner ear hair cell regeneration were characterized in adult zebrafish following noise-induced hair cell loss (described in Chapter 2). Based on the visible cellular reactions to damage, the inner ear tissue samples were collected at different time-points during the subsequent hair cell regeneration. Then gene expression profiles were generated from the tissue samples with a high-throughput profiling technique named Digital Gene Expression (DGE) (Morrissy et al., 2009). By comparing the regenerative profiles to an untreated control profile, candidate genes whose expression level had significantly changed during hair cell regeneration were identified. The gene expression profile generation and comparison is described in Chapter 3. Lastly, we did follow-up studies in the functions of the candidate genes/pathway of greatest interest: stat3/socs3 (described in Chapter 4).

The results from the profile generation and comparison provided a comprehensive view of the hair cell regeneration mechanism by examining the changes in gene expression levels during the regeneration in a high-throughput way. The functional studies confirmed the important functions of stat3/socs3 in hair cell/supporting cell production during both development and regeneration. In addition, my project also provided protocols for similar *de novo* candidate gene screening in nonmammalian vertebrates with a next-generation sequencing platform.

Chapter 2 Inner Ear Hair Cell Regeneration after Noise-Induced Hair Cell Loss in Adult Zebrafish

2.1 Background review

2.1.1 Hair cells and supporting cells

The inner ear sensory epithelium (Figure 2.1) is mainly composed of hair cells and supporting cells (Fritzsch et al., 2006). The most distinguishing morphological feature of a hair cell is the hair cell bundle which is located at the apical end of the cell. The hair cell bundle is composed of numerous short stereovilli and one single long kinocilium (lost in auditory hair cells in postnatal mammals). The stereovilli are microfilaments arranged in a staircase fashion with the longest ones closest to the kinocilium, a true cilium consisting of microtubules. The hair cells are innervated by the afferent (cranial nerve VIII) and efferent neurites on the basolateral surface of the cell body. In between hair cells, there are always one or more supporting cells. Supporting cells are less distinguishable morphologically than hair cells and are not innervated.

Inner ear hair cells are the basic mechanosensory receptors for hearing and balancing (Vollrath et al., 2007). The reflection and deflection of the hair cell bundle transforms the energy of sound waves to electrophysiological signals that are sent to the brain via cranial nerve VIII. When the hair bundle is pushed toward the kinocilium (deflection), the mechanotransductory channels on the bundle are opened. As a result, the influx of positive ions (mostly K^+ and Ca^{2+}) through the channels

depolarizes the hair cell, which triggers the release of neurotransmitters (mostly glutamate) onto the afferent synapses formed by the VIII cranial nerve (Fuchs, Glowatzki, & Moser, 2003; Gillespie & Walker, 2001; Hudspeth, 1997). On the other hand, when the hair bundle is pushed away from the kinocilium (reflection), the mechanotransductory channels are closed, resulting in hyper-polarization of the hair cell. Although the supporting cells are not working as mechanotransducers, they have many other important functions, including hair cell insulation, structural support (Tanaka & Smith, 1978), fluid homeostasis maintenance (Wangemann, 2006), secretion of otoconia/tectorial membrane building materials (Goodyear, Killick, Legan, & Richardson, 1996; Thalmann, Ignatova, Kachar, Ornitz, & Thalmann, 2001), as well as being a postembryonic source of new hair cells and supporting cells (discussed below).

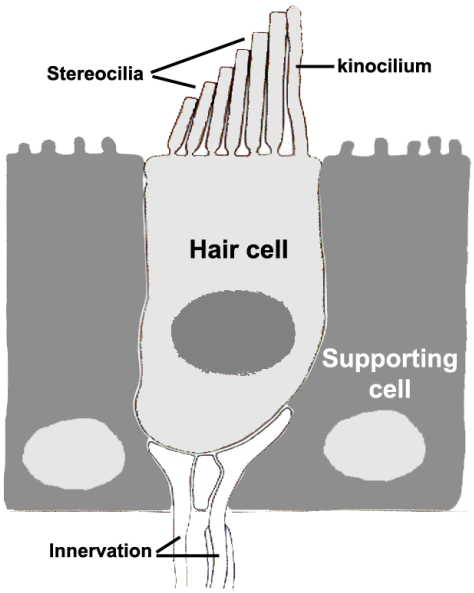

Figure 2.1. A schematic illustration of the sensory epithelium. The sensory epithelium is mainly composed of hair cells and supporting cells. A hair cell is characterized by the apical hair cell bundle (consisting of one kinocilium and several stereovilli) and basolateral innervation. Supporting cells locate in between hair cells.

In addition to inner ears, fishes and aquatic amphibians also possess a superficial mechanosensory organ, the lateral line system, for detecting water movement along the body (McHenry, Feitl, Strother, & Trump, 2009; Montgomery, Carton, Voigt, Baker, & Diebel, 2000). The lateral line system is composed of numerous units called neuromasts that consist of mainly hair cells and supporting cells. The lateral line hair cells and supporting cells are highly similar to those in the inner ear sensory epithelia at both the morphological and molecular levels (Nicolson, 2005).

2.1.2 Hair cell regeneration: mammals vs. non-mammals

In mammals, hair cell production ceases during the late embryonic stages (Ruben, 1967). There is no spontaneous cell addition in mature mammalian auditory or vestibular sensory epithelia (Roberson & Rubel, 1994). New hair cell production is not triggered by hair cell loss in mammals (Chardin & Romand, 1995; Roberson & Rubel, 1994) except for the rare cases where limited hair cell regeneration was observed in vestibular sensory epithelia (Kuntz & Oesterle, 1998; Lambert, 1994; Rubel, Dew, & Roberson, 1995; Warchol, Lambert, Goldstein, Forge, & Corwin, 1993). As a result, loss of inner ear hair cells from over-exposure to noise (Lim, 1976; Mcgill & Schuknecht, 1976), ototoxic drugs (Lim, 1976), or aging (Soucek, Michaels, & Frohlich, 1986; Ter Haar, De Groot, Venker-van Haagen, Sluijs, & Smoorenburg, 2009) is the major cause of permanent auditory and vestibular deficiencies in mammals.

Different from mammals, spontaneous postembryonic hair cell production has been observed in many nonmammalian vertebrates, including the otolithic end organs of fishes (Corwin, 1981; Popper & Hoxter, 1984) and the vestibular end organs of birds (Jørgensen & Mathiesen, 1988). Damage-induced postembryonic hair cell production has also been observed in nonmammalian vertebrates: auditory and vestibular end organs of birds (Corwin & Cotanche, 1988; Cruz et al., 1987), vestibular end organs of frogs (Baird et al., 1996), and otolithic end organs of fish (Schuck & Smith, 2009; Smith et al., 2006). Functional recovery accompanying hair cell regeneration has also been reported in fish (Smith et al., 2006) and birds (Dooling, Ryals, Dent, & Reid, 2006; Levic et al., 2007; Müller, Smolders, Ding-

Pfennigdorff, & Klinke, 1996; Woolley, Wissman, & Rubel, 2001). In addition, both spontaneous (Harris et al., 2003) and damage-induced (Balak, Corwin, & Jones, 1990; Harris et al., 2003; Jones & Corwin, 1993; Song, Yan, & Popper, 1995) hair cell production have been observed in the lateral line system.

Supporting cells are considered the progenitor cells of new hair cells in regeneration. The first direct evidence was from the time-lapse imaging of hair cell regeneration after laser ablation of lateral line hair cells in salamanders (Balak et al., 1990; Jones & Corwin, 1993). Supporting cells can give rise to new hair cells in two ways: by cell division and differentiation and by direct transdifferentiation (DT). Important as they are to our understanding of the regenerative process, the molecular mechanisms of hair cell regeneration are poorly understood. However, previous publications do reveal the complexity of the process and suggest some overlap or similarity between the regulation signaling used in cell differentiation during development, and regenerative events in sensory epithelia (Cafaro, Lee, & Stone, 2007; Ma, Rubel, & Raible, 2008; Millimaki, Sweet, Dhason, & Riley, 2007; Stone & Rubel, 1999; Woods, Montcouquiol, & Kelley, 2004).

2.1.3 Cell cycle regulation in supporting cells

Evidence of hair cell regeneration from supporting cell division comes from both time-lapse imaging (Balak, Corwin, & Jones, 1990; Jones & Corwin, 1993) and from DNA synthesis tracking with chemicals like [^{3}H] thymidine or bromo-deoxyuridine (BrdU) (Harris et al., 2003; Presson & Popper, 1990; Raphael, 1992; Stone & Cotanche, 1994). Damage-induced supporting cell proliferation is mostly restricted to the sensory epithelial area where hair cell loss has been induced (Corwin & Cotanche,

1988; Ryals & Rubel, 1988; Stone & Cotanche, 1994; Warchol & Corwin, 1996). The extent of supporting cell division seems to be directly related to that of hair cell loss (Kil, Warchol, & Corwin, 1997; Stone & Cotanche, 1994; Williams & Holder, 2000). Temporary over-production of supporting cells and hair cells was observed in avian inner ear sensory epithelia after damage, but the cell numbers were reduced to normal levels later (pigeons (*Columba livia*) (Dye, Frank, Newlands, & Dickman, 1999), chickens (*Gallus gallus*) (Girod, Tucci, & Rubel, 1991; Wilkins, Presson, & Popper, 1999)).

The molecular triggering of supporting cell division induced by hair cell loss is poorly understood. A few genes/pathways have been suggested as inducing/promoting supporting cell division, most of which were identified in *in vitro* studies in chicken sensory epithelium explants. Various growth factors, their corresponding receptors, and associated proteins are expressed in the normal and damaged sensory epithelia in chickens (Bermingham-McDonogh, Stone, Reh, & Rubel, 2001; Lee & Cotanche, 1996; Pickles & Heumen, 1997; Umemoto et al., 1995). Insulin-like growth factor 1 (IGF-1), insulin (Oesterle, Tsue, & Rubel, 1997), and Transforming Growth Factor-α (TGF- α) (Warchol, 1999) showed mitogenic effect in vestibular sensory epithelium explants from post-hatched chickens, while basic Fibroblast Growth Factor (bFGF) inhibited cell division in auditory and vestibular sensory epithelium explants (Oesterle, Bhave, & Coltrera, 2000). Fibroblast Growth Factor Receptor 1 (FGFR1), a high-affinity receptor of Fibroblast Growth Factor 2 (FGF2), re-distributes from hair cells to supporting cells after hair cell loss in chicken basilar papilla, suggesting a possible role of FGF2/FGFR1 in

regulating supporting cell division during hair cell regeneration (Pickles & Heumen, 1997; Umemoto et al., 1995). Similarly, FGFR3 is reported as down-regulated in supporting cells after hair cell loss, but then up-regulated as supporting cells re-entered post-mitotic phase (Bermingham-McDonogh et al., 2001). In addition to various growth factors, N-cadherin and retinoic acid were reported as cell division inhibitors in sensory epithelium explants (Warchol, 2002) while intracellular signaling including the MAPK pathway, Phosphatidylinositol-3 Kinase (PI3K), Target of Rapamycin (TOR), and Protein Kinase C (PKC), were considered as required for S-phase entry of supporting cells (Witte, Montcouquiol, & Corwin, 2001). Some epigenetic influences have also been characterized, e.g. histone deacetylation up-regulates cell proliferation during hair cell regeneration in cultured chicken utricles (Slattery, Speck, & Warchol, 2009).

Other understanding of cell cycle control mechanisms in sensory epithelial cells comes from studies in the cochlea of embryonic and neonatal mice. The best studied cell cycle regulation genes in the developing organ of Corti include cyclin-dependent kinase inhibitor 1b (cdkn1b/p27kip1) and retinoblastoma 1 (rb1), both of which promote cell cycle exit of precursor cells prior to hair cell/supporting cell differentiation (Chen & Segil, 1999; Sage et al., 2005). Cdkn1b is also required for holding the supporting cells in a post-mitotic status in mice (Löwenheim et al., 1999; Ono et al., 2009). In addition, the ability to down-regulate cdkn1b partially accounts for the age-dependent changes in the proliferative ability of supporting cells (White, Doetzlhofer, Lee, Groves, & Segil, 2006). In chicken, the cdkn1b expression first decreases in noise-damaged utricle and then returns to normal levels as regeneration

progresses (Hawkins et al., 2007). Meanwhile, rb1, cyclin-dependent kinase inhibitor 1a (cdkn1a/p21cip1), and cyclin-dependent kinase inhibitor 2d (cdkn2d/p19ink4d) are also involved in the maintenance of the post-mitotic status of hair cells (Chen et al., 2003; Laine et al., 2007; Mantela et al., 2005; Weber et al., 2008). Cyclin D1 (ccnd1) has recently been found to play a role in cell cycle control in the mouse cochlea: down-regulation in ccnd1 expression correlates with the decline in the proliferative ability of differentiating hair cells and supporting cells (Laine, Sulg, Kirjavainen, & Pirvola, 2010).

2.1.4 Cell differentiation regulation in sensory epithelia

Regulatory mechanisms of cell differentiation during hair cell regeneration are similar to those employed during development (Figure 2.2). A good example is the Notch signaling pathway (Driver & Kelley, 2009; Stone & Cotanche, 2007). Notch receptors are a group of large trans-membrane proteins, activated by their ligands, Delta (Dl) or Serrate/Jagged (Ser/Jag) (Rebay et al., 1991; Wharton, Johansen, Xu, & Artavanis-Tsakonas, 1985). Once activated, the Notch intracellular domain (NICD) is cleaved from the receptor and transferred into the nucleus (Gordon, Arnett, & Blacklow, 2008). NICD, together with DNA-binding protein CBF1/RBPjκ/Su(H)/Lag-1 (CSL), promotes transcription of genes from the Hairy and Enhancer of Split (HES) family that, in turn, inhibit the transcription of Notch ligands, completing a feedback loop (Fortini, 2009). This intercellular pathway regulates cell differentiation in many development processes, resulting in neighboring cells acquiring distinct cell fates, e.g. the mosaic pattern of hair cells and supporting cells in sensory epithelia (Driver & Kelley, 2009; Kelley, 2007). Hair cell/supporting

cell differentiation in the developing mouse cochlea requires up-regulation of jagged 2 (jag2) and delta-like 1 (dll1) in nascent hair cells and strong expression of notch1, hes1, and hes5 in their neighboring supporting cells (Puligilla & Kelley, 2009). Accordingly, during hair cell regeneration in the chicken basilar papilla, dll1 is expressed first symmetrically in pairs of daughter cells from mitosis and then highly up-regulated in hair cell precursors while down-regulated in supporting cell precursors (Stone & Rubel, 1999). Disruption of the Notch signaling results in precocious differentiation and overproduction of hair cells during development in the inner ear of mice (Kiernan, Xu, & Gridley, 2006; Lanford et al., 1999; Zine, Water, & Ribaupierre, 2000) as well as the inner ear and lateral line of zebrafish (Haddon, Jiang, Smithers, & Lewis, 1998; Haddon et al., 1999). Similarly, pharmacological blockage of Notch signaling in damaged chicken basilar papilla induced excessive hair cell production at the cost of supporting cells, while over-expression of activated Notch receptors after damage resulted in the opposite effect (Daudet et al., 2009). Notch signaling also regulates the hair cell regeneration in zebrafish lateral line, preventing precocious hair cell differentiation at the cost of supporting cells (Ma et al., 2008).

In addition to Notch ligands, atonal homolog 1 (atoh1), a basic helix-loop-helix (bHLH) transcription factor, is also inhibited by HES at the transcriptional level (Skeath & Carroll, 1992; Woods et al., 2004). Atoh1 is a key player in hair cell differentiation in development, during which it is first expressed in all undifferentiated precursors and later only in differentiating hair cells to promote cell fate commitment, but atoh1 is down-regulated in differentiating supporting cells as a

result of HES up-regulation (Millimaki et al., 2007; Woods et al., 2004). While atoh1 expression is absent from undamaged mature chicken basilar papilla, it is triggered in transdifferentiating and proliferating supporting cells and later present only in newly produced hair cell precursors during hair cell regeneration (Cafaro et al., 2007), suggesting a similar role of the gene in development and regeneration. In addition, forced expression of atoh1 in mouse cochlea *in vitro* (Woods et al., 2004; Zheng & Gao, 2000) and *in vivo* (Gubbels, Woessner, Mitchell, Ricci, & Brigande, 2008) results in the differentiation of ectopic hair cells. Some of the ectopic hair cells have morphological as well as physiological resemblances to normal hair cells (Gubbels et al., 2008). Forced expression of atoh1 in cultured pluri-potent stem cells leads to the commitment of hair cell fate in those cells (Han et al., 2010; Liu et al., 2006). In addition, new hair cells are induced in mammalian sensory epithelia after hair cell loss by atoh1 transfection, which results in functional recovery in auditory as well as vestibular end organs (Baker, Brough, & Staecker, 2009; Izumikawa et al., 2005). However, the capability of forced atoh1 expression to induce new hair cell in damaged sensory epithelium seems to be context-dependent. The supporting cells often fail to maintain their differentiated status once the hair cells are eliminated, resulting in a "flat epithelium," Transfecting the flat epithelium with atoh1 can not induce hair cell regeneration, suggesting the existence of supporting cells is required for atoh1-induced hair cell differentiation during regeneration in mammalian sensory epithelia (Izumikawa, Batts, Miyazawa, Swiderski, & Raphael, 2008).

In addition to HES, atoh1 is also antagonized by inhibitors of DNA binding (Ids), SRY-box containing gene 2 (sox2), and prospero homeobox 1 (prox1), all of which

promote supporting cell fate commitment during development (Dabdoub et al., 2008; Jones, Montcouquiol, Dabdoub, Woods, & Kelley, 2006; Kirjavainen et al., 2008). The transcription factors involved in chicken hair cell regeneration include prox1 (Stone, Shang, & Tomarev, 2004) and repressor element-1 silencing transcription factor (REST) (Roberson, Alosi, Mercola, & Cotanche, 2002), both of which show dynamic changes of their expression patterns in the basilar papilla during hair cell regeneration.

In contrast to hair cells, the regulatory mechanism of supporting cell differentiation is poorly understood. Notch signaling and related genes (e.g. sox2) are required for supporting cell differentiation as the blocking of Notch signaling causes the production of supernumerary hair cells at the cost of nearly all supporting cells in development (Haddon et al., 1999; Zine et al., 2000) as well as regeneration (Daudet et al., 2009; Ma et al., 2008). In addition, FGF-signaling is found to regulate the differentiation of different subtypes of supporting cells in the mouse cochlea. The fgf8/sprouty2/fgfr3 signaling pathway regulates the commitment and differentiation of pillar/Deiters cells in developing mouse cochlea (Jacques, Montcouquiol, Layman, Lewandoski, & Kelley, 2007; Mueller, Jacques, & Kelley, 2002; Puligilla et al., 2007; Shim, Minowada, Coling, & Martin, 2005). A Notch ligand, hairy/enhancer-of-split related with YRPW motif 2 (hey2), is also required for normal differentiation of pillar cells (Doetzlhofer et al., 2009). Interestingly, the function of hey2 in pillar cell is regulated by FGF signaling via fgfr3 rather than by Notch signaling (Doetzlhofer et al., 2009).

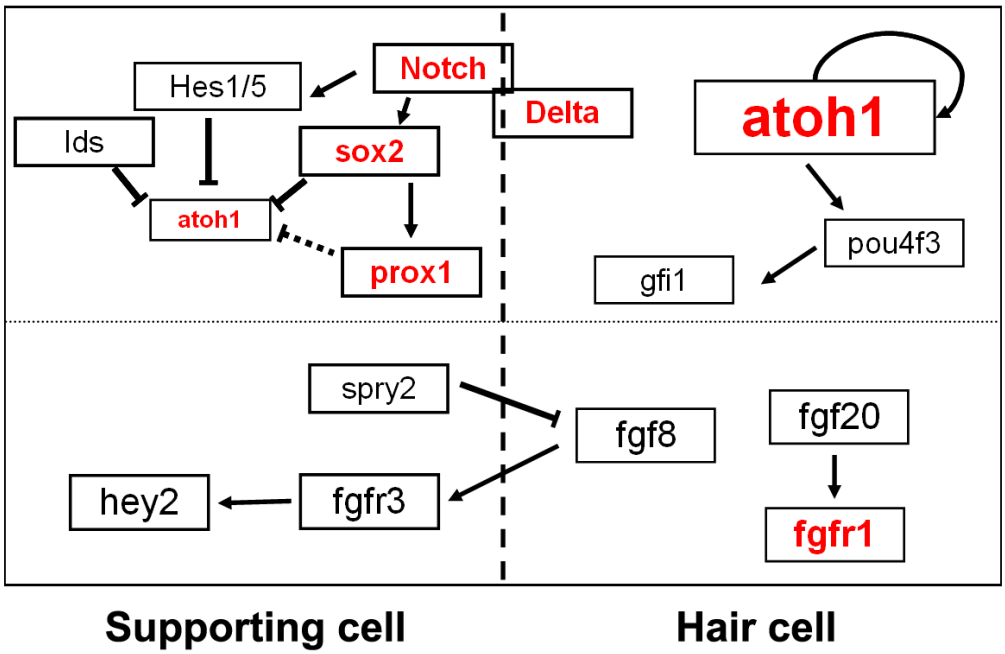

Figure 2.2. Signaling pathways known to be involved in hair cell/supporting cell differentiation during development. Genes in red are also known to be involved in hair cell regeneration.

2.1.5 Direct transdifferentiation

In addition to supporting cell division, there is a second way to replenish the lost hair cells: direct transdifferentiation (DT). DT is an event during which the differentiated supporting cells convert themselves to hair cells without cell cycle re-entry. The early supporting evidence of direct transdifferentiation was morphological: the translocation of nuclei from the supporting cell layer to the hair cell layer without an addition of new cells was observed in cultured bullfrog saccules after aminoglycoside treatment (Baird, Torres, & Schuff, 1993). More compelling evidence comes from hair cell regeneration studies in the chicken basilar papilla (Roberson, Alosi, & Cotanche, 2004). Continuous infusion of [^{3}H] thymidine or

BrdU during hair cell regeneration after gentamicin treatment only labeled a proportion of the new hair cells, suggesting the rest might come from direct transdifferentiation. Additional supporting data are from studies that showed normal hair cell regeneration in the presence of DNA synthesis blockers (bullfrog (*Rana catesbeiana*) saccule (Baird, Burton, Fashena, & Naeger, 2000); newt (*Notophthalmus viridescens*) saccule (Taylor & Forge, 2005); chicken basilar papilla (Adler & Raphael, 1996)).

Both supporting cell division and direct transdifferentiation contribute to hair cell regeneration in the chicken basilar papilla (Cafaro et al., 2007; Roberson et al., 2004). Direct transdifferentiation takes place earlier than the peak of supporting cell division, even before the extrusion of the dying hair cells in the damaged area (Cafaro et al., 2007; Roberson et al., 2004). In addition, previous studies show that new hair cells in the neural half of basilar papilla are more likely to be produced via supporting cell division, while those in the abneural half of BP are more likely to be produced by DT (Cafaro et al., 2007).

Interesting as it is, the molecular mechanism of direct transdifferentiation is not known. Meanwhile, there are also controversial ideas suggesting that direct transdifferentiation is actually the differentiation of hair cell precursors that have been committed to hair cell fate, but have yet to terminally differentiate (Morest & Cotanche, 2004).

2.1.6 Hair cell regeneration in zebrafish

Zebrafish have gained popularity for studies in hair cell development/death/regeneration/protection (Behra et al., 2009; Harris et al., 2003;

Hernández, Olivari, Sarrazin, Sandoval, & Allende, 2007; Ma et al., 2008). Most of the hair cell regeneration studies were done using the lateral line neuromasts of zebrafish larvae because they are readily accessible. In those studies, hair cells are eliminated by water-borne ototoxic chemicals (e.g. aminoglycosides, copper, and cisplatin) and full regeneration is usually completed in as short as three days (Hernández et al., 2007; Ma et al., 2008). In the lateral line neuromasts, hair cell regeneration is primarily through cell division after elimination of the hair cells (Hernández et al., 2007; Ma et al., 2008). During regeneration, in accordance with its role in developing sensory epithelia, the Notch signaling pathway is crucial for hair cell/supporting cell differentiation because interruption of Notch signaling resulted in precocious differentiation and over-production of new hair cells (Ma et al., 2008). In addition, sox2, a transcription factor involved in prosensory domain specification and hair cell differentiation during development (Dabdoub et al., 2008), is also considered as an important component of lateral line hair cell regeneration (Hernández et al., 2007). Behra et al. (2009) characterized a novel gene, phoenix, which is specifically required for cell proliferation during hair cell regeneration, but not for lateral line development or regeneration in other organs (e.g. fin).

In addition to the lateral line neuromasts, there are studies that tried to explore the hair cell regeneration mechanism in developing sensory epithelia in the otic vesicles in zebrafish embryos after laser ablation of the hair cells (Millimaki, Sweet, & Riley, 2010). However, because of the high level of spontaneous cell division and differentiation during the early development of the maculae, it is not an appropriate system for studying regenerative processes.

Hair cell regeneration also occurs in the inner ear of adult zebrafish after noise-induced hair cell loss, accompanied by an up-regulation in cell proliferation in the sensory epithelium (Schuck & Smith, 2009). Because the rate of spontaneous hair cell production is relatively low in adult zebrafish inner ears under normal conditions (Bang, Sewell, & Malicki, 2001; Higgs, Souza, Wilkins, Presson, & Popper, 2002), the inner ear in the adult fish provides a better system for studying the mechanism of hair cell regeneration, enabling the comparison with the mechanisms involved in hair cell production during development. However, no publication, to the best of my knowledge, has used genomic approaches to globally characterize the molecular mechanisms involved in the inner ear hair cell regeneration in adult zebrafish.

2.2 Experiment overview

To get a comprehensive understanding of the molecular mechanisms involved in hair cell regeneration in adult zebrafish, we first characterized the regenerative process at the cellular level. We induced hair cell loss in the saccular sensory epithelia (maculae) in adult zebrafish with a noise exposure setup modified from a previous study (Smith et al., 2006). The saccular maculae were dissected out from fish at different time points after noise exposure and examined with immunohistological staining with hair cell markers.

My results confirmed the noise-induced hair cell loss in the saccular maculae and found the recovery of hair cell density occurred within 96 hours after noise exposure. These results also provided a reference for deciding the time-points for collecting the inner ear tissue samples for gene expression profiling experiments afterwards (See Chapter 3).

2.3 Materials and methods

2.3.1 Animal husbandry

Zebrafish were maintained as previously described (Westerfield 2000) in compliance with guidelines for animal care from NIH and the University of Maryland.

2.3.2 Noise exposure of adult zebrafish

Adult wildtype (TAB-5) (Amsterdam et al., 1999) zebrafish (~ 1yr old) were exposed to white noise (100-10,000 Hz) for 48 h at 28-29 ºC according to a protocol modified from Smith et al. (2006): a steel exposure bucket was used instead of a plastic one in the previous publication. After exposure, the fish were maintained under regular husbandry conditions until sacrificed. The control fish were not exposed to noise.

2.3.3 Immunohistochemistry

The primary and secondary antibodies used include rabbit myosin VI antibody and myosin VIIa antibody (Proteus biosciences, 1:200-dilution), Alexa Fluor 568 goat anti-rabbit IgG (Invitrogen, 1:1,000-dilution). Other common reagents included PBT (1XPBS and 1% Triton X-100 (Sigma)), blocking buffer (10 mg/mL bovine serum albumin (Sigma) and 10% goat serum (Vector laboratories) in PBT), and staining buffer (1:5-dilution of blocking buffer in PBT).

Adult zebrafish were anesthetized with 0.03% buffered MS-222 and fixed in 4% paraformaldehyde (Sigma) at 4°C overnight. The fixed embryos were rinsed with PBS three times before dissection. The inner ear sensory epithelia were dissected as

previously described (Liang & Burgess, 2009). They were stained with Alexa 488 phalloidin (Invitrogen, 1:1,000-dilution in PBT) for 30 min at room temperature and rinsed with PBT for 3 times, 10 min each time. The tissues were then blocked with blocking buffer for 6 h at room temperature or 4°C overnight, followed by myosin VI/VIIa antibody staining at 4°C overnight. The tissues were then rinsed (3 times, 10 min each time) and mounted onto slides with Vectashield hard set mounting medium with DAPI (Vector laboratories).

2.3.4 Microscopy and image analysis

To capture the whole saccular epithelia, several overlapping pictures were taken for each epithelium using an AxiovertNLO confocal microscope (Zeiss) with Carl Zeiss AIM software (Zeiss) or using an Axiovert200M with an Apotome Grid Confocal (Zeiss) with Carl Zeiss Vision software (Zeiss). The individual pictures were then tiled with Photoshop 7.0 software (Adobe).

2.3.5 Statistical analysis

One-way ANOVA and *post-hoc* test were used to compare the hair cell numbers at different time-points after noise exposure. The calculations were done using Excel software (Microsoft).

2.4 Results

2.4.1 Noise induced hair cell loss in saccular maculae in adult zebrafish

We induced inner ear hair cell loss in adult zebrafish using a modified version of a previously published noise exposure protocol established in goldfish (Figure 2.3A)

(Smith et al., 2006). Using this setup, we could consistently induce hair cell loss in the saccular maculae (Figure 2.3B) in adult zebrafish (approximately one year old). Hair cell staining with phalloidin showed an extensive area of hair cell loss took place in the anterior-medial region of the saccular macula (Figure 2.3B, red boxes). Such hair cell loss was not observed in the utricle or lagena at 0 hour post noise exposure (hpe). Because hair cell bundles are the morphological feature of a late differentiation stage of hair cells, we counted phalloidin-stained hair cell bundles in saccular maculae to quantify the number of hair cells during hair cell loss and regeneration. Quantification of phalloidin-stained hair cells in a 20 µm X 20 µm area at 40% total length of the anterior-posterior axis of the saccular maculae confirmed the observation with ~80% hair cell loss in the specific region ($p < 0.05$, Figure 2.3B and C). Co-staining of the saccular macula with a phalloidin and myoVI/VIIa antibody-mix confirmed no phalloidin or myoVI/VIIa staining indicating complete elimination of hair cells as opposed to surviving bundleless hair cells in the damaged area (Figure 2.4B).

2.4.2 Hair cell regeneration after noise-induced hair cell loss

To establish the time-line of hair cell regeneration in zebrafish inner ears, we quantified the hair cells in the 20 µm X 20 µm area at 40% total length of the anterior-posterior axis of the saccular macula at 24-h intervals from 0 hpe up to 120 hpe. Hair cells in the damaged area regenerated rapidly. The number of hair cells in the area showed no significant difference to control levels at 96 hpe (Figure 2.3C). The regeneration curve showed two faster phases of hair cell addition: 0-24 hpe and

48-96 hpe (Figure 2.3C), whereas the curve remains more flat during the times between the two phases (Figure 2.3C).

Based on the regeneration time-line, we decided to collect inner ear tissue sample at 0, 24, 48, and 96 hpe for expression profile comparison described in Chapter 3.

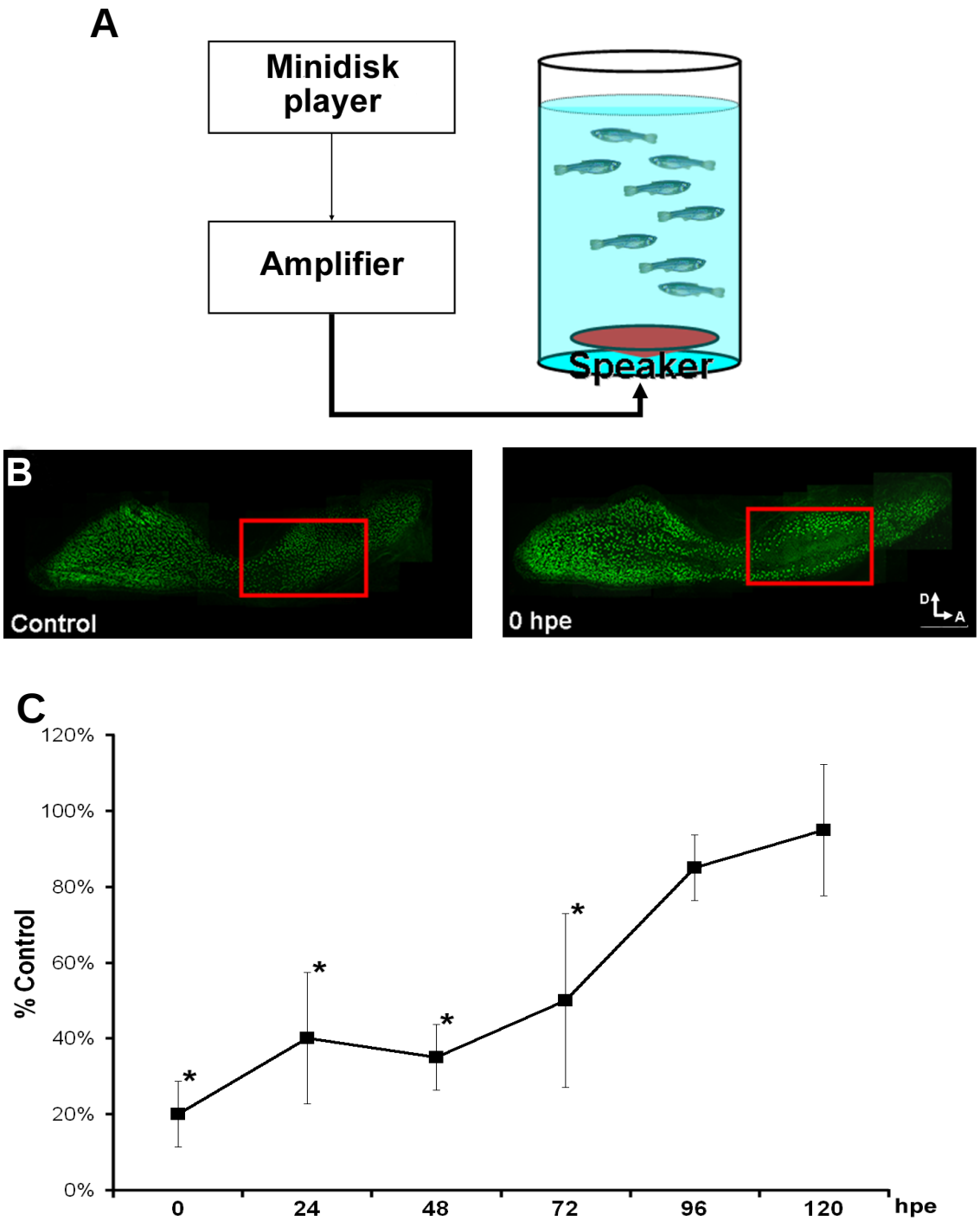

Figure 2.3. Noise-induced hair cell loss and regeneration in saccular maculae in adult zebrafish. A) The noise exposure apparatus used to induce hair cell loss in adult zebrafish. **B)** Phalloidin staining of the saccular hair cells. Hair cell loss

occurred in the anterior-medial area of the saccular sensory epithelium (red boxes). hpe: hours post exposure, D: dorsal, A: anterior, scale bar = 100 µm. **C)** Quantification of hair cell numbers in a 20 µm X 20 µm area at 40% total length of the anterior-posterior axis of the saccular maculae at different time-points after sound exposure (One-way ANOVA and *post-hoc* test, n = 3, *p < 0.05; all error bars in this dissertation demonstrate standard deviation).

2.4.3 Sensory epithelial morphology during hair cell loss and regeneration

Bundleless hair cells were rarely seen in control saccular maculae (Figure 2.4A). After noise exposure, bundleless hair cells were seen occasionally in the damaged areas (0 hpe, Figure 2.4B). These cells appeared without bundles but with myosin VI/VIIa antibody staining that was much weaker than the other hair cells (Figure 2.4B). It is unclear if these were viable or dying hair cells. An apical actin ring stained with phalloidin was often observed over the bundleless hair cells (Figure 2.4B). Such actin rings of various sizes were also found in the damaged area where no myosin VI/VIIa labeling was present (Figure 2.4B). Hair cells with shorter or splayed bundles were also observed in the vicinity of the damaged area (Figure 2.4B).

During hair cell regeneration, hair cells without a bundle or with a short/thin bundle were often seen in the damaged area (Figure 2.4C and D). Similar to those found right after noise exposure, the presence of the apical actin rings were often found where this type of hair cell was present (Figure 2.4C and D). At 96 hpe, although the density of hair cells (with bundles) was no longer significantly different (85% of control density, p > 0.05, Figure 2.3C), hair cells without or with short bundles could still be found in the regenerating area (Figure 2.4D).

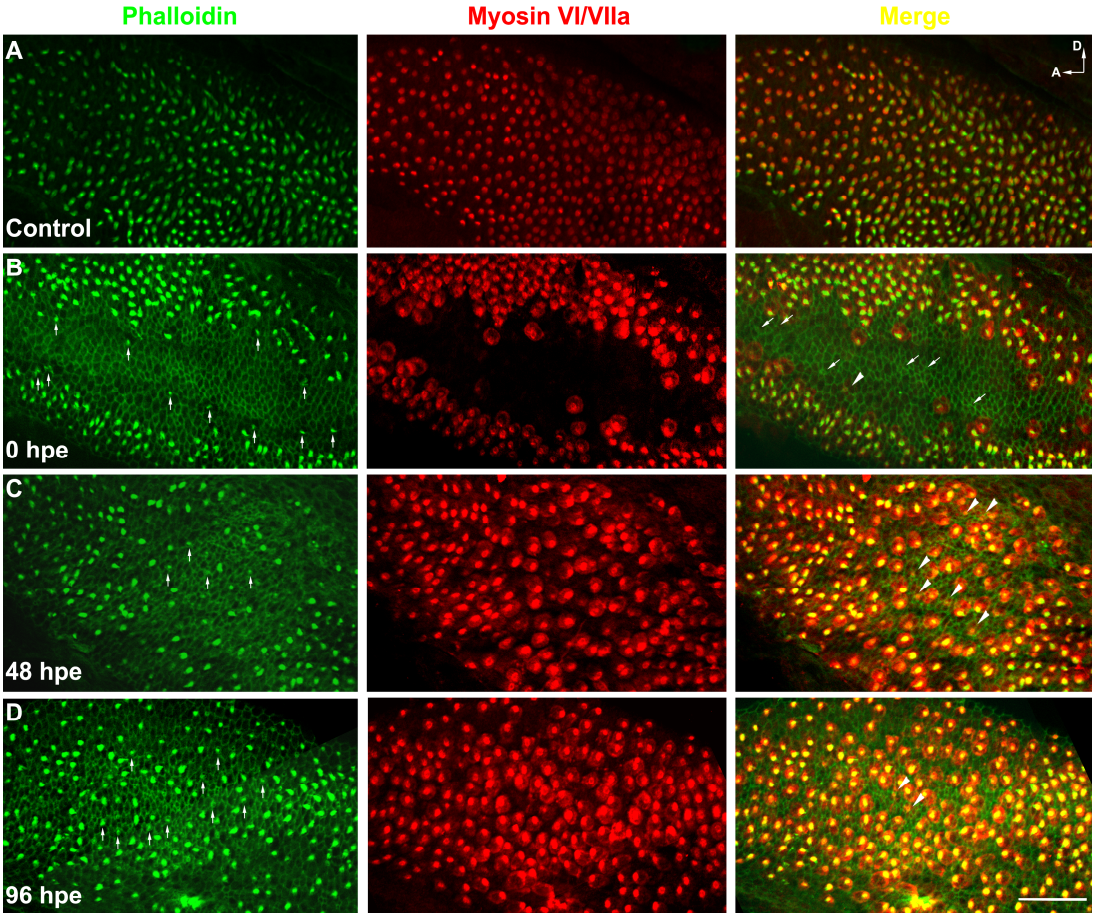

Figure 2.4. Morphology of the damaged area in the saccular maculae after noise exposure and during regeneration. Saccular maculae were stained with phalloidin (green, left panel) and a mixture of myosin VI and VIIa antibodies (red, middle panel). **A)** Saccular macula from control tissue. D: dorsal, A: anterior. **B)** Saccular macula from zebrafish sacrified at 0 h post noise exposure (hpe). Arrows in the left panel point at short and splayed hair cell bundles observed after noise exposure. Arrows in the right panel point at actin rings of different sizes without the presence of hair cells. Arrowhead in the right panel points at a bundle-less hair cell with the apical actin ring. **C)** and **D)** Saccular maculae from zebrafish sacrified at 48 hpe (**C**) and 96 hpe (**D**). Arrows in the left panel point at young hair cell bundles with apical actin

rings. Arrowheads in the right panel point at bundle-less hair cells with apical actin rings. Scale bar = 40 µm.

2.5 Discussion

2.5.1 The pattern of noise-induced hair cell loss suggests a tonotopic arrangement in saccular maculae in adult zebrafish

In early hair cell regeneration studies in fish, due to the lack of good hair cell markers, scanning electron microscopy (SEM) was used to examine hair cell loss. Those studies clearly showed the absence of hair cell bundles after ototoxic drug administration but not the elimination of the cells (Lombarte et al., 1993). Later studies used DAPI as the nuclear marker to show the loss of nuclei at the hair cell level in the pseudo-stratified sensory epithelia in goldfish (Smith et al., 2006) and zebrafish (Schuck & Smith, 2009) after noise exposure. Myosin VI and myosin VIIa have been identified as hair cell markers labeling both the hair cell bundle and cell body in zebrafish (Coffin, Dabdoub, Kelley, & Popper, 2007). In this study, noise-induced hair cell loss (rather than only hair cell bundle loss) was confirmed using a myosin VI/VIIa antibody mixture (Figure 2.4B). In addition, our results further confirmed the noise exposure setup had consistent performances in inducing inner ear hair cell loss, similar to those reported in previous studies (Schuck & Smith, 2009; Smith et al., 2006).

After exposure to white noise, adult zebrafish showed significant hair cell loss in the saccular maculae (Figure 2.3). Previous studies in goldfish with similar noise exposure setup also induced hair cell loss only in the saccules (Smith et al., 2006)

which has been considered as the major auditory end organ in goldfish (Fay, 1978). The inner ear of zebrafish shares high similarity with that of goldfish (Platt, 1993), which explains why noise-induced hair cell loss was only observed in the zebrafish saccule.

In chickens, hair cells at different locations on the basilar papilla showed different vulnerabilities to the over-exposure of pure tones with different frequencies (Cotanche, Saunders, & Tilney, 1987), which is consistent with the tonotopic mapping of the basilar papilla. Similar results have also been observed, though less clearly understood, in the saccule of goldfish (Smith et al., 2006), zebrafish (Schuck & Smith, 2009), and cod (Enger, 1981). These results suggest the existence of a tonotopic mapping in the auditory epithelium in fish. In our data, over-exposure to white noise induced significant hair cell loss in the anterior-medial region in the saccular maculae (Figure 2.3B). In the previous study where adult zebrafish were exposed to 100 Hz pure tone for 36 h, hair cell loss was observed only the posterior area in a sporadic pattern (Schuck & Smith, 2009). The difference in the region of most severe hair cell loss in the two studies may be due to the energy distribution across the frequencies: an intensive pure tone at 100 Hz vs. broadband (100-10,000 Hz) white noise. The audiogram of adult zebrafish expands from 100 Hz (or lower) to 4,000 Hz with 800 Hz as the most sensitive frequency (Higgs et al., 2002). The most severely damaged anterior-medial region in our data may be responsible for detecting sound of ~800 Hz, while the damaged area in the posterior region observed in the previous study (Schuck & Smith, 2009) may correspond to the tonotopic area responsible for detecting sound of lower frequencies.

2.5.2 Supporting cell “scar formation” after noise-induced hair cell loss

At 0 hpe, apical actin rings stained with phalloidin was often observed in the damaged area in saccular maculae (Figure 2.4B). The actin rings formed by the surrounding supporting cells were seen either with or without a myosin VI/VIIa-positive cell underneath (Figure 2.4B). Such structure has been described in aminoglycoside-treated sensory epithelia in bullfrogs as “scar formation,” in which the apices of the supporting cells expanded to seal the extra space resulted from hair cell death/damage (Baird et al., 1996; Gale, Meyers, Periasamy, & Corwin, 2002; Hordichok & Steyger, 2007). Similar to what was seen in our data, the actin rings were observed simultaneously with the extrusion of the dying hair cells (Hordichok & Steyger, 2007) as well as when the bundleless hair cells survived underneath (Baird et al., 1996). In addition, the rings were also observed surrounding immature hair cells during hair cell regeneration in bullfrog (Baird et al., 1996), similar to the observation during hair cell regeneration in zebrafish saccules (Figure 2.4C and D).

2.5.3 Hair cell regeneration with or without mitosis

Extensive studies in birds and amphibians have shown the two cellular mechanisms of hair cell regeneration: regeneration via mitosis (Raphael, 1992; Stone & Cotanche, 1994) and regeneration via direct transdifferentiation (Baird et al., 1993; Roberson et al., 2004). Previous studies in zebrafish lateral line neuromasts suggest the majority of new hair cells deriving from supporting cell division after complete hair cell loss induced by neomycin (Ma et al., 2008). An increase in BrdU incorporation after noise-induced hair cell loss in the damaged area suggests mitosis also plays a role in the hair cell regeneration in zebrafish (Schuck & Smith, 2009).

Incorporation of BrdU peaked at two days after noise exposure in the previous study (Schuck & Smith, 2009), which corresponds to the second phase of hair cell addition from 48-96 hpe, assuming a lag between cell division and hair cell differentiation.

However, we do not have enough data to confirm or rule out the possibility of hair cell addition from direct transdifferentiation. At early time points post noise exposure (24 and 48 hpe), there were young hair cells (identified based on the presence and length of the bundles) found in the damaged area. According to a previous publication, bundleless hair cells can also survive and repair their bundles after ototoxic treatment (Gale et al., 2002), so it is difficult to know whether these hair cells were newly produced by supporting cell transdifferentiation or were survivors from noise exposure that were going through repair. The number of hair cells returned to control levels within 96 hpe (Figure 2.3C), which seems to be more rapid than previously reported as seven days (Schuck & Smith, 2009). However, the authors did not collect data between two and seven days after noise exposure, which makes it difficult for such comparison. In addition, the presence of hair cells with short bundles in the damaged area at 96 hpe (Figure 2.4D) suggests they need a longer time frame to become fully matured.

2.5.4 Zebrafish as a model system for understanding hair cell regeneration in nonmammalian vertebrates

Adult zebrafish are known to produce new hair cells spontaneously (Bang et al., 2001; Higgs et al., 2002) as well as after hair cell loss (Schuck & Smith, 2009). There are several other reasons making it attractive as a model system for understanding the molecular mechanisms involved in hair cell regeneration. First of all, it has been a

model organism for genetic studies for decades, which facilitates the functional studies of any gene of interest involved in hair cell regeneration. Secondly, the availability of a whole-genome sequence and a relatively well-annotated transcriptome make it possible to carry out large-scale screening for candidate genes involved in hair cell regeneration. Last but not least, the existence of the superficial neuromasts facilitates the functional studies of candidate genes involved in the hair cell regeneration (Behra et al., 2009; Harris et al., 2003; Hernández et al., 2007; Ma et al., 2008).

To establish zebrafish as the model system for hair cell regeneration studies, a series of protocols need to be established and streamlined, starting with the induction of hair cell death. Ideally the protocol should be able to induce massive hair cell loss within a short period of time. In this study, the noise exposure equipment is easy to set up, and performs consistently in inducing hair cell regeneration. However, it can only induce hair cell loss in a relatively small region in saccular maculae in 48 h. Aminoglycosides have been widely used as an ototoxic treatment to induce hair cell loss. However, the administration of systemic aminoglycoside did not have ototxic effects on zebrafish for unknown reasons. Other categories of chemicals, e.g. cisplatin (Ou, Raible, & Rubel, 2007) and copper (Hernández et al., 2007), which are toxic to zebrafish lateral line hair cells, may be ototoxic as well. However, the accessibility and side effects of systemic administration of these chemicals into adult zebrafish remain to be determined.

The most promising strategy at the moment is the nitroreductase (NTR) system which allows time- and tissue-specific targeting of cell death (Pisharath, Rhee,

Swanson, Leach, & Parsons, 2007). Expression of nitroreductase driven by a tissue-specific promoter allows for tissue-specific targeting, while the timing is controlled by the administration of Metronidazole (Mtz), a substrate that can be converted to cytotoxin by nitroreductase to induce cell death. It has been successfully used in regenerative and other studies in zebrafish to induce specific cell death in pancreatic beta cells (Curado, Stainier, & Anderson, 2008; Pisharath et al., 2007), liver and heart (Curado et al., 2008), gonads (Hsu, Hou, Wu, & Her, 2009; Hu et al., 2009), and retina (Montgomery, Parsons, & Hyde, 2010). To properly utilize the NTR-induced cell death, a cell/tissue-specific promoter is needed to drive the expression of nitroreductase (Curado et al., 2008). As for specifically inducing hair cell death, a couple of promoters with such potential have been identified, e.g. pou4f3 (Xiao, Roeser, Staub, & Baier, 2005) and pvalb3b (McDermott et al., 2010)., while the promoter region used to drive nitroreductase expression needs to be optimized to minimize off-target effects. To successfully apply the NTR system to inducing massive hair cell death in adult zebrafish, the penetration efficiency of Mtz also needs to be tested in adult fish.

Chapter 3 Generation and Comparison of Expression Profiles of Inner Ear Tissues during Hair Cell Regeneration

3.1 Background review

An intriguing question in molecular biology is how cells with identical genetic materials can have diverse structures and functions. A general answer to this question is that not all the genes are equally expressed in different cells. In other words, the specific structure and function of a certain type of cell rely on the expression of a specific set of genes. Therefore, to get a more detailed answer to the question, we need to know what genes are expressed and at what level they are expressed (i.e. the gene expression profile) in any specific cell/tissue.

3.1.1 Sequencing-based gene expression profiling techniques: the early approaches

The most naive approach is to sequence all the mRNAs in the target tissue/cells to get the expression profile. The first attempts to do so were by cDNA library construction. To construct the library, mRNAs were extracted from the sample usually from a specific tissue/organ and reversed-transcribed into double-stranded (ds) cDNAs which were subsequently cloned. Due to the high cost and laborious execution of the Sanger sequencing technique, it is not feasible to routinely sequence full-length cDNA clones. An alternative way to deal with the cost issue was to sequence only a small fragment of the cloned cDNA. These fragments are called Expressed Sequence Tags (ESTs) (Adams et al., 1991). They are 150-800 nt long unedited, randomly selected single-pass sequence reads derived from cDNA libraries.

The ESTs are usually generated from 5'- or 3'- end of a cDNA clone and are named 5'-ESTs and 3'-ESTs. After the EST sequences are obtained, the annotation of the sequences requires sequence clustering and assembly, sometimes using the genomic sequences as references. Although the cost was greatly reduced by sequencing ESTs instead of full-length cDNAs, it was mainly used for novel gene discoveries and genome annotation (Adams et al., 1991). As for expression profiling, it informs the researchers the presence/absence of certain transcripts in a tissue sample rather than providing a true quantitative expression profile because it was not a cost-efficient way to get the data depth needed for the quantification of gene expression level. In addition, due to the cloning process required for generating ESTs, the EST data often show biased representation for certain groups of transcripts that were tolerated in *E. coli*-based plasmid construction.

A great advance in quantitative gene expression profiling was the development of Serial Analysis of Gene Expression (SAGE) (Velculescu, Zhang, Vogelstein, & Kinzler, 1995). The idea was to generate one single short (14-27 bp) fragment (called "tag") from each individual mRNA transcript to represent the original transcript. The sequence of the fragment was mapped back to the original transcript based on the sequence similarity. The number of times a fragment with the same sequence occurred in a sample serves as a direct measurement of the copy number of the transcript. SAGE starts from reverse-transcription of mRNAs from samples into ds cDNAs. The cDNAs are first digested with a frequent-cutting restriction enzyme (anchoring enzyme) and the 3'-fragments of the ds cDNAs are isolated. The cDNAs are divided in half and ligated with two different 5'-adaptors respectively. Both

adaptors contain a recognition site for a type II endonuclease. After adaptor ligation, the digestion with the corresponding type II endonuclease (tagging enzyme) generates the tag from the cDNA fragment a specific number of bases (15-27) downstream of the 5'-adaptor. Two sets of tags with different adaptors are ligated to form an adaptor A-ditag-adaptor B molecule that can be amplified by PCR reactions with adaptor-specific primers. After the amplification, the adaptor-ditag-adaptor molecules are digested with anchoring enzyme again to release the ditags from the flanking adaptors. The ditags are then concatemerized with each other by ligation and cloned into *E. coli* cells. The ditags are then sequenced by Sanger sequencing technique, quantified, and assigned to the transcripts that they represent using bioinformatic tools. The primary advantage of the SAGE technique is that it provides the copy number of different mRNA molecules in the sample as a direct measurement of gene expression level. Unfortunately, SAGE never gained popularity as a profiling technique because of the labor-intensive cloning of ditags and the high costs of the Sanger sequencing technique.

Another profiling technique, Massively Parallel Signature Sequencing (MPSS) was developed later and shared the same principle with SAGE (Brenner et al., 2000). MPSS differed from SAGE in that it adopted a sequencing method that involves involved a series of hybridization and ligation of oligonucleotide fragments with known sequences to tags immobilized on microbeads. The sequencing method allows reading out the sequences of hundreds of thousands of tags in parallel, which yields higher sequencing efficiency and thus deeper data set than traditional SAGE (Reinartz et al., 2002). However, due to the high cost of MPSS technique and the

issues of reproducibility, MPSS was also not widely adopted for expression profiling studies.

3.1.2 Microarray

Microarray techniques were developed based on the hybridizing affinity between complementary DNA or RNA molecules (Schena, Shalon, Davis, & Brown, 1995). A large number of single-stranded DNA molecules with known sequences are immobilized onto a solid surface to create the array. Those molecules are called probes. To examine the gene expression profile of certain biological sample, mRNAs purified from the sample are reverse-transcribed into ds cDNAs. Amplified RNAs (aRNAs, also called "targets") are synthesized with the cDNAs as templates. During the synthesis, fluorophore-labeled NTPs are used to label the aRNA molecules. The targets are then hybridized with the probes and the fluorophores are excited. The microarray is scanned and the fluorescent signals from the hybridized targets are captured and analyzed. The targets are identified by the probes that they hybridize with and the relative abundance of the targets is indirectly determined by measuring the fluorescent intensities. The microarray platforms used for gene expression profiling can be divided into two categories based on the probes used: cDNA microarray and oligonucleotide microarray. In cDNA microarrays, the probes (600-2,400 nt) are amplified from EST/cDNA libraries (Duggan, Bittner, Chen, Meltzer, & Trent, 1999). In oligonucleotide microarrays, the probes (25-60 nt) are designed and synthesized based on the known/predicted gene sequences (Hughes & Shoemaker, 2001). Based on the labeling and hybridization methods of the targets, microarrays can be divided into one-color (Hughes & Shoemaker, 2001) and two-color

microarrays (Schena et al., 1996). In one-color microarrays, the targets are generated only from the biological sample of interest and labeled with one single fluorophore. In two-color microarrays, there are two sets of targets. One set is generated from the biological sample of interest, while the other is from certain universal reference RNAs. The two sets of targets are labeled with two different fluorophores and hybridized with the array at the same time. The expression level of any gene of interest is read out as the ratio of fluorescent intensity of the target from biological sample relative to that of the reference target.

Microarrays are probably the most widely used high-throughput technique for gene expression profiling studies. However, the approach also suffers from various limitations. First of all, the technique requires knowing the sequence of the target genes examined, thereby limiting the detection of novel genes that might be expressed in biological samples. This becomes a major disadvantage when the transcriptome of the organism of interest is poorly understood. Secondly, the reproducibility of the microarray data has been a long-standing issue . The well-known publication by Tan et al. (2003) compared three commercially available microarrays and found poor reproducibility of data generated from them. Similar issues were also found in other studies (Kothapalli, Yoder, Mane, & Loughran, 2002; Kuo, Jenssen, Butte, Ohno-Machado, & Kohane, 2002; Li, Pankratz, & Johnson, 2002; Severgnini et al., 2006).

The cross-platform inconsistency in microarray data can be attributed to many factors. First of all, there is intrinsic cross-hybridization problem between the probes and the targets. The lengths of the probes (Järvinen et al. 2004; Wheelan et al. 2008)

as well as the experimental conditions (Kuo et al. 2006) contribute to the specificity of probe-target binding. Secondly, a surprisingly high number of probes on the microarrays were mis-annotated. Although the problem is more severe in custom-made cDNA microarrays because of the library contamination (Halgren, Fielden, Fong, & Zacharewski, 2001; Järvinen et al., 2004; Kothapalli et al., 2002), the annotation of the commercial microarrays are not mistake-free. For example, Harbig et al. (2005) BLAST the Affymetrix U133 plus 2.0 arrays against known human transcripts and found that re-annotation of ~37% of the probes were needed. Last but not least, the interpretation of microarray data is tremendously influenced by different data analysis strategies (Lei Guo et al., 2006; Shi et al., 2005; Yauk & Berndt, 2007). Because microarrays do not provide direct measurement of gene expression level, it has been suggested that the direction of changes rather than the magnitude of the changes in gene expression level should be emphasized when doing cross-platform comparisons (Kawasaki, 2006).

3.1.3 Revisiting sequencing-based gene expression profiling techniques

The high cost and relatively low throughput of the Sanger sequencing technique for large-scale sequencing tasks was the major drawback in the traditional sequencing-based gene expression profiling techniques. With the recent development and adoption of Next-generation Sequencing technologies, sequencing-based strategies for gene expression profiling become more and more favorable due to the dramatic increase in sequencing efficiency and the accompanying sharp drop in sequencing costs.

3.1.3.1 Next-generation sequencing technologies

Several conceptually novel sequencing methods are often referred to as "Next-Generation Sequencing technologies" (NGS). The commercially available sequencing platforms that adopt these technologies include Roche 454 (Margulies et al., 2005), Illumina (Bennett, 2004; Bennett, Barnes, Cox, Davies, & Brown, 2005), SOLiD (Shendure et al., 2005), and SMRT (Eid et al., 2009). The major features of these platforms are summarized in Table 3.1. The innovation in sequencing chemistry and signal detection techniques allow sequencing tens of millions of short DNA fragments at the same time. In addition, bacterial cloning of the target sequences is no longer necessary. All these changes greatly enhance the throughput and reduce the cost.

Table 3.1. Comparison of different DNA sequencing platforms

Sequencing platform	Sanger	454	Illumina	SOLiD	SMRT
Sequencing chemistry	Dye-terminator sequencing	Sequencing by synthesis	Sequencing by synthesis	Sequencing by hybridization and ligation	Sequencing by synthesis
Template amplification method	Bacterial cloning	Emulsion PCR	Bridge PCR	Emulsion PCR	N/A
Read length	700-900 bases	400 bases	100 bases X 2	75 bases X 2	>1,000 bases
Sequencing efficiency	2Mb/day	1Gb/day	25Gb/day	100Gb/day	-
Cost	~$10.00/kb	~$60.00/Mb	~$2.00 /Mb	~$2.00/Mb	-

3.1.3.2 Sequencing transcriptomes with NGS technologies

Previous research sequencing full-length cDNAs/ESTs with the Sanger sequencing technique has provided valuable information for gene annotation (Adams et al., 1991). However, due to the low throughput and sampling rates, those studies revealed only 60% of total transcripts in the cells and most of them are of higher abundance in the samples (Brent, 2008). Deep sequencing of the transcriptome with NGS technologies enables us to capture those low-abundance transcripts not detected in previous studies. Transcriptome sequencing with NGS technologies is usually called RNA-sequencing (RNA-seq). In RNA-seq, mRNAs are converted into short

cDNA fragments which are subjected to in-depth sequencing. After that, the short cDNA fragments are assembled and annotated. RNA-seq results are highly informative because they provide transcriptome sequences (Sultan et al., 2008; Wilhelm et al., 2008), transcription start/ending sites (Guttman et al., 2010; Wilhelm, Marguerat, Goodhead, & Bahler, 2010), exon-intron boundaries (Wilhelm et al., 2008; Guttman et al., 2010), splicing patterns (Sultan et al., 2008; Wilhelm et al., 2008; Trapnell et al., 2010), post-transcriptional modification (Picardi et al., 2010), single nucleotide polymorphisms (SNPs) (Cloonan et al., 2008), and transcription level quantification (Marioni, Mason, Mane, Stephens, & Gilad, 2008; Mortazavi, Williams, McCue, Schaeffer, & Wold, 2008; Wilhelm & Landry, 2009).

3.1.3.3 Quantitative gene expression profiling with NGS technologies

One application of the NGS technologies is for quantitative gene expression profiling by sequencing and quantifying short cDNA "tags" derived from mRNAs. The 454 platform has been used for sequencing and quantifying SAGE ditags, e.g. DeepSAGE (Nielsen, Høgh, & Emmersen, 2006). Solexa/Illumina (Digital Gene Expression, DGE) and Applied Biosystems (SOLiD SAGE) have developed their own SAGE-like protocols to generate short tags (21-nt for DGE and 27-nt for SOLiD SAGE) compatible with their own sequencing platforms. These protocols are greatly simplified compared to the original SAGE protocol in that they do not require the concatemerization or bacterial cloning of the tags. Digital Gene Expression (also called "tag profiling") starts from reverse transcription of mRNAs purified from biological samples into ds cDNAs. The cDNAs are digested with DpnII or NlaIII (corresponding to the anchoring enzyme in SAGE protocol). The 3'-cDNA fragments

are isolated and ligated with a 5'-adaptor which contains a MmeI recognition site. Another round of digestion with MmeI (corresponding to the tagging enzyme in SAGE protocol) generates cDNA tags of 20-nt (starting with DpnII) or 21-nt (starting with NlaIII) long. The tags are then ligated to a 3'-adaptor. The tag flanked by two adaptors are immobilized onto solid surface in flow cells and amplified by bridge PCR. After amplification, the tags are sequenced and quantified with an Illumina Genome Analyzer sequencer (sequencing-by-synthesis) and quantified the same way as in the SAGE protocol. The tag sequences are then mapped to the transcripts they represent to get the final version of a comprehensive gene expression profile with direct quantitative measurement of gene expression level.

3.1.3.4 Advantages of sequencing-based gene expression profiling techniques

The biggest advantage of RNA-seq compared to microarray is that *a priori* knowledge of the transcriptome of interest (sometimes even the corresponding genomic sequences) is not required and thus will not limit the application of RNA-seq. In addition to the fruitful re-annotation of extensively studied transcriptomes (Mortazavi et al., 2008; Nagalakshmi et al., 2008), RNA-seq has also demonstrated its power in *de novo* transcriptome sequencing without existing genomic sequences (Vera et al., 2008).

Although tag profiling has more dependence on what is known about the transcriptome/genome, it is not limited to profiling only known/predicted transcripts as in microarrays. For the purpose of generating gene expression profiles, RNA-seq is probably the most powerful technique for accurately identifying full-length transcripts and different splicing isoforms of the genes expressed in the biological

samples. When it comes to the quantification of gene expression level, RNA-seq (10^5 or higher) and tag profiling (15-20 million tags per lane in Illumina GA IIx) (Asmann et al., 2009) have a larger dynamic range compared to microarray (100-1,000-fold) (Wang, Gerstein, & Snyder, 2009) for measuring gene expression level. Both RNA-seq (Cloonan et al., 2008; Nagalakshmi et al., 2008) and tag profiling (Asmann et al., 2009; Feng et al., 2010; Hegedűs et al., 2009; 't Hoen et al., 2008) have shown high levels of reproducibility in biological repeats and technical repeats. For example, profiling of human brain RNA libraries generated in different labs with DGE executed in different lanes in same/different runs on an Illumina sequencer yielded highly reproducible profiles (Person Correlation $r > 0.95$) (Asmann et al., 2009). Moreover, much less efforts in data generation and analyses were needed to achieve such high reproducibility compared to those required for microarray studies. Although all profiling techniques tend to have difficulty capturing rare transcripts, all the previous studies comparing tag profiling with different microarray platforms showed a more sensitive and reliable measurement of transcripts of low abundance in tag profiling (Asmann et al., 2009; Hegedűs et al., 2009; 't Hoen et al., 2008). Deep sequencing, the direct measurement of copy numbers of transcripts, and simplified sample preparation (no bacterial cloning required) all contribute to the more desirable performance of RNA-seq and tag profiling (especially the latter one) over microarray for quantitative analysis of gene expression profiles. What is more, these features also facilitate the inter-lab sharing of profiling data which is extremely difficult to achieve for microarray studies (MAQC Consortium, 2006; Yauk & Berndt, 2007).

3.1.3.5 Challenges for the new sequencing-based gene expression profiling techniques

The new sequencing-based gene expression profiling techniques are not flawless. There are still challenges in every step of the experiment.

Starting from the library preparation, fragmentation of cDNAs or mRNAs is required for RNA-seq experiments to make their length compatible with most of the NGS platforms. cDNA fragmentation tends to over-represent 3'-end of the transcript, probably due to the existence of RNA secondary structure and/or biased priming during reverse transcription (Mortazavi et al., 2008; Nagalakshmi et al., 2008; Shendure, 2008). While mRNA fragmentation overall has a unanimous coverage of the transcripts, it tends to lose both ends of the transcripts (Mortazavi et al., 2008; Wang et al., 2009). As for tag profiling, it is obvious that the transcripts without a cutting site of the anchoring enzyme (~6.68% of human Refseq RNAs) will be missing from the profile (Asmann et al., 2009). Priming with internal poly-adenylation sequences and incomplete enzyme digestion give rise to tags located upstream to the 3'-most anchoring enzyme cutting site, which makes the mapping of the tags to the original transcripts more complicated (Discussed below).

Another major challenge arises from the short length of the sequencing reads, which leads to failures in mapping the short reads to the genome/transcriptome. There are mainly two types of mapping problems: no mapping and multiple mapping. Sometimes the short sequencing reads can not be mapped to any location on the genome/transcriptome, which can be attributed to exon-spanning reads, alternative splicing isoforms, post-transcriptional editing, polymorphisms, and sequencing errors.

While it has been estimated that more than 75% of the 21-nt tags are expected to occur only once in the human genome (Saha et al., 2002), the chance of mapping short RNA-seq reads and DGE tags to a specific gene or genome location is further lowered by repetitive sequences, polymorphisms (e.g. SNPs), and sequencing errors. Using the 454 platform or pair-end sequencing on the Illumina and SOLiD platforms to get longer RNA-seq reads (200-500 nt) will definitely be helpful to the mapping problems. Bioinformatic and statistical strategies can also partially alleviate the problems. For example, in case of low-copy repetitive sequences, multi-mapping RNA-seq reads can be assigned to a genome location based on the information from their unique-mapping neighbors (Cloonan et al., 2008; Mortazavi et al., 2008). The mapping of the DGE tags to a specific genome/transcriptome location is even more challenging due to even shorter lengths (20-27 nt). Several studies tried to assign tags with more than one mapping sites to a unique gene by calculating the probabilities of those tags derived from different genes (Ge, Jung, Wu, Kibbe, & Wang, 2006; Malig, Varela, Agosin, & Melo, 2006). Many factors were taken into account for the probability calculation, including the sequence context of the putative mapping loci (e.g. internal poly-adenylation sequences) (Malig et al., 2006) and the gene expression data from previous SAGE and microarray studies (Ge et al., 2006). In most cases, the tags are mapped to the 3'-most anchoring enzyme cutting sites, but exceptions have been observed as well (Asmann et al., 2009). Moreover, while such a method is useful for DGE in organisms with a relatively well-annotated transcriptome, it may induce more biases when the experiment is done in an organism

with a poorly studied transcriptome and the mapping is mainly based on EST sequences rather than curated, full-length transcript sequences.

While RNA-seq clearly has advantages over DGE when it comes to the accurate mapping of short sequence reads, DGE, at the moment, is still favored over RNA-seq for generating a quantitative gene expression profile for two main reasons. First, compared to DGE, RNA-seq needs a much greater sequencing depth in order get adequate coverage of transcripts for measuring the gene expression level. For example, it was estimated that RNA-seq required at least 40 million reads to cover 90% of a transcriptome library while DGE required no more than 5 million tags (Wold & Myers, 2008). The great difference in required sequencing depth is directly translated into the more expensive sequencing cost when RNA-seq is used for quantification. The other reason lies in the more complicated statistics needed for quantifying gene expression level from RNA-seq data. Because a single transcript gives rise to multiple cDNA fragments "randomly" in RNA-seq, the total number of cDNA fragments mapped to the transcript can not be used to represent the copy number of the transcript until they are normalized according to the length of the transcript (Marioni et al., 2008). Further normalization may also be required given the biased coverage of full-length transcripts resulting from library preparation.

With further reduction of the sequencing cost and optimization of the protocol, RNA-seq will become more applicable for quantification profiling studies. However, instead of being replaced by RNA-seq, DGE will more likely be adapted as a quick gene expression profiling routine in the future. Under current circumstances, a combination of low-coverage RNA-seq and DGE would allow large-scale

quantitative analysis of gene expression profiles at relatively low costs (Wang et al., 2010).

3.2 Experiment overview

Previous studies on hair cell regeneration mechanisms generally focused on one or a small number of genes/pathways at a time (Daudet et al., 2009; Ma et al., 2008; Roberson et al., 2002; Stone et al., 2004; Stone & Rubel, 1999) with the exception of very few microarray studies with limited data depth (Hawkins et al., 2003, 2007). To avoid these limitations, we used a new high throughput gene expression profiling technique, Digital Gene Expression (DGE, i.e. tag profiling) (Morrissy et al., 2009) to examine the changes in gene expression during hair cell regeneration in adult zebrafish.

In order to have a comprehensive understanding of the genes/pathways involved in inner ear hair cell regeneration after noise exposure in adult zebrafish, we generated expression profiles from inner ear samples of adult zebrafish using DGE at different time points (based on Section 2.4.2) during hair cell regeneration. By comparing the regeneration profiles to the control profile, we screened for genes whose expression level significantly changed during regeneration. These genes are considered as “candidate genes” because they are more likely to play important roles in hair cell regeneration. Pathway analyses were performed to identify key pathways strongly enriched in the regeneration response.

3.3 Materials and methods

3.3.1 Inner ear tissue collection and RNA extraction

Adult wildtype (TAB-5) (Amsterdam et al., 1999) zebrafish (~ 1yr old) were exposed to white noise as described in Section 2.3.2. After exposure, the fish were maintained under regular husbandry conditions until sacrifice. The control fish were not exposed to noise. Fish were euthanized with 0.03% buffered MS-222 (Sigma) at 0, 24, 48, and 96 hpe. The heads were immediately removed and rinsed in the RNAlater (Ambion). Both saccule and lagena were collected for RNA extraction because separating them in fresh tissue is far too difficult to be performed rapidly. Total RNA from saccules and lagenae was extracted with Trizol (Invitrogen) according to manufacturer's instructions. The RNA concentration and purity was determined by a Nanodrop spectrophotometer.

3.3.2 Generation of expression profiles from inner ear tissues with Digital Gene Expression (DGE)

Gene expression profiles of the inner ear samples were generated by Illumina, Inc. using the Digital Gene Expression (DGE) technique, i.e. tag profiling. mRNAs were reverse-transcribed and converted to double-stranded cDNAs that were then digested with DpnII. The 3'-fragments were purified and ligated to a 5'-adaptor containing an MmeI restriction site. Digestion by MmeI cut 20 bps into the cDNA fragments. After ligation to a 3'-adaptor, a 20-nt long cDNA fragment ("tag"), flanked by 5'- and 3'-adaptors, was generated from the original mRNA. All the tags were then

sequenced by the Illumina Genome Analyzer. After sequencing, the number of tags with identical sequences in each experiment were counted and pooled.

3.3.3 Tag mapping and annotation

Tags detected only once in the five expression profiles were discarded to simplify analysis. The remaining tags were mapped against transcriptome and genomic sequence databases: Refseq RNAs, UniGene, Ensembl RNAs, Ensembl RNA *ab initio*, and the zebrafish genome (Zv.8). A C++ program was developed to efficiently map the tags to specific databases. The program starts by building a prefix tree of the divergent part of the tags (16-nt sequence after the DpnII cutting site "GATC") and by linearly scanning the database for potential matches to the common prefixes (DpnII cutting site "GATC"). Upon finding a match, the prefix tree was searched for the remainder of the database string. Those tags that failed to be mapped were re-mapped when single-nucleotide mismatch was allowed to accommodate the high frequency of polymorphism in zebrafish genome. However, the mis-match data were not used for further analyses in this study. For candidate gene screening, only the mapping results in Refseq RNA and UniGene were used because they provided the most useful information about known/predicted genes. To be included for further analyses, a tag needed to be "unambiguously mapped," i.e. mapped to only one Refseq RNA entry (and the corresponding UniGene entry if existing) or to only one UniGene entry (when no mapping in the Refseq database). UniGene IDs were used as the primary index (except for those Refseq RNAs without corresponding UniGene IDs). Potential miRNA-encoding genes in the profiles were examined separately (See Section 3.3.7).

3.3.4 Comparisons of expression profiles

The expression level of a certain gene (identified by a unique UniGene ID) was the summation of counts of the "unambiguously mapped" tags normalized by the total counts of all tags obtained in the profile, resulting in expression units of "Transcripts Per Million (TPM). χ^2-tests (genes with tag count > 5) and Fisher's Exact Tests (genes with tag count $\leq$ 5) were used to compare the expression levels of the genes quantified by tag profiling. The calculation was done using R software. Expression data from inner ear samples collected at different time-points during regeneration were compared to those from the control sample. Candidate genes were identified for further analysis if they showed significant differences in expression level during regeneration compared to the control sample, i.e. $\geq$ 1.5-fold increase or $\geq$ 2-fold decrease in expression level with a p value < 0.01 as determined by χ^2-test or Fisher's Exact Test.

3.3.5 Verification of candidate genes

Candidate genes identified by expression profile comparison were confirmed with qRT-PCR. qRT-PCR reactions were carried out with the SYBR GreenER two-step qRT-PCR kit for iCycler according to the manufacture's instructions. Glyceraldehyde-3-phosphate dehydrogenase (gapdh) was used as the reference gene for all experiments. The relative change in expression level of a gene X in a certain experimental (EXP) sample compared to the control (CON) sample is calculated as $2^{\wedge}(\Delta Ct_{EXPx} - \Delta Ct_{CONx})$ while $\Delta Ct_{EXPx} = (Ct_{EXPref} - Ct_{EXPx})$ and $\Delta Ct_{CONx} = (Ct_{CONref} - Ct_{CONx})$. Ct is the cycle number at which amplification rises above the background threshold. The qRT-PCR primers are listed in Table 3.2.

Table 3.2. Sequences of qRT-PCR primers

Target gene	Primer sequences
atoh1a	F: 5'-GCG AAG AAT GCA CGG ATT GAA CCA-3'
	R: 5'-TGC AGG GTT TCG TAC TTG GAG AGT-3'
dld	F: 5'-TCC AAC CCT TGC TCG AAT GAT GCT-3'
	R: 5'-TCG ATG TTG TCT TCG CAG TGC GTT-3'
dre-miR-21-1	F: 5'-GGC GTG GAT ATA AGT CTT TCC CAG TGT G-3'
	R: 5'- AGA CAG CCT ACA GAC TGT TGT CGC-3'
jak1	F: 5'-ACG AGT GCT TGG GAA TGG CTG TTT-3'
	R: 5'-AGT TGC GTT GCT TAA TGG TGC GGT-3'
socs3a	F: 5'-TAA AGC AGG GAA GAC AAG AGC CGA-3'
	R: 5'-TGG AGA AAC AGT GAG AGA GCT GGT-3'
socs3b	F: 5'-CGG ATA ACG CTT TGA AGC TGC CTT-3'
	R: 5'-TAC TAT GCG TTA CCA TGG CGC TCT-3'
stat3	F: 5'-AGT GAA AGC AGC AAA GAG GGA GGA-3'
	R: 5'-TGA GCT GCT GCT TAG TGT ACG GTT-3'

3.3.6 Data analyses

Sample clustering analysis was done using Genesifter software (Geospiza). The distances between different inner ear tissue samples were calculated based on the overall expression profile from each sample. Pathway analysis was done with candidate genes using the MetaCore software (GeneGo) by utilizing known relationships between the human orthologs of the zebrafish candidate genes. The

results were then examined manually to identify the genes/pathways of highest interest.

Gene expression data were obtained from the Zebrafish Information Network (ZFIN, www.zfin.org). χ^2-test was used to examine if the genes known to be expressed in the developing ears and lateral line system were significantly enriched in the list of candidate genes compared to all the genes identified from the expression profiles. Z-scores were also used to show similar enrichment and was calculated by Z-score = (r-n*(R/N))/(n*(R/N)*(1-R/N)*(1-(n-1)/(N-1)) where R = the total number of candidate genes, N = total number of genes identified from the profiles, r = the number of candidate genes known to be expressed in the developing ear/lateral line system, and R = the number of genes known to be expressed in the developing ear/lateral line system in the profiles. When the Z-score is greater than 2, the genes known to be expressed in the developing ear/lateral line system occur more often in the group of candidate genes than expected as if the group of candidate genes had been randomly selected from the profiles.

3.3.7 Identification of candidate genes encoding miRNAs

Tags with no Refseq or UniGene mappings and with only one genome mapping locus were mapped against the known zebrafish miRNAs from Release 15 (miRBase). A tag was considered as associated with a miRNA when the tag locates 1) on the same strand of chromosome as the miRNA and 2) less than 10kb away (up- or down-stream) from the miRNA. The statistical analyses were performed as mentioned in Section 3.3.4.

3.4 Results

3.4.1 Gene expression changes in inner ear tissues collected during hair cell regeneration

We generated transcriptional expression profiles from inner ear tissue samples (saccules and lagenae) collected from noise-exposed zebrafish at 0, 24, 48, and 96 hpe as well as from control fish. The expression profiles were generated by the "Digital Gene Expression" (DGE) technique, i.e. tag profiling. The raw data from profiling included sequences of 944,347 transcript-representing tags (20-nt) and a "count" associated with each tag (Supplemental file 1; Table 3.3). Here "count" means the number of times that a tag with a specific sequence was detected from a specific tissue sample, which is a direct readout of the expression level (mRNA copy number) of the represented gene. Each tissue sample yielded ~300,000 unique tag sequences from ~3,000,000 total tags. Closer examination of the tag sequences showed 6.8% of the unique tag sequences containing one or more "N"s where the sequencer failed to make an accurate base call.

Around 68% of the tags, consisting of ~4% of the total tag counts, were detected only once in the five profiles and excluded from the tag mapping process for quality control purposes (Table 3.3). After filtering out these tags, there were 303,342 unique tag sequences remaining, with a total number of 15,103,943 sequenced tags. Only these tags were included further in the analyses.

Table 3.3. Summary of tag profiling results

	Total		After filtration[b]	
	Count	**Unique tag sequences**	**Count**	**Unique tag sequences**
Control	3,339,753	327,240	3,199,598	187,085
0 hpe[a]	2,758,836	279,532	2,646,064	166,760
24 hpe	3,615,956	317,505	3,486,384	187,933
48 hpe	3,476,027	331,687	3,337,409	193,069
96 hpe	2,554,376	289,177	2,434,488	169,289
Total	15,744,948	944,347	15,103,943	303,342

a. hpe: hour post exposure
b. Tags that were detected only once in five profiles are excluded.

3.4.2 The distribution of tag abundance

Each profile was composed of 166,760-193,069 unique tag sequences (Table 3.3). The number of tag counts were transformed to the normalized unit called transcripts per million (TPMs) by dividing the number of tag counts by the total number of sequences in one profile, then multiplying by 1 million. The distribution of tag abundance was consistent across all five profiles (Figure 3.1). In each profile, ~85% of the tag sequences were detected at the level of no more than 3 TPMs which is equivalent to an average of no more than one copy of the transcript per cell. A much smaller percentage (~15%) of tag sequences were detected medial abundance (3-1,000 TPMs). Very few tag sequences (~0.05%) were highly enriched (>1,000 TPMs) in each profile.

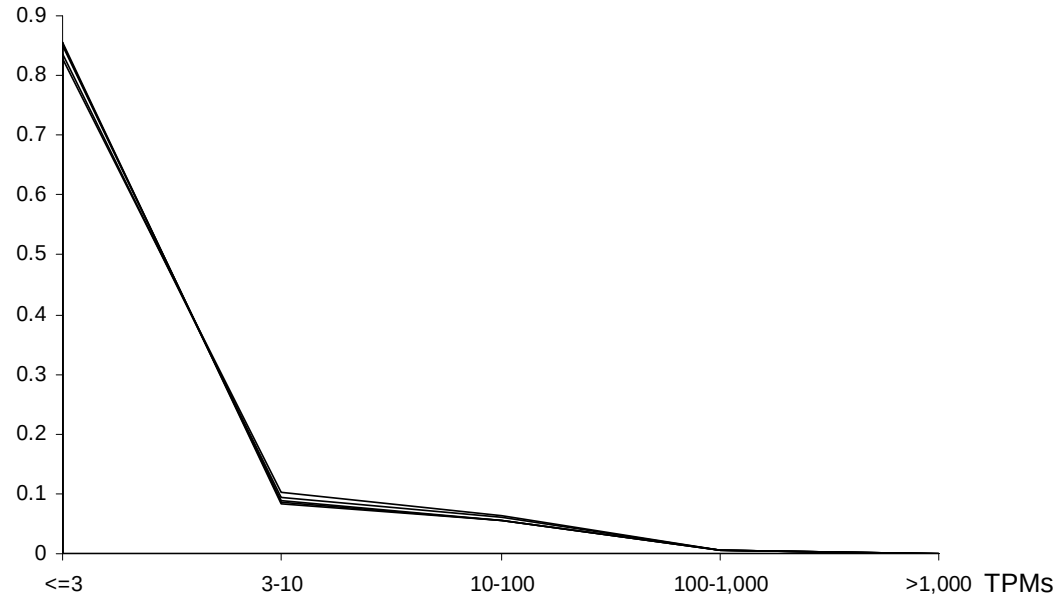

Figure 3.1. Distribution of tag abundance in five expression profiles. The numbers of unique tag sequences were plotted against the different level of abundances. The tag abundance was normalized to units of Transcripts Per Million (TPMs). Each line in the figure represents data from one expression profile. Five lines representing five profiles are superimposed in the figure to show the similar distribution pattern in all five profiles.

3.4.3 Tag mapping to transcriptome and genome databases

A total number of 303,342 unique tag sequences were mapped to multiple databases: RefSeq RNA, UniGene, Ensembl RNA, Ensembl *ab initio* and the zebrafish genome (Zv8). For further analyses, only the mapping results from RefSeq RNA, UniGene, and genomic sequences were taken into account while those based on Ensembl databases were only used as references. ~60% of the unique tag sequences were mapped to at least one known/predicted transcript or at least one

location in the genome (Figure 3.2A). ~34% of the tag sequences were mapped to one or more known/predict transcripts. Among those sequences, ~78% or as many as 80,604 sequences were unambiguously mapped to one known/predicted transcript (Figure 3.2A) and used for gene identification and expression level calculations. From the tag sequences unambiguously mapped to only one transcript, 22,324 UniGene clusters were identified (Supplemental file 2).

No mismatch was allowed in the mapping results presented in Figure 3.2A and as the bars with solid colors in Figure 3.2B. Figure 3.2B shows the break-downs of mapping results according to the number of the tags in the control profile (normalized to TPMs). Tag sequences detected at the level of no more than 3 TPMs showed the worst "overall mappability" (the percentage of tag sequences mapped to at least one transcript or genome location) with nearly 40% of the sequences failing to be mapped to any transcript or genomic location (Figure 3.2B). The overall mappability improved as the abundance of the tags increased (Figure 3.2B). However, the percentage of ambiguous mapping (mapped to more than one transcript or genome location) also increased with the overall mappability (Figure 3.2B). There was only ~1.2% of tag sequences with >1,000 TPM abundance that failed to be mapped to the transcriptome or genome, but the percentage of ambiguously mapped sequences in this group was as high as 67%. Tag sequences with medial abundance showed a much higher percentage of unambiguous mapping (mapped to only one transcript or genome location). For example, tag sequences with 10-100 TPMs abundance showed highest percentage (~60%) of unambiguous mapping, followed by tag sequences with abundance of 3-10 TPMs and 100-1,000 TPMs (Figure 3.2B).

Due to the high rate of polymorphisms in zebrafish genome and possible sequencing errors, we also performed tag mapping allowing one sequence mismatch (bars with shaded colors in Figure 3.2B). When one-mismatch was allowed, overall mappability and the percentage of unambiguous mapping increased with all tag sequences regardless of their abundances. The low-abundance group (≤3 TPMs) showed the greatest improvement: less than 7% of the tag sequences failed to be mapped, while the percentage of unambiguous mapping increased from 46% to 67% (Figure 3.2B). However, due to the low abundance of these tag sequences, the increased mappability resulted from one-mismatch strategy did not lead to significant changes to the overall expression profiles, so only the expression profiles annotated by no-mismatch mapping were used for further analyses for higher stringency. In this study, the tag sequences were only considered associated with genes or genome locations based on no-mismatch mapping. Only data calculated from the control profile are presented in Figure 3.2B, but all five profiles showed similar mappability patterns across different tag abundances.

3.4.4 Unexpected tags related to the transcripts

Theoretically tags can only be generated from the 3'-most DpnII cutting site in the cDNA molecule. However, due to the incomplete DpnII digestion and priming to internal poly-A sequences, other DpnII cutting sites farther from the 3'-end of the cDNA molecules can also give rise to tags. Previous publications suggest giving priority to 3'-most DpnII site-mapping when a tag sequence can be mapped to multiple transcripts (Blackshaw et al. 2004), so we examined the probability of tags generated from different DpnII cutting sites on the cDNA molecules. Only tag

sequences that mapped to the sense strand of one Refseq RNA transcript were used. In addition, tag sequences containing any "N" were also excluded. After examining 27,193 such tag sequences, we found only 46% of the tag sequences mapped to the 3'-most DpnII cutting sites (Figure 3.2C). As high as 50% of the tag sequences were mapped to the 2^{nd} to 10^{th} DpnII cutting sites from 3'-ends of the transcripts.

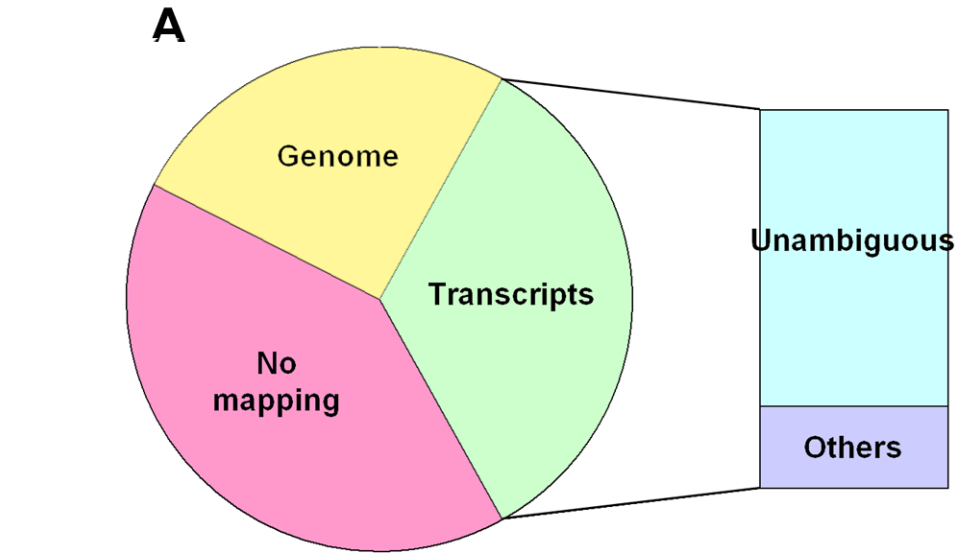
A
Genome
Transcripts
No mapping
Unambiguous
Others

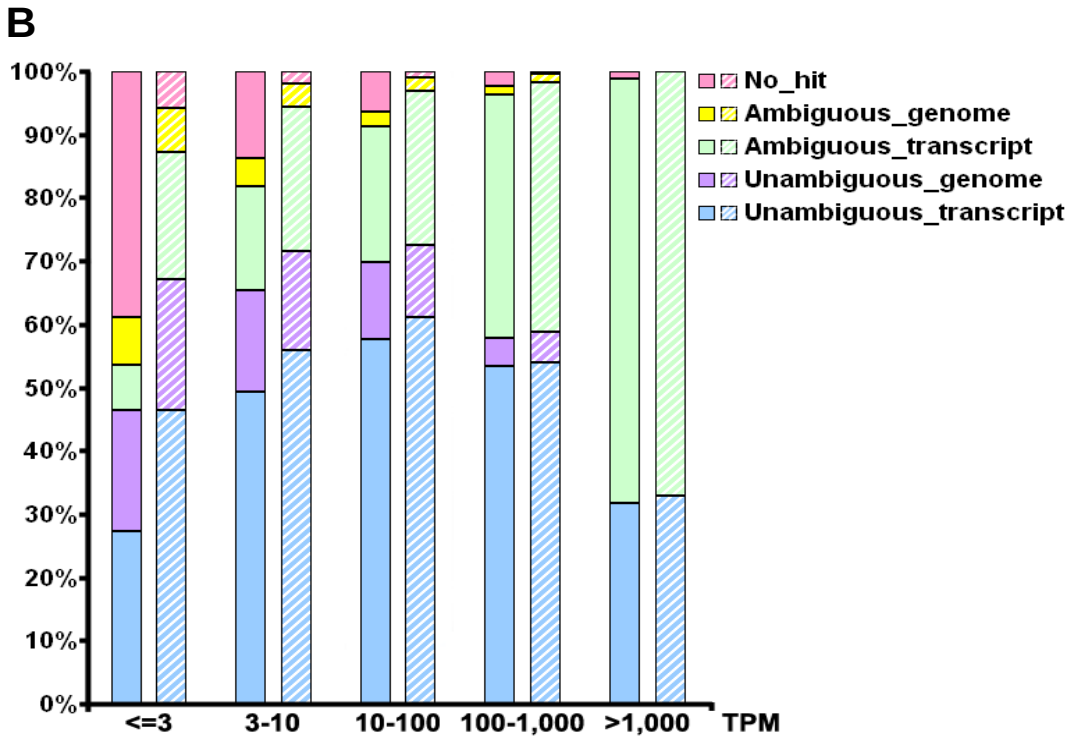
B
100%
90%
80%
70%
60%
50%
40%
30%
20%
10%
0%
<=3
3-10
10-100
100-1,000
>1,000
TPM
No_hit
Ambiguous_genome
Ambiguous_transcript
Unambiguous_genome
Unambiguous_transcript

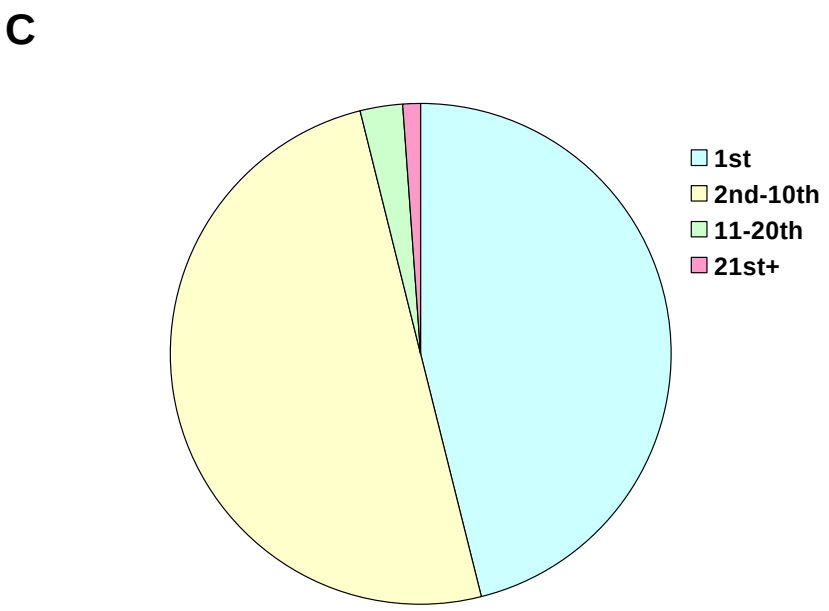

Figure 3.2. **Summary of mapping results of tag sequences.** 303,342 unique tag sequences from five time-points were mapped against transcriptome and genome databases. **A)** ~34% of the tag sequences were mapped to one or more known/predicted transcripts and ~26% to one or more loci in genome (without a known transcript), leaving ~40% of the tag sequences without transcriptome or genome mapping. Among those mapped to known/predicted transcripts, ~78% were unambiguously mapped. **B)** Analysis of mapping results in tag sequences of different abundances. The bars with solid colors are results from no-mismatch mapping and those with shaded colors are results from one-mismatch mapping. The results presented here are from the control profile. **C)** The mapping of tag sequences to different DpnII cutting sites in the transcripts. The cutting sites are numbered from the 3'-end of the transcripts, i.e. "1st" means the 3'-most cutting site.

3.4.5 Candidate gene identification and confirmation

We used χ^2-tests and Fisher's exact tests to compare the gene expression level during regeneration to the control level. 2,269 genes (identified as unique UniGene clusters) with significant changes in their expression levels in at least one time-point during regeneration were identified as candidate genes (Supplemental file 3). These genes were identified by a p value cutoff of 0.01 and a fold-change ratio $\geq$1.5 or $\leq$0.5. Several candidate genes identified by DGE were confirmed with qRT-PCR (Figure 3.3A).

Over 60% of the candidate genes were up-regulated during regeneration while the others were down-regulated (Supplemental file 3). Out of the four regenerative profiles, 1,628 candidate genes were identified from the 0-hpe profile (Figure 3.3B). The number of candidate gene decreased with time, with the 96-hpe profile containing the smallest number of candidate genes (Figure 3.3B).

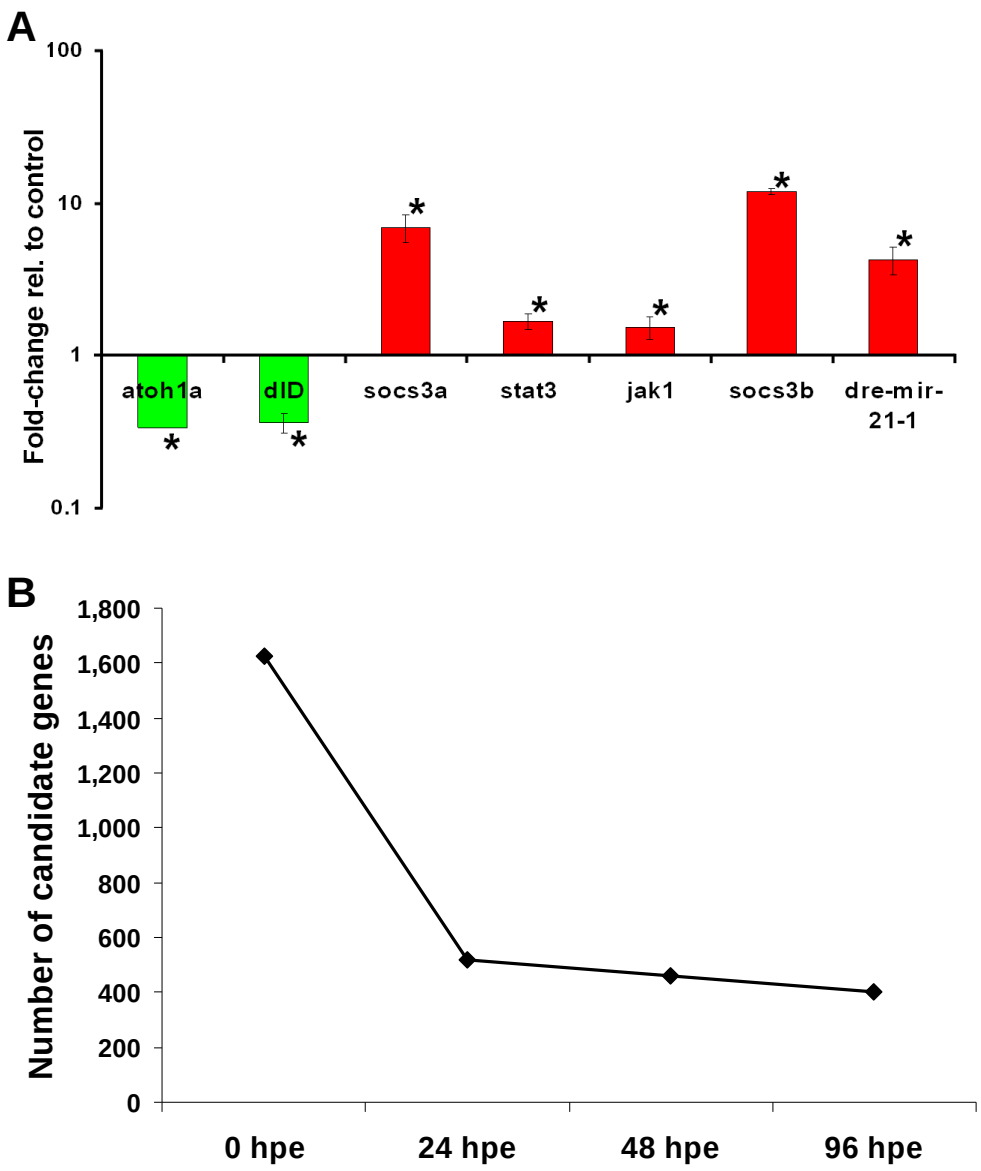

Figure 3.3. Confirmation and characterization of candidate genes. A) Some of the candidate genes (0 hpe) identified by tag profiling were confirmed by qRT-PCR using gapdh as a reference gene (n = 3, one-tail t-test, *p < 0.01). **B)** The numbers of candidate genes identified from four regenerative profiles respectively.

3.4.6 Involvement of candidate genes during inner ear and lateral line system development

Based on data from the Zebrafish Information Network (ZFIN), 186 candidate genes were known to be expressed in the developing ears/lateral line systems (Supplemental file 4). Statistical analyses suggested a greater enrichment of the genes known to be expressed in the developing ears/lateral line systems in the group of candidate genes than expected as if the group of candidate genes had been randomly selected from the profiles ($p < 0.0001$ from χ^2-test and Z-score = 102.5).

3.4.7 Clustering analysis of five gene expression profiles

Clustering analysis of the five expression profiles with Genesifter software (Geospiza) based on the calculation of the overall differences between profiles showed that the 96-hpe profile shared the highest similarity with the control profile, followed by the 24-hpe and the 48-hpe profiles, which were highly similar to each other, and then by 0-hpe profile that differed the most from the control profile (Figure 3.4A, top part). Essentially the transcriptional profiles are most different immediately after sound exposure and slowly return to normal over the course of four days.

3.4.8 Pathway analysis with identified candidate genes

Pathway analyses were carried out for the 2,269 candidate genes using the Metacore software package (GeneGo). Approximately 50% of the genes were included in the analysis because their homologs in human could be identified based on the HomoloGene database. The functions of the most enriched interaction network

calculated from the candidate genes in each experimental time-point are listed in Figure 3.4A (bottom part).

When manually examining the interaction networks, we focused on nodes or sub-networks that shared significant connections with other part of the network. Based on that preference, we identified the stat3/socs3 pathway as the dominant signaling pathway to become activated at the earliest time-point of recovery (0 hpe) (Figure 3.4B). Signal transducer and activator of transcription 3 (stat3) and suppressor of cytokine signaling 3a (socs3a, a zebrafish homolog of human socs3) were both significantly up-regulated at 0 hpe (Supplemental file 3). Some of the related genes, e.g. socs3b (the paralog of socs3a), Janus kinase 1 (jak1), and matrix metalloproteinase 9 (mmp9), also showed significant changes in their expression levels (Supplemental file 3).

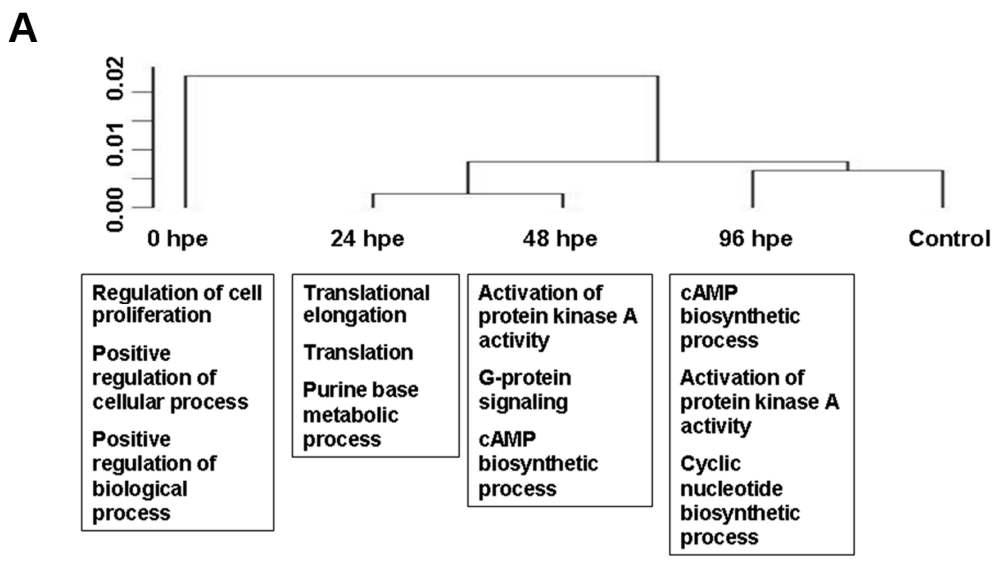

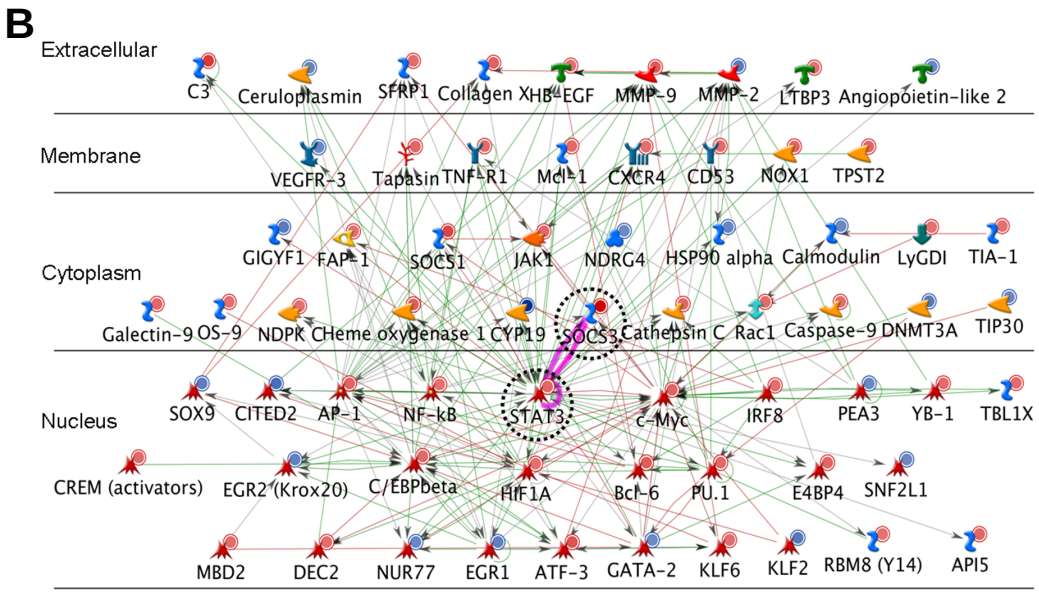

Figure 3.4. Analyses of the expression profiles and candidate genes. A) Clustering analysis of the five expression profiles with Genesifter software showed the relationship between different profiles (top diagram). The clustering results had the predicted relationship where the 0 hpe expression was the most different from control and then the samples progressively returned to "normal" over time. Pathway analysis showed cell signaling pathways represented by the candidate genes that are critical for specific phases of regeneration, *e.g.* cell proliferation-related at 0 hpe and cell

differentiation-related at later time-points (bottom boxes). **B)** Pathway analysis of the candidate genes (identified at 0 hpe) involved inner ear hair cell regeneration highlighted the interactions between *stat3* and *socs3* (dashed circles) with other identified candidate genes. The known interactions (red: positive; green: negative; grey: unspecified) between the human orthologs of the candidate genes were extracted in batch to predict the candidate pathways involved in the hair cell regeneration. Different colors of the circles indicate those genes being up- (red) or down- (blue) regulated during hair cell regeneration.

3.4.9 Candidate genes encoding miRNAs

A total of 55,930 tag sequences were not associated with any Refseq or UniGene entry and mapped to only one location in the genome. Those tags were compared to the 127 zebrafish miRNAs (Release 15 from miRBase). From those miRNAs, we identified 12 candidate miRNAs (from eight clusters) whose expression level significantly changed during hair cell regeneration (Table 3.4). Most of those miRNA were down-regulated during regeneration, except for three: dre-mir-21-1, dre-mir-29a-1, and dre-mir-29b-3 with the latter two being in one cluster. qRT-PCR results further confirmed the up-regulation of dre-mir-21-1 (Figure 3.3A).

Table 3.4. Candidate genes encoding miRNAs

miRNA	Fold-change relative to control				Expressed in[a]	
	0 hpe	24 hpe	48 hpe	96 hpe	Ear	Neuromast
dre-let-7b	0.3	-[b]	-	-	N	N
dre-mir-133a-2	-	0.4	-	-	Y	Y
dre-mir-182 dre-mir-183 dre-mir-96	0.5	0.4	-	-	Y	Y
dre-mir-199-3	0.3	-	-	-	N	N
dre-mir-21-1	1.6	-	-	-	Y	N
dre-mir-23a-1	-	0.3	-	-	N	Y
dre-mir-24-4 dre-mir-27e	-	0.2	0.4	-	N	Y
dre-mir-29a-1 dre-mir-29b-3	3.7	-	-	-	N	N

a. Based on data from Wienholds et al. 2005.
b. Expression level not significantly different from control

3.5 Discussion

3.5.1 Deep profiling data generated by DGE

We generated one expression profile from control tissue and four expression profiles from regenerative tissues. Each of the five profiles contains approximately three million tags (Table 3.3). However, due to the nature of DGE and other SAGE-like techniques, the transcripts without a DpnII cutting site would be missing from the

profiles. The Illumina sequencing platform is not perfect as 6.8% of the unique tag sequences (944,347) contains one or more unidentified bases (marked as "N"s in Supplemental File 1). For quality control, tags detected only once in all five profiles were eliminated (Table 3.3) because they are more likely to result from rare DpnII cutting events (See Section 3.5.2), sequencing errors or other artifacts and would not, regardless of whether they were artifacts, impact the final analysis. In each profile, most of the tag (~85%) sequences fell into the category of low-abundance tag sequences (≤ 3 TPMs) while high-abundance tag sequences (>1,000 TPMs) were detected much less frequently (Figure 3.1). Similar abundance distribution has also been found in other DGE studies (Hegedűs et al., 2009).

3.5.2 Mapping of tag sequences to known/predicted transcripts and genome

Approximately 49% of the tag sequences were not mapped to any transcript or genome location (Figure 3.2A). The unmapped sequences were mostly composed of sequences from the low-abundance group (Figure 3.2B, bars with solid colors). There are several possible reasons for the existence of unmapped sequences, including sequencing errors, SNPs, unidentified splicing isoforms or RNA editing event, and gaps in genome sequences. It is not surprising that the overall mappability increased when one mismatch was allowed in the mapping (Figure 3.2B, bars with shaded colors) because it allowed a certain level of tolerance for SNPs and sequencing errors. The improvement was most prominent in the low-abundance group (Figure 3.2B), suggesting most of the unmapped sequences in this group were resulted from SNPs or sequencing errors.

Approximately17% of the tag sequences failed to be mapped to any known/predicted transcripts, but could be mapped to certain intergenic locations on the genome (Figure 3.2A). These tags may represent non-protein coding genes (e.g. miRNA, see Section 3.5.4) or novel genes, suggesting the potentials of using DGE for transcriptome annotation.

Sometimes a tag sequence could be mapped to multiple transcripts or multiple locations in the genome, which is considered a case of "ambiguous mapping" (Figure 3.2A). Tag sequences with unidentified bases are more likely to be mapped to multiple transcripts/genome locations. Moreover, the ambiguous mapping is more likely to happen in organisms like zebrafish due to a genomic duplication and significant stretches of repeated sequence. Ambiguous mapping was found in tag sequences of different abundances, but most frequently in the group of sequences with high abundance (Figure 3.2B), probably resulted from tags originated from the highly homogenous regions of different transcripts.

Theoretically all the tags should be generated from the 3'-most anchoring enzyme cutting site (DpnII in this study) in the transcripts. This is true in most cases in practice while sometimes tags are generated from other anchoring enzyme cutting sites due to internal priming and/or incomplete digestion with the anchoring enzyme (Asmann et al., 2009). Some of the studies only took the 3'-UTR sequences into account when mapping the tags (Taft et al., 2009). Such methods may cause biases because 1) some tags are found mostly originated from anchoring enzyme cutting sites other than the 3'-most ones in some transcripts (Asmann et al., 2009) and 2) the identification of 3'- boundary of the transcripts can be incorrect due to the lack of

well-curated full-length transcript sequences or the unidentified splicing isoforms. In this study, tags were found originated from DpnII cutting sites other than the 3'-most ones at a frequency that is not omittable (Figure 3.2C), so we only took unambiguously mapped tag sequences for further analysis regardless of whether they were originated from the 3'-most DpnII cutting sites. Leaving out all the ambiguously mapped tag sequences did result in a smaller amount of usable data. However, due to the depth of data generated by DGE, there were still as many as 80,604 unique tag sequences unambiguously mapped to one known/predicted transcript (Figure 3.2A). To get a more efficient use of the DGE data, certain algorithms developed for assigning ambiguously mapped SAGE tags to one transcript (Malig et al., 2006) can be used for further studies.

3.5.3 Capturing the biology of inner ear hair cell regeneration by gene expression profiling

One way to validate the gene expression profiling data is to see how well they correlate to the biological processes examined. By clustering analysis, we found the similarity between different expression profiles corresponded nicely with the morphological changes (see Chapter 2) observed during hair cell regeneration (Figure 3.4A). In addition, the pathway analysis showed enriched biological processes based on the expression profiles further confirmed such correspondence (Figure 3.4A). In line with that, the number of genes with significant changes in their expression levels was the highest at 0 hpe and gradually decreased during regeneration (Figure 3.3B).

It is known that similar regulatory mechanisms are shared by developmental and regenerative events in sensory epithelia of inner ears and the lateral line system (Ma

et al., 2008; Millimaki et al., 2007; Stone & Rubel, 1999; Woods et al., 2004). It is reasonable to predict that genes expressed during ear/lateral line development are more likely to play some roles during hair cell regeneration. Here we found an enrichment of genes known to be expressed in developing ears/lateral line system in the candidate genes identified based on their expression patterns during hair cell regeneration (Supplemental file 4), which serves as an indirect confirmation of the candidate genes with potential functions during hair cell regeneration.

3.5.4 Potential functions of miRNAs in hair cell regeneration

In addition to the protein-coding genes, comparison of the expression profiles also revealed the roles of miRNAs during hair cell regeneration. Most of the candidate miRNAs were down-regulated during regeneration (Table 3.4), suggesting an alleviation of inhibitory effects on their target genes, which corresponds nicely with the up-regulation in the majority of the protein-coding candidate genes.

miRNAs are expressed during inner ear and lateral line development in mammals (Weston, Pierce, Rocha-Sanchez, Beisel, & Soukup, 2006) and zebrafish (Friedman et al., 2009; Li, Kloosterman, & Fekete, 2010; Wienholds et al., 2005). Most of the candidate miRNAs were detected in the ear and/or lateral line neuromasts in developing zebrafish (Table 3.4 comparing with data from Wienholds et al., 2005). Moreover, disruption of mir-182/183/96 cluster expression during zebrafish development results in abnormalities in hair cell production in the inner ear (otic vesicle) and lateral line neuromasts (Li et al., 2010). Previous studies have identified the involvement of many miRNAs in a variety of regenerative processes and many of the candidate miRNAs (or their mammalian homologs) are included. For example,

dre-mir-133 is down-regulated and dre-mir-21 is up-regulated during fin regeneration in zebrafish (Yin et al., 2008), which is the same as their expression patterns detected in our experiments (Table 3.4). Over-expression of dre-mir-133 after fin amputations attenuates regeneration by reducing blastemal cell proliferation (Yin et al., 2008). In mouse, mir-21 is up-regulated during the proliferative phase of liver regeneration (Marquez, Wendlandt, Galle, Keck, & McCaffrey, 2010). In addition, let-7, mir-21, and mir-29 were suggested as translational regulators during liver regeneration (Kren et al., 2009). let-7 is a blocker of self-renewal in embryonic stem cells (Melton, Judson, & Blelloch, 2010). During hair cell regeneration, dre-let-7b was down-regulated at 0 hpe (Table 3.4), probably for unblocking cell division.

3.5.5 Potential issues in DGE application

3.5.5.1 Experimental design for DGE

In this DGE experiment, each profile was generated by pooling tissue samples from ~40 fish. While sample pooling is known to cause bias in the detection of changes in gene expression level (Hegedűs et al., 2009), it was unavoidable in this experiment due to the small size of the target tissue and the minimum total RNA required (2 µg) when the experiment was done in 2006. In addition, due to the relatively high cost of the DGE experiments in 2006, it was financially challenging to have multiple biological and/or technical replications. These difficulties in the early application of DGE will definitely have negative effects on the quantification and comparison of profiles. However, with the cost reduction of deep sequencing with NGS platforms and the improvement of tag preparation protocol and statistical analyses, these issues have been greatly alleviated. For future studies, more reliable

detection of changes in gene expression levels can be achieved by minimizing tissue pooling and performing biological and technical replications.

3.5.5.2 Sampling for DGE

The first issue with tissue preparation lies in the “contamination” from non-sensory epithelial tissues due to the technical difficulties of manual dissection. It is possible that the expression changes detected in certain genes was due to different severity of such “contamination” in different biological samples. Because of the high sensitivity of DGE acquired by deep sequencing, such contamination would result in skewed expression profiles in DGE experiments (Hegedűs et al., 2009) while it would probably not be picked up by other low-throughput techniques. It is possible to detect profiles with such “contamination” by comparing biological replications (Hegedűs et al., 2009). On the other hand, we can not rule out the possibility that non-sensory epithelial tissues in the saccule also directly or indirectly involved in hair cell regeneration.

It is note-worthy that noise exposure only killed a restricted region of hair cells in the saccular maculae (see Section 2.4). Even if only the saccular maculae had been used for profile generation and comparison, we would still be likely to detect changes in gene expression due to more “global” responses of the sensory epithelia induced by noise exposure, e.g. stress responses, in addition to the responses specifically induced by local hair cell death. It is unclear if those “global” responses are related to the hair cell regeneration, but any responses for the purpose of maintaining inner ear homeostasis would very likely be helpful in understanding hair cell regeneration.

There was a 48 hour time lag between the onset of noise exposure and the first sampling time-point (0 hpe). A certain amount of hair cell death definitely took place before 0 hpe because dead hair cell debris was detected by hair cell marker labeling at 0 hpe in the most severely damaged area. Meanwhile, supporting cells had started active cytoplasmic movements creating “scar formation” in response to the death of their neighboring hair cells (see Section 2.4.3). This suggests that the earliest responses triggered in the supporting cells by the first sign of hair cell death were likely missing from the transcriptional profiling results. These responses may be crucial for hair cell regeneration. In order to examine them, further studies are required that start sampling additional time-points between the onset and the ending of the noise exposure.

Chapter 4 Functional Studies of Stat3/Socs3 Signaling Pathway in Hair Cell Regeneration

4.1 Background review

4.1.1 Stat3

4.1.1.1 Stat3 protein

Signal transducer and activator of transcription 3 (stat3) is a member of a group of transcription factors that transduce signals from the cell membrane to the nucleus to regulate gene expression. It was first identified as a member of the gp130-mediated signaling pathway (Akira et al., 1994). Seven mammalian STATs have been identified: stat1-4, stat5a, 5b, and stat6 (Lim & Cao, 2006). Mammalian stat3 (as well as most other STATs) protein is composed of six domains: the N-terminal domain, the coiled-coil domain, the DNA binding domain, a linker, the SH2 domain, and the transcriptional activation domain (TAD). The N-terminal domain is involved in protein dimerization (Sasse et al., 1997). The coiled-coil domain is important for receptor-binding (Zhang, Kee, Seow, Fung, & Cao, 2000), nuclear import (Ma, Zhang, Novotny-Diermayr, Tan, & Cao, 2003), and nuclear export (Begitt, Meyer, van Rossum, & Vinkemeier, 2000). In addition, it also interacts with other proteins (Collum, Brutsaert, Lee, & Schindler, 2000; Lufei et al., 2003; Zhang, Wrzeszczynska, Horvath, & Darnell, 1999). The DNA binding domain recognizes and binds to the consensus binding sequences in the promoter: $TTCCN_2GAA$ (Kidder, Yang, & Palmer, 2008). It is also involved in binding to importins, which

mediate nuclear translocation of activated stat3 (Ma & Cao, 2006). The linker domain has been reported to be involved in the interaction between stat3 and GRIM-19 which negatively regulates stat3 activity (Lufei et al., 2003). The SH2 domain is the most conserved region in all of the STAT genes. It is essential for receptor binding (Stahl et al., 1995), stat3 activation (Heim, Kerr, Stark, & Darnell, 1995; Inoue, Minami, Matsumoto, Kishimoto, & Akira, 1997), and dimerization (Becker, Groner, & Muller, 1998; Shuai et al., 1994). The phosphorylation of a conserved tyrosine residue (Y705 in human STAT3) is considered as a requirement for stat3 activation in most cases studied. The TAD domain, on the other hand, is the least conserved region. In addition to activating transcription (Sasse et al., 1997), it also contains a conserved serine residue (S727 in human STAT3) and a conserved lysine residue (K685 in human STAT3). Phosphorylation of the serine residue can regulate stat3 activity (Decker & Kovarik, 2000) and acetylation of lysine residue is considered critical for stabilizing stat3 dimers (Yuan, Guan, Chatterjee, & Chin, 2005).

There are three isoforms of the STAT3 protein in humans, a result of alternative splicing. STAT3 isoform 1 (NP_644805) is the longest version of protein, consisting of 770 aa. STAT3 isoforms 2 (NP_003141) and 3 (NP_998827) lack amino acid residues in N-terminus and C-terminus respectively. Isoform 3 is of special interest to researchers because the truncation in the C-terminus results in no TAD in the protein. Some fragments of stat3 protein generated by proteolytic digestion have been found in different cell types with putative functions in transcription regulation (Darnowski et al., 2006; Hevehan, Miller, & Papoutsakis, 2002; Xia et al., 2001).

4.1.1.2 Stat3 activation

Stat3 is activated in response to various extracellular signaling molecules, including cytokines and growth factors. Interleukin 6 (IL-6) was the first one to be identified (Akira et al., 1994). Other cytokines include IL-5 (Stout, Bates, Liu, Farrington, & Bertics, 2004), 9-12 (Demoulin et al., 1996; Jacobson et al., 1995; Williams, Bradley, Smith, & Foxwell, 2004; Yanagisawa et al., 2000), 21 (Wei, Laurence, Elias, & O'Shea, 2007), 22 (Radaeva, Sun, Pan, Hong, & Gao, 2004), 27 (Lang, 2005), Interferon gamma (IFN-γ) (Kordula, Bugno, Goldstein, & Travis, 1995), Ciliary Neurotrophic Factor (CNTF) (Ji et al., 2004), Macrophage Inflammatory Protein 1 alpha (MIP-1α) (Wong & Fish, 1998), Regulated on Activation Normal T cell Expressed and presumably Secreted (RANTES) (Wong & Fish, 1998).

Growth factors that can activate stat3 include Epidermal Growth Factor (EGF) (Zhong, Wen, & Darnell, 1994), Granulocyte Colony-Stimiulating Factor (G-CSF) (Nishiki et al., 2004), Platelet-Derived Growth Factor (PDGF) (Vignais, Sadowski, Watling, Rogers, & Gilman, 1996), to name a few. In addition, some other factors have also been reported to trigger stat3 activation, e.g. UVB exposure (Ahsan, Aziz, & Ahmad, 2005) and osmotic shock (Gatsios et al., 1998). Once activated, stat3 forms dimers and translocates into the nucleus to execute the function of a transcription factor (Sadowski & Gilman, 1993; Wegenka, Buschmann, Lutticken, Heinrich, & Horn, 1993). The nuclear translocation is mediated by importins (Liu, McBride, & Reich, 2005; Ma & Cao, 2006; Ushijima et al., 2005). The downstream transcriptional targets of stat3 include cyclin D1 (ccd1) (Masuda et al., 2002), bcl-xl (Catlett-Falcone et al., 1999), bcl6 (Tsuyama et al., 2005), c-myc (Kiuchi et al.,

1999), survivin (Gritsko et al., 2006), miRNA-21 (Loffler et al., 2007), suppressors of cytokine signaling (SOCS) (Auernhammer, Bousquet, & Melmed, 1999; Naka et al., 1997; Xu, Sylvester, Tighe, Chen, & Gudas, 2008), as well as stat3 itself (Kidder et al., 2008).

4.1.1.3. Regulation of stat3 activity by phosphorylation

In most studies, stat3 is considered activated when the tyrosine residue in the SH2 domain is phosphorylated (Lim & Cao, 2006). The phosphorylation is mediated by receptor and non-receptor protein tyrosine kinases. Most of the kinases are the corresponding receptors or related kinases to the cytokines and growth factors mentioned above. Those kinases include Janus Kinases (JAKs) (Lütticken et al., 1994), EGF receptor (Garcia et al., 1997), PDGF receptor (Vignais & Gilman, 1999), Src (Yu et al., 1995), and so on.

In addition to the tyrosine residue, the serine residue in the TAD is also a target for phosphorylation in response to similar extracellular factors (Jain, Zhang, Kee, Li, & Cao, 1999; Wen, Zhong, & Darnell, 1995; Yokogami, Wakisaka, Avruch, & Reeves, 2000). In STATs, there is a highly conserved PMSP motif in the least conserved domain, TAD (Wen et al., 1995). The serine residue in the motif is phosphorylated by Mitogen Activated Protein Kinases (MAPKs) (Chung, Uchida, Grammer, & Blenis, 1997; Plaza-Menacho et al., 2007), p38 (Zauberman, Zipori, Krupsky, & Ben-Levy, 1999), mammalian target of rapamycin (mTOR) (Yokogami et al., 2000), and PKC isoforms (Gartsbein et al., 2006; Aziz et al., 2007) to name a few. However, the regulatory mechanism seems to be more complicated and context-dependent. For example, the phosphorylation of serine residue was not considered as

obligatory to stat3 activation but as an amplifier to the tyrosine phosphorylation for stat3 to achieve maximal transcriptional activity in COS-1 cells (Wen et al., 1995). However, a decrease in stat3 transcriptional activity was found later in the presence of serine phosphorylation in different cells, e.g. NIH3T3 (Jain, Zhang, Fong, Lim, & Cao, 1998). The different effects of serine phosphorylation are summarized by Decker & Kovarik (2000). The serine phosphorylation-mediated increase in stat3 transcriptional activity may be explained by the increase in DNA binding (Ng & Cantrell, 1997; Zhang, Blenis, Li, Schindler, & Chen-Kiang, 1995) and/or in nuclear translocation (Qin et al., 2008). There is no evidence of an enhancement in tyrosine phosphorylation resulted from serine phosphorylation so far. On the other hand, a decrease in tyrosine phosphorylation as a result of serine phosphorylation has been reported (Chung et al., 1997). However, the presence of serine phosphorylation doesn't seem to account for all cases of down-regulation in tyrosine phosphorylation: a decrease in tyrosine phosphorylation was also detected as independent of serine phosphorylation (Sengupta, Talbot, Scherle, & Ivashkiv, 1998). In addition, contrary to the previous idea of serine phosphorylation as an additive regulatory factor to tyrosine phosphorylation, the phosphorylated serine residue can activate stat3 activation independent of tyrosine phosphorylation (Kim, Yoon, & Chen, 2009; Lim & Cao, 2006; Ng & Cantrell, 1997; Qin et al., 2008). Meanwhile, constitutive activated stat3 is only phosphorylated at serine residue, but not at tyrosine residue in some cancer cells (Hazan-Halevy et al., 2010). Although the relationship between serine phosphorylation and tyrosine phosphorylation remains unclear, stat3 activated

by either residue share some common transcriptional targets, e.g. c-myc, survivin, and socs3. (Kim et al., 2009; Qin et al., 2008).

Phosphorylation of stat3 protein has been considered as a requirement for stat3 activation. However, several publications have claimed the activation of stat3 signaling without stat3 protein phosphorylation (Yang et al., 2005, 2007; Yang & Stark, 2008). It is note-worthy that most of the studies did not take into account the possibility of stat3 activation by serine phosphorylation, so whether those activated stat3 protein was really "unphosphorylated stat3 protein" remains questionable. In Drosophila, unphosphorylated stat92E binds to heterochromatin protein 1 (HP1) and stabilizes heterochromatin (Shi et al., 2008). Phosphorylation of stat92E by JAK causes dispersal of stat92E and HP1 from heterochromatin, resulting in deconstruction of the heterochromatin structure and facilitation of transcription (Shi et al., 2006, 2008). Intriguing as it is, such epigenetic function of unphosphorylated stat92E in Drosophila has not yet been detected in vertebrates.

The phosphorylation of stat3 protein is reversible. Tyrosine phosphorylation can be reversed by Protein Tyrosine Phosphatase Receptor D (PTPRD) (Veeriah et al., 2009) and T (PTPRT) (Zhang et al., 2007) in the cytoplasm and by T-cell Protein Tyrosine Phosphatase in the nucleus (Tc-PTP) (Tetsuya Yamamoto et al., 2002). Serine phosphorylation can be reversed by Protein Phosphatase 2A (PP2A) in the nucleus (Woetmann et al., 1999).

4.1.1.4 Regulation of stat3 activity by other mechanisms

In addition to phosphorylation, stat3 activity can also be regulated by acetylation. Yuan and colleagues (2005) first reported that the acetylation of a lysine residue in

the TAD domain (K685 in human STAT3) was critical for forming stable stat3 dimers. The acetylation of stat3 was mediated by histone acetyltransferase p300 and reversed by type I histone deacetylase (Yuan et al., 2005). In addition, CD44 could form a complex with stat3 and p300 to elicit the acetylation and nuclear translocation (Lee, Wang, & Chen, 2009).

The activity of stat3 can also be modulated by interacting with proteins other than kinases or phosphatases. For example, Protein Inhibitor of Activated STAT 3 (PIAS3) (Chung et al., 1997) and suppressors of cytokine signaling (SOCS, see below) negatively regulate stat3 activity.

STAT3 protein isoform 3 lacks the TAD due to alternative splicing. It is also activated by tyrosine phosphorylation (Caldenhoven et al., 1996). It was first considered as a negative regulator of STAT3 isoform 1 in COS cells (Caldenhoven et al., 1996). However, later studies show that STAT3 protein isoform 3 is capable of activating the transcription of some known stat3-target genes *in vivo* in the presence of IL-6 (Maritano et al., 2004).

4.1.1.5 Nuclear stat3 vs. cytoplasmic stat3

While stat3 activation sometimes requires the tyrosine phosphorylation of stat3 protein, the nuclear import of stat3 is independent of tyrosine phosphorylation and possibly independent of stat3 dimerization (Liu et al., 2005). Liu and colleagues (2005) transfected cells with DNA construct encoding mutated stat3 protein which could neither be phosphorylated at the tyrosine residue nor form dimers with mutated or endogenous STAT proteins and detected nuclear retention of the mutated stat3 protein. Whether such observation can be made in other cells remains unknown.

Nuclear import of stat3 is mediated by importin-α/β pathway, in which stat3 interacts with importin-α3 (Liu et al., 2005) and possibly other importin-α proteins (Ma & Cao, 2006; Ushijima et al., 2005). Nuclear export of stat3 is mediated by the interaction between the coiled-coil domain of stat3 and Chromosomal Region Maintenance 1 (CRM1) (Sato et al., 2005).

It has been taken for granted that stat3 can only function as a transcription factor in the nucleus. However, stat3 has been found in the mitochondria as a regulator of mitochondrial metabolism (Wegrzyn et al., 2009). Mutated stat3 protein that can not be imported into the nucleus is exclusively targeted to mitochondria and facilitates Ras-dependent malignant transformation (Gough et al., 2009). In addition, cytoplasmic stat3 also directly interacts with stathmin and Superior Cervical ganglia protein 10-LIke Protein (SCLIP) to adjust the microtubule stability and regulate cell morphology and cell migration (Ng, Lim, Lin, Zhang, & Cao, 2010; Ng et al., 2006; Verma et al., 2009).

4.1.1.6 Biological functions of stat3

Stat3 is known as a crucial gene in multiple biological processes, including mitogenesis, oncogenesis, metastasis, immune response, cell survival, cell differentiation, tissue repair, and pluripotency maintenance. Stat3-null mice are embryonically lethal at E6.5-7.5 (Takeda et al., 1997). Dominant-negative mutation in human STAT3 causes Hyper-IgE Syndrome (Minegishi et al., 2007). Hyper-activation of stat3 is responsible for oncogenesis, metastasis, and inflammation (Aggarwal et al., 2009). First identified as an Acute Phase Response Protein (APRP) (Akira et al., 1994), stat3 has been found to play an important role in the

inflammatory response mediated by various cytokines, e.g. IL-6 (Zhong et al., 1994) and IL-11 (Ernst et al., 2008). Stat3 is also involved in oncogenesis through its downstream targets, e.g. cyclin D1, which promote cell proliferation (Masuda et al., 2002). In addition, the interaction between stat3 and c-myc and pim-1 also contributes to the stat3-mediated enhancement of cell proliferation (Shirogane et al., 1999). The survival-promoting effects of stat3 is executed by a group of its down-stream targets, e.g. bcl-xl (Catlett-Falcone et al., 1999), bcl2 (Zushi et al., 1998), bcl6 (Tsuyama et al., 2005), survivin (Mahboubi et al., 2001), and Mcl-1 (Puthier et al., 1999), all of which encode anti-apoptotic proteins. Stat3 also mediates metastasis via transcriptional regulation of related genes, e.g. Matrix Metalloproteinases (MMPs) (Xie et al., 2004), MUC1 (Gaemers, Vos, Volders, Valk, & Hilkens, 2001), and COOH terminal tensin-like focal adhesion kinase (Cten) (Barbieri et al., 2010). In mouse embryonic stem cells (ESCs), stat3 binds to the promoter/enhancer region of multiple genes crucial for the maintenance of the stem cell state (Kidder et al., 2008).

4.1.1.7 Stat3 in non-mammalian animals

Homologs to mammalian stat3 have been found in vertebrates, e.g. zebrafish (Oates et al., 1999), frog (Nishinakamura et al., 1999), and chicken (Caldwell et al., 2004), and invertebrates, e.g. stat92E in Drosophila (Xie et al., 2004). In zebrafish, the stat3 gene is located on chromosome 3 (Oates et al., 1999). Two alternative splicing isoforms of stat3 have been reported in zebrafish, a longer version encoding 806 aa and a C-terminal truncated one encoding 720 aa (Oates et al., 1999). The amino acid sequence of the longer isoform shares 85% identity with STAT3 isoform 2 (STAT3-alpha) in human and the residues important for regulating stat3 activity are

conserved (Y708, S751, and K686 in zebrafish stat3). The shorter isoform seems lacking the TAD domain. In zebrafish, stat3 expression starts as early as the midblastula transition (MBT) stage (Oates et al., 1999). Knocking-down stat3 during early development disrupted the epithelial-mesenchymal transition (EMT) during gastrulation (Yamashita et al., 2002), in accordance with the known functions of stat3 in organogenesis, healing, and metastasis in mammals. The function of stat3 in the inner ear is barely studied in mammals except that it was detected in the nuclei of outer hair cells in the organ of Corti in neonatal mice (Hertzano et al., 2004). Stat3 expression is detected by *in situ* hybridization in the otic vesicle and lateral line neuromasts during zebrafish early development (Oates et al., 1999; Thisse & Thisse, 2004), while its function remains unclear.

4.1.2 Socs3

4.1.2.1 Socs3 protein

Suppressor of cytokine signaling 3 (socs3) was first identified as a STAT-induced-STAT inhibitor (Minamoto et al., 1997). It is a member of the SOCS family proteins, socs1-7 and cytokine inducible SH2-containing protein (cis), which suppress cytokine signaling via inhibiting the STAT/JAK pathway downstream of the cytokine receptors (Croker, Kiu, & Nicholson, 2008; Piessevaux, Lavens, Peelman, & Tavernier, 2008; Starr et al., 1997). All members in the family contain three domains: a central SH2 domain flanked by a variable N-terminal region and a conserved C-terminal SOCS box (Piessevaux et al., 2008). There is a kinase inhibitory region (KIR) in the N-terminal region of socs1 and socs3 that is responsible for binding to the tyrosine kinase domain in Jaks and thus blocking their kinase activity (Sasaki et

al., 1999). The SH2 domain is involved in binding to the phosphotyrosine motif of interacting proteins, e.g. Y1007 in JAK2 (Sasaki et al., 1999). In addition, two small regions in the N- and C-termini (N- and C-extended SH2 domain, N-ESS and C-ESS) are also important for stabilizing binding (Babon et al., 2006). The SOCS box binds to an E3 ubiquitin ligase complex, an E1 ubiquitin-activating enzyme, and an E2 ubiquitin-conjugating enzyme, which enables the poly-ubiquitination and degradation of SOCS proteins as well as their binding partners (Piessevaux et al., 2008).

4.1.2.2 Socs3 activity in cytokine signaling pathways

Socs3 is involved in the signaling pathways initiated by specific cytokines, including GCSF (Croker et al., 2004), IL-6 (Croker et al., 2003; Yasukawa et al., 2003), IL-23 (Chen et al., 2006), leptin (Mori et al., 2004), and Leukemia Inhibitory Factor (LIF) (Robb et al., 2005). Its SH2 domain shows only a weak affinity with Y1007 in JAK2 (Sasaki et al., 1999), but preferably binds to the phosphorylated tyrosine residue in receptor subunits, e.g. Y757 in gp130 (Nicholson et al., 2000). Surprisingly, the SH2 domain in socs3 can also bind to tyrosine phosphatase SHP2, suggesting multiple functions for the protein (De Souza et al., 2002). Socs3 can be transcriptionally activated by STATs, while it inhibits STAT/JAK signaling in a negative-feedback loop (Murray, 2007). It can also be epigenetically silenced by methylation of the CpG islands in its promoter (He et al., 2003). At post-translational level, socs3 activity can be regulated by phosphorylation of its tyrosine residues in the SOCS box (Y204 and Y221) in response to many cytokines and growth factors, e.g. IL-6 (Sommer et al., 2005) and insulin (Peraldi, Filloux, Emanuelli, Hilton, & Obberghen, 2001). The phosphorylated socs3 fails to interact with elongin C, which

destabilizes the socs3 protein (Haan et al., 2003). Meanwhile, phosphorylated socs3 inhibits p120, a Ras inhibitor, in favor of cell survival and proliferation mediated by the Ras-MAPK pathway (Cacalano, Sanden, & Johnston, 2001). In addition to tyrosine phosphorylation, the unstructured PEST sequence in C-ESS also contributes to the turnover of socs3 (Sasaki et al., 1999).

4.1.2.3 Biological functions of socs3

Similar to stat3, socs3 is also involved in multiple biological processes. It modulates a variety of processes by dampening cytokine-induced STAT/JAK-dependent responses in cells (Croker et al., 2008). The Socs3-null mouse is embryonically lethal possibly due to excessive erythropoiesis (Marine et al., 1999) or abnormal placenta development (Roberts et al., 2001). As a key negative regulator of cytokine-induced signaling, it controls the intensity and duration of immune responses. When socs3 is conditionally knocked out in hematopoietic and endothelial cells in mouse, the animal dies young due to severe inflammatory lesions (Croker et al., 2004). Elevated level of socs3 is associated with human inflammatory diseases, e.g. atopic dermatitis (Ekelund et al., 2006) and rheumatoid arthritis (Shouda et al., 2001). Hyper-silencing of socs3 by methylation and the accompanying hyper-activation of STAT/JAK signaling have been found in a variety of tumor cells and considered as one of the explanations for the abnormal proliferation of those cells (He et al., 2003; Martini et al., 2008).

4.1.2.4 Socs3 in zebrafish

The zebrafish homologs to mammalian socs3 are socs3a and socs3b, sharing 55% and 59% identity respectively with human SOCS3 protein and 67% identity with

each other. According to a very limited number of publications, socs3a/b was found playing a similar role in zebrafish as in mammals: a negative regulator of cytokine-induced STAT/JAK signaling (Studzinski, Almeida, Lanes, Figueiredo, & Marins, 2009; Yamashita et al., 2004).

4.1.3. Stat3 and socs3 in regeneration

Both stat3 and socs3 contribute to the regenerative process in many organs, either working with each other or with other proteins involved in STAT/JAK signaling pathways.

4.1.3.1 Stat3 and socs3 in liver regeneration

In liver, stat3 is rapidly activated after hepatectomy (Salazar-Montes, Ruiz-Corro, Sandoval-Rodriguez, Lopez-Reyes, & Armendariz-Borunda, 2006; Taub, Greenbaum, & Peng, 1999). In addition, liver-specific knockout of stat3 impaired hepatocyte mitogenic events and disrupted liver regeneration severely (Li, Liang, Kellendonk, Poli, & Taub, 2002). Originally, the studies on stat3 function in liver regeneration focused on the IL-6-induced gp130-mediated activation of stat3 because IL-6 is a well-known activator of stat3 signaling (Akira et al., 1994). IL-$6^{-/-}$ mice showed disrupted liver regeneration and lack of stat3 activation (Cressman et al., 1996). In addition, after hepatectomy, mice with liver-specific knockout of stat3 showed abnormal immediate-early gene (IEG) activation largely correlated with similar abnormalities observed in IL-$6^{-/-}$ mice (Li et al., 2002). Socs3 has been identified as a negative regulator of IL-6-induced stat3 signaling in undamaged liver (Croker et al., 2003). IL-6 signaling during liver regeneration induced rapid up-regulation of socs3, which correlated with the subsequent down-regulation of

phosphorylated stat3 and therefore terminated IL-6 signaling (Campbell et al., 2001). Hepatocyte-specific knockout of socs3 led to an increase in DNA synthesis and cell cycle progression and thus accelerated liver regeneration in mice, which was accompanied by an enhancement in IL-6/stat3 signaling (Riehle et al., 2008). Meanwhile, keeping the cytokine signaling tempered by the negative feedback of socs3 on stat3 signaling is crucial for liver regeneration (Taub, 2004). This idea is further supported by the observation that over-expression of IL-6 inhibited regeneration after hepatectomy in mice (Wüstefeld, Rakemann, Kubicka, Manns, & Trautwein, 2000). In addition to IL-6, other cytokines also play a role in liver regeneration, which is through stat3 and modulated by socs3 as well. For example, IL-22 promotes liver cell regeneration by increasing hepatic cell proliferation and hepatocyte migration through the activation of Akt and STAT signaling, which is abrogated by SOCS-1/3 over-expression (Brand et al., 2007).

It is worth noting that the conditional knockout of gp130 in mice severely impaired early activation of stat3 but not DNA synthesis after partial hepatectomy (Wüstefeld et al., 2003). In contrast, mice with the conditional knockout of stat3 showed severe deficits in DNA synthesis in liver regeneration (Li et al., 2002), indicating another IL-6/gp130-independent mechanism for late stat3 activation to initiate DNA synthesis. Two growth factors, EGF (mediated by EGFR) and hepatocyte growth factor (HGF, mediated by met) have been proposed to induce stat3 activation during liver regeneration (Seki et al., 2008) because they have been shown to induce stat3 signaling in liver cells (Ruff-Jamison et al., 1994; Schaper et al., 1997). While a conditional knockout of either met (Borowiak et al., 2004) or EGFR

(Natarajan, Wagner, & Sibilia, 2007) was adequate to disrupt DNA synthesis and cell cycle progression after hepatectomy, stat3 activation after hepatectomy was not affected in the EGFR knockout (Natarajan et al., 2007) and was even prolonged in the met knockout (Borowiak et al., 2004). Although both EGF and HGF were able to induce stat3 activation in hepatocytes (Seki et al., 2008), it still remains unclear if either of them is responsible for stat3 activation during liver regeneration. Interestingly, IL-6 level remains correlated to stat3 activity in both conditional knockout studies (Borowiak et al., 2004; Natarajan et al., 2007), suggesting a closer link between IL-6 and stat3 activity and a possible compensatory effect of IL-6/stat3 to HGF/met signaling in liver regeneration.

4.1.3.2 Stat3 and socs3 in neuronal regeneration

Stat3 and socs3 are involved in neuronal regenerative processes. In spinal cord, stat3 activation was found immediately after compression (Yamauchi et al., 2006). Conditional knockout of stat3 in astrocytes resulted in a decrease in astrocyte migration and more severe motor deficits after spinal cord injury, while up-regulation of stat3 signaling by conditional knockout of socs3 had the opposite effects (Okada et al., 2006). Axon injury also leads to stat3 activation (Lee, Neitzel, Devlin, & MacLennan, 2004) and socs3 expression (Miao et al., 2006). In retinal ganglion neurons (RGN), CNTF-induced activation of stat3 signaling promotes axon regeneration (Müller, Hauk, Leibinger, Marienfeld, & Fischer, 2009; Park, Luo, Hisheh, Harvey, & Cui, 2004). Accordingly, conditional knockout of socs3 or gp130 in RGN promoted the axon regeneration (Smith et al., 2009). Similar observations have also been found in sensory neurons and motoneurons (Lee et al., 2004; Qiu,

Cafferty, McMahon, & Thompson, 2005; Toth et al., 2008). CNTF-induced activation of stat3 signaling also promoted the regeneration of photoreceptors in retina (Kassen et al., 2009).

4.1.3.3 Stat3 and socs3 in skin regeneration

Stat3 and socs3 are involved in epithelial cell regeneration in skin and other inner organs (e.g. lung (Kida et al., 2008) and intestine (Pickert et al., 2009)). The skin regeneration after wounding requires the migration, proliferation, and differentiation of keratinocytes (Sano, Chan, & DiGiovanni, 2008). Stat3 activation was detected at the wound edge in mouse skin (Sano et al., 2008). Mice with keratinocyte-specific knockout of stat3 showed delayed wound healing as a result of the failure in keratinocyte migration instead of the failure in keratinocyte proliferation (Sano et al., 1999). The stat3 signaling in keratinocyte migration was induced by growth factors and cytokines (EGF, transforming growth factor-α, heparin-binding EGF-like factor, HGF, and IL-6 (Tarnawski & Jones, 1998; Tokumaru, Sayama, Shirakata, et al., 2005; Tokumaru, Sayama, Yamasaki, et al., 2005). One of the effectors of stat3 signaling is p130cas which regulates the cell adhesiveness and thus migration ability (Kira et al., 2002). Socs3 was also found to be induced during acute wound inflammation (Goren, Linke, Muller, Pfeilschifter, & Frank, 2005). gp130-stat3 signaling was up-regulated in the wound healing in socs3-deficient mice, accompanied by a surprisingly impaired healing process (Zhu et al., 2008). Hyperactivation of gp130-stat3 signaling by depressing socs3 activity resulted in hyperproliferating keratinocytes, which secreted cytokines and chemokines to prolong the immune response and delay the healing process (Zhu et al., 2008). Both

hypo- and hyper-activation of stat3 signaling pathway result in impaired wound healing in skin, suggesting a critical balance needed to be achieved, at least in part by the negative feedback from socs3, for normal wound healing.

4.1.3.4 Stat3 and socs3 in regeneration in non-mammals

The importance of stat3 and socs3 in regeneration has also been found in nonmammalian vertebrates and invertebrates. Stat3 expression was found to be up-regulated in dividing cells during zebrafish retinal photoreceptor regeneration (Kassen et al., 2009). Stat92E, the Drosophila homolog to vertebrate stat3, was required in the epithelial stem cells of the midgut after cell damage caused by bacteria (Jiang et al., 2009). Socs3 was found to be required for epithelial wound healing in Xenopus embryos (Kuliyev, Doherty, & Mead, 2005). It is also found to be up-regulated in the regeneration of fins (Schebesta, Lien, Engel, & Keating, 2006) and retinas (Qin, Barthel, & Raymond, 2009) of zebrafish.

4.1.4. Background summary

As a transcription factor, stat3 remains latent in the cytoplasm until cytokine/growth factor-induced and kinase-mediated activation. The activity of stat3 is regulated through multiple complicated mechanisms in a context-dependent manner. One way to negatively regulate stat3 activity is through SOCS proteins, one of which is socs3. Stat3 can activate the transcription of socs3 gene, the protein product of which inhibits stat3 activity and completes a negative feedback loop between stat3 and socs3. Both stat3 and socs3 play important roles in development, tumorigenesis, immune responses, as well as regeneration. Here their functions in the regeneration of liver, nervous system, and skin are reviewed in detail. In addition to

regeneration, stat3 also has protective functions in injured liver (Taub, 2004) and in the nervous system (Dziennis & Alkayed, 2008). For example, stat3 signaling induced by IL-6 can protect hepatocytes in injured liver by up-regulating genes with anti-apoptotic functions as well as those with antioxidant functions (Haga et al., 2003).

Although stat3 activation is required for a variety of regenerative processes, hyperactivation of stat3, either by over-expressing IL-6 (Wüstefeld et al., 2000) or by depressing socs3 (Zhu et al., 2008), hampers normal regeneration. Because hyperactivation of stat3 and/or silencing of socs3 contribute to both inflammation (Gao & Ward, 2007; Zhu et al., 2008) and tumorigenesis (Baltayiannis, Baltayiannis, & Tsianos, 2008; Yu et al., 2009), the proper functioning of the self-regulating stat3/socs3 pathway seems crucial for a well-controlled regeneration in various organs.

4.2 Experiment overview

Stat3 and socs3 were found transcriptionally up-regulated during inner ear hair cell regeneration in adult zebrafish (Supplemental file 3). It is known that stat3 and socs3 form a self-restrictive feedback loop which plays an important role in a variety of regenerative processes (See Section 4.1.3), so we tested if the stat3/socs3 pathway was involved in hair cell regeneration in zebrafish.

Instead of determining the role of the stat3/socs3 pathway in inner ear hair cell regeneration, we performed functional studies in the lateral line system, another mechanosensory structure in zebrafish highly similar to the inner ear sensory epithelia and used for detecting water movements over the body (McHenry et al., 2009;

Montgomery et al., 2000). The neuromasts in the lateral line are composed of hair cells and supporting cells similar to those in the inner ear sensory epithelium (Nicolson, 2005). In addition, the hair cell regeneration in the lateral line neuromasts shares similar molecular mechanisms with that in the inner ear (Behra et al., 2009; Harris et al., 2003; Ma et al., 2008), Rubel, and Raible. Last but not least, the neuromasts are located on the surface of the fish body, making them a convenient system for testing the functions of candidate genes involved in hair cell regeneration.

My results suggest that stat3/socs3 signaling is triggered during hair cell regeneration in the lateral line neuromasts. Pharmacological up-regulation of stat3 signaling accelerates hair cell regeneration by promoting supporting cell division. In addition, stat3 also seems to be involved in development and stem cell maintenance of the neuromasts.

4.3 Materials and methods

4.3.1 Quantification of hair cell numbers and mitotic events and characterization of stat3's involvement during lateral line hair cell regeneration

Five days post fertilization (dpf)-old zebrafish larvae were treated with $CuSO_4$ (10 µM in system water) for 2 h to kill the lateral line hair cells as previously described (Hernández et al., 2007). The larvae were then kept at 28.5 ºC up to 72 h post $CuSO_4$ treatment (hpt). For hair cell quantification, the Tg(pou4f3:GFP) larvae (Xiao et al., 2005) were raised in Holtfreter's buffer containing S3I-201 (EMD Biosciences, 40 µL stock in DMSO/10 mL buffer, final concentration = 400 µM) or DMSO (Sigma, 40 µL/10 mL buffer). Lateral line hair cells (GFP-positive cells) in

living larvae were quantified at 24, 48, and 72 hpt using an inverted epifluorescence microscope (Axiovert200M from Zeiss). In addition, myosin VI antibody staining was also used as an alternative for hair cell quantification. The mitotic events during lateral line hair cell regeneration were quantified by Bromo-deoxyuridine (BrdU) incorporation assays (Ma et al., 2008) using Tg(scm1:GFP) larvae (Behra et al., 2009). BrdU was dissolved in DMSO and added to Holtfreter's buffer to achieve a final concentration of 10 mM. In addition, Tg(scm1:GFP) larvae (Behra et al., 2009) were also collected at different time-points for immunohistochemical staining to examine the involvement of stat3 during hair cell regeneration.

4.3.2 Whole-mount *in situ* hybridization

Fragments of the target cDNAs were amplified with PCR primers containing T7 or T3 promoter in their 5'-ends. All primers are listed in Table 4.1. The anti-sense RNA probes were synthesized with DIG RNA labeling kit (Roche) according to manufacturer's instructions. Whole-mount *in situ* hybridization of zebrafish embryos was done as previously described (Oxtoby & Jowett, 1993) with modification. Instead of using 1-phenyl-2-thiourea (PTU) to prevent pigmentation in living embryos, H_2O_2 (10%) was used to bleach pigments after rehydration of the fixed embryos. The hybridization temperature was 60 ºC.

Table 4.1. Sequences of primers and morpholinos

Experiment	Target gene	Sequence
qRT-PCR	atoh1a	F: 5'-GCG AAG AAT GCA CGG ATT GAA CCA-3'
		R: 5'-TGC AGG GTT TCG TAC TTG GAG AGT-3'
	bactin1	F: 5'-GAC CCA GAC ATC AGG GAG TGA TGG-3'
		R: 5'-AGG TGT GAT GCC AGA TCT TCT CCA TG-3'
	bcl6	F: 5'-TGT TCT GCT CAA CCT GAA CCG ACT-3'
		R: 5'-TAG AAG AGC CCA CTG CAT GCC ATA-3'
	mmp2	F: 5'-GCT GGT GTG CAA CCA CTG AAG ATT-3'
		R: 5'-AAG ACA CAG GGT GCT CCA TCT GAA-3'
	mmp9	F: 5'-AAA TCG AGA AGC TCG GCC TAC CAA-3'
		R: 5'- TCC TCT GTC AAT CAG CTG AGC CTT-3'
	socs3a	F: 5'-TAA AGC AGG GAA GAC AAG AGC CGA-3'
		R: 5'-TGG AGA AAC AGT GAG AGA GCT GGT-3'
	stat3	F: 5'-AGT GAA AGC AGC AAA GAG GGA GGA-3'
		R: 5'-TGA GCT GCT GCT TAG TGT ACG GTT-3'
***In situ* hybridization probe synthesis**[a]	stat3	F: 5'-ATT AAC CCT CAC TAA AGG GAT ACT GGA ACA CAA CCT GCA GGA CA-3'
		R: 5'-TAA TAC GAC TCA CTA TAG GGA GAT CGA CCC ACG TGA ATG TGA TTC CT-3'
	socs3a	F: 5'-ATT AAC CCT CAC TAA AGG GAA AGA CTG TGA ACG GAC ACA CGG AT-3'
		R: 5'-TAA TAC GAC TCA CTA TAG GGA GAA GTG TCT GGC ATG AGA AGG CTG AA-3'
Morpholino	socs3a[b]	MO1: CCCTGAGCTGCCGGGAAGCAGATCT
		MO2: CGTGTAATATACAGAGTGTCGAGTC
	stat3[c]	MO1: GCCATGTTGACCCCTTAATGTGTCG

a. Underlined sequences are T3 (F) and T7 (R) promoters.
b. Both morpholinos gave rise to similar phenotypes. Results reported here are from embryos injected with MO1.
c. Stat3 MO sequence was synthesized according to Yamashita et al. (2002).

4.3.3 Morpholino and mature mRNA injection

The morpholino (MO) injections were done in fertilized eggs of TAB-5 (Amsterdam et al., 1999) and Tg(cldnb:GFP) (Haas & Gilmour, 2006) lines. MOs against stat3 and socs3a were injected at a concentration of 500 µM. The mature mRNA of socs3a was synthesized with a mMESSAGE mMACHINE kit (Ambion) and injected at a concentration of 37.8 ng/µL. Control injections were done with PBS

solution containing traces amounts of phenol red (Sigma). The sequences of all MOs are listed in Table 4.1.

4.3.4 Immunohistochemistry

The primary and secondary antibodies used included rabbit myosin VI antibody (Proteus biosciences, 1:200-dilution), mouse anti-BrdU with Alexa Fluor 546 conjugates (Invitrogen, 1:200-dilution), goat GFP antibody (FITC-conjugated, Abcam, 1:200-dilution), rabbit $STAT3^{pS727}$ (Abcam, 1:50-dilution) and Alexa Fluor 568 (or 488) goat anti-rabbit IgG (Invitrogen, 1:1,000-dilution). Other common reagents included PTWD (1X PBS, 0.1% Tween-20 (Sigma), and 1% DMSO), blocking buffer (10 mg/mL bovine serum albumin (Sigma) and 10% goat serum (Vector laboratories) in PTWD), and staining buffer (1:5-dilution of blocking buffer in PTWD).

Zebrafish embryos/larvae were anesthetized with 0.03% buffered MS-222 and fixed with 4% paraformaldehyde (Electron Microscopy Sciences) at 4°C overnight or at room temperature for 2 h. The fixed embryos were rinsed with PTWD for 3 times, 10 min each time before different pretreatments according to the primary antibodies used. For myosin VI antibody staining, the embryos were incubated with distilled water for 1-3 h followed by acetone treatment (7 min at room temperature 5 dpf or younger embryos/larvae and 20 min at -20 ºC for 5 dpf+ larvae) and several rinses (1 rinse with distilled water for 5 min and another 2 rinses with PTWD, 10min each time). For $STAT3^{pS727}$ antibody, embryos were rinsed in distilled water for 5 min after acetone treatment and then incubated with 100% methanol over night. The rest steps of the pretreatment was the same as anti-BrdU staining (Ma et al., 2008), except

for skipping the proteinase K digestion. After pretreatment, the embryos were incubated first in blocking buffer at 4°C overnight or at room temperature for 4-6 h and then in primary antibody diluted in staining buffer at 4°C overnight. After incubation, the embryos were rinsed with PTWD for 3 times (10 min each time), followed by another round of blocking, secondary antibody incubation, and rinsing. The staining for detecting BrdU incorporation was done as previously described (Ma et al., 2008) with different antibodies: mouse anti-BrdU with Alexa Fluor 546 conjugate and goat GFP antibody. DAPI (Invitrogen, 50 pg/mL) was used for counter-staining the nuclei in the embryos. Stained embryos were stored in glycerol (50% in 1X PBS) at 4°C before viewing. If needed, the embryos were mounted onto slides with Aqua Poly/Mount (Polysciences).

4.3.5 Microscopy and image analysis

The antibody staining results of embryos/larvae were visualized using an AxiovertNLO confocal microscope (Zeiss) with Carl Zeiss AIM software (Zeiss). The *in situ* hybridization results were captured under the Stemi SV 11 microscope (Zeiss) with Openlab software (Improvision). The imaging in the living larvae was done using an epitflurescence microscope Axiovert200M (Zeiss).

4.3.6 Cell culture and chemical administration

The zebrafish cell line Pac2 were maintained in as previously described (Lin et al., 1994). Before treated with S3I-201, Pac2 cells were plated in culture dishes coated with poly-L-lysine (Sigma) and cultured overnight to reach approximately 40% confluence. The cells were treated with S3I-201 (5 µL stock/10 mL media, final

concentration = 50 µM) or DMSO (5 µL/10 mL media) for 2 h at 32ºC before they were collected for total RNA extraction.

4.3.7 RNA extraction and qRT-PCR

Total RNA was extracted from embryos and cultured cells as described in Section 3.3.1 with additional cleanup steps using RNeasy Minelute Cleanup kit (Qiagene) according to the manufacturer's instructions. qRT-PCRs with the extracted RNA were performed as described in Section 3.3.5.

4.3.8 Statistical analysis

Student's t-test was used to compare data from experimental groups and control groups. The calculations were done using Excel software (Microsoft).

4.4 Results

4.4.1 Stat3 and socs3a expression in the lateral line neuromasts of zebrafish larvae

According to a previous publication, stat3 expression has been detected in the lateral line neuromasts by *in situ* hybridization (Thisse & Thisse, 2004). At 5 dpf, stat3 expresses in a "donut" pattern in the neuromast, reminiscent of the localization of the supporting cells (Thisse & Thisse, 2004). My *in situ* hybridization results also showed the expression of socs3a in the neuromasts in 5-dpf larvae (Figure 4.1). Socs3a seemed only expressed in a subgroup of hair cells and/or supporting cells rather than unanimously in all cells in the neuromasts (Figure 4.1, close-up).

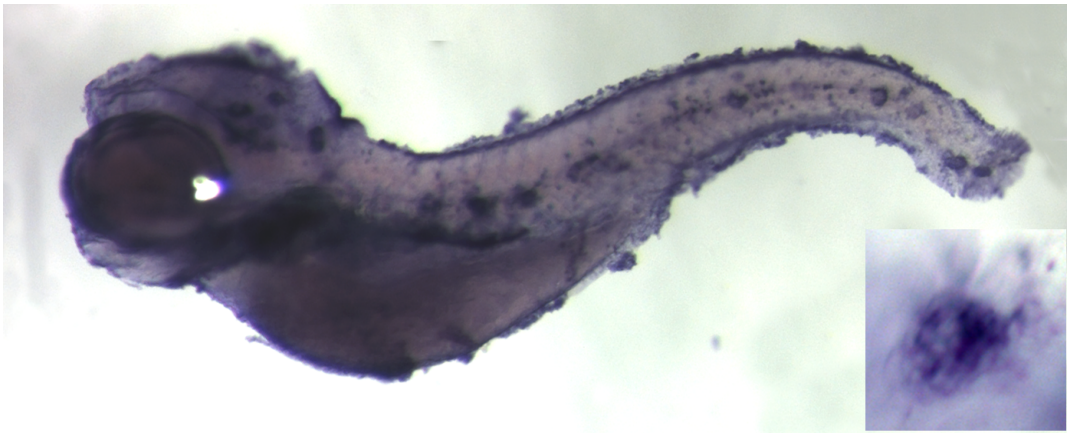

Figure 4.1. Socs3a expresses in the lateral line neuromasts in zebrafish larvae. Socs3a expression was detected in anterior and posterior lateral line neuromasts in 5-dpf larvae by *in situ* hybridization (a close-up of one neuromast in bottom right corner). D: dorsal, A: anterior, dpf: days post fertilization.

4.4.2 The self-restrictive regulation between stat3 and socs3a in zebrafish embryos

Both stat3 (Mid-Blastula Transition (Oates et al., 1999)) and socs3a (20 hpf) express very early during zebrafish embryo development, so we used morpholino (MO) injection to knock down the expression of stat3 or socs3a during the early development of zebrafish embryos to determine if reduced expression in one of the two genes has an effect on the other. We found a significant decrease in stat3 and socs3a mRNAs in stat3 morphants, while a significant increase in stat3 and socs3a mRNAs in socs3a morphants (Table 4.2) consistent with the negative feedback loop experimentally determined in other systems.

4.4.3 Disruption of stat3/socs3a signaling during zebrafish development

The genes/pathways involved in hair cell production during development often overlap with those used in hair cell regeneration (Cafaro et al., 2007; Ma et al., 2008; Millimaki et al., 2007; Stone & Rubel, 1999; Woods et al., 2004), so studying the function of stat3/socs3 signaling pathway in inner ear/neuromast development will not only reveal its function, if exists, in hair cell production during development, but also indirectly confirm its functions in hair cell regeneration. When we reduced either stat3 or socs3a expression with MOs, we observed deficits in lateral line neuromast development: the morphants exhibited fewer neuromasts and smaller numbers of hair cells per neuromast (Figure 4.2A; $p < 0.01$ in both cases). In order to examine the role of stat3/socs3 signaling in hair cell differentiation, we measured the mRNA level of atonal homolog 1a (atoh1a) in stat3 and socs3a morphants. Atoh1a is the zebrafish homolog of atoh1, which is an essential gene required for hair cell fate commitment (Bermingham et al., 1999; Millimaki et al., 2007; Woods et al., 2004). Both knocking-down of stat3 and over-expression of socs3a resulted in a reduction in atoh1a mRNA level (Table 4.2). In contrast, a strong increase in atoh1a mRNA level was observed in socs3a morphants where stat3 was presumably hyper-activated (Table 4.2). In addition, the cross-talk between stat3/socs3 and atoh1 was further confirmed by *in situ* hybridization of the socs3a morphants (Figure 4.2B).

Table 4.2. Summary of qRT-PCR results in morpholino- and mRNA-injected embryos

	Target gene		
	Atoh1a	**Stat3**	**Socs3a**
Socs3a MO (36 hpf [a])	1.35 (9.91e-3)[b]	1.76 (0.0284)	8.37 (0.0324)
Socs3a mRNA (12 hpf)	0.615 (2.70e-3)	0.720 (0.0235)[c]	-
Stat3 MO (32 hpf)	0.547 (0.0105)	0.294 (1.77e-4)	0.600 (0.041)

a. hpf: hour post fertilization
b. Fold change (p value)
c. Data collected from 6-hpf embryos

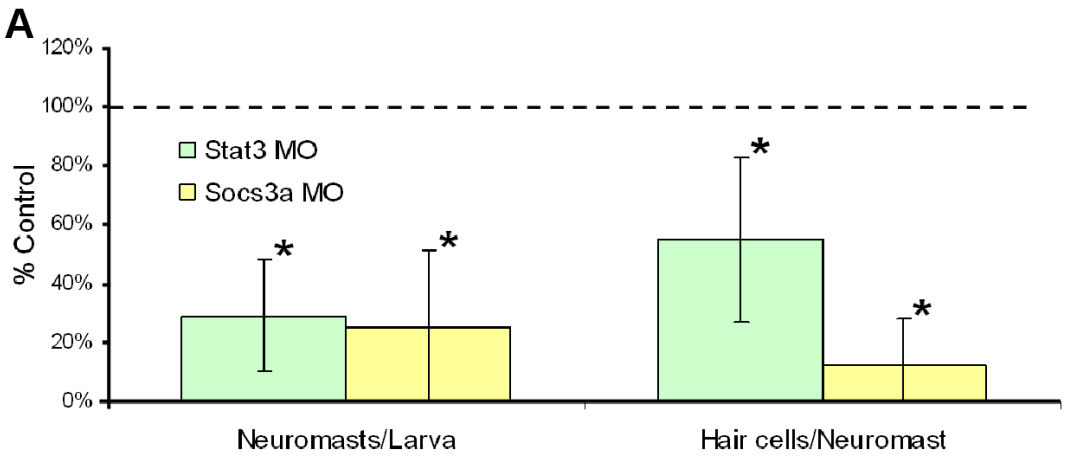

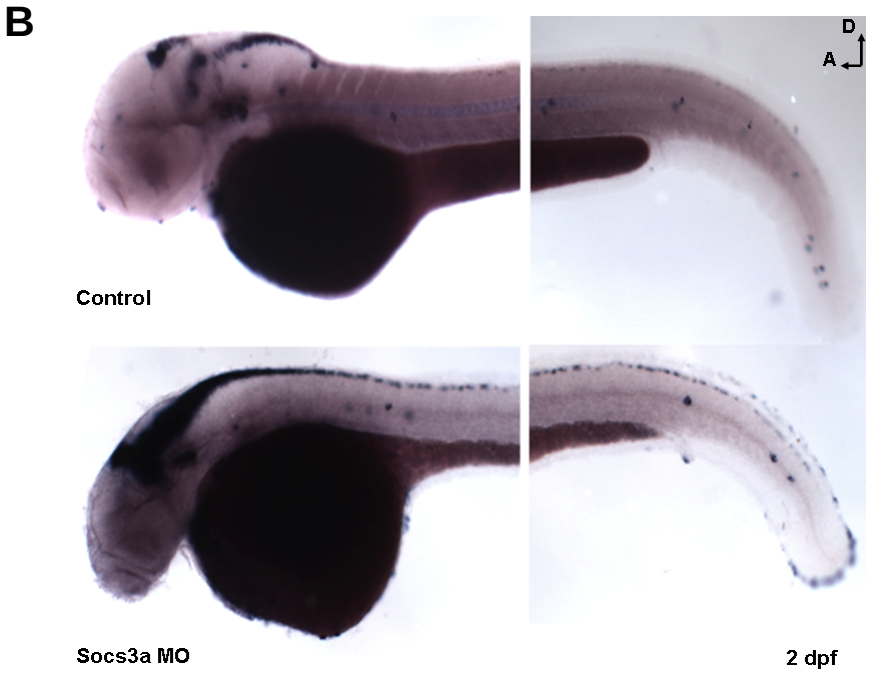

Figure 4.2. Socs3a and stat3 knock-downs disrupted hair cell production in lateral line neuromasts as well as the expression of atoh1a during zebrafish development. A) Both stat3 and socs3a morphants possessed fewer posterior lateral line neuromasts (left, n = 10 in all groups, one-tail t-test, *$p < 0.01$) with a smaller number of hair cells per neuromast (right, one-tail t-test, *$p < 0.01$) compared to control larvae at 2.5 dpf (days post fertilization). **B)** In addition, in socs3a morphants, an expansion of atoh1a expression was detected by *in situ* hybridization in both the brain and the lateral line. MO: morpholino, D: dorsal, A: anterior.

In addition to the lateral line neuromasts, stat3 was also found expressed in the anterior region of the otic vesicle by *in situ* hybridization from around 24 hpf (Oates et al., 1999), while no socs3a expression was detected in the otic area by *in situ* hybridization in this study (24 hpf to 5 dpf). Correspondingly, stat3-morphants often had otic vesicles missing the anterior otolith (Figure 4.3A-H), while socs3a morphants showed no gross defect in the otic vesicles. The missing otolith either never appeared (in most cases up to 3 dpf), or occasionally appeared later in a reduced size. Using the hair cell marker, myosin VI, we found that the morphants showed a significant decrease in the number of hair cells in the anterior macula but not in the posterior macula at 32 hpf (Figure 4.3I and J).

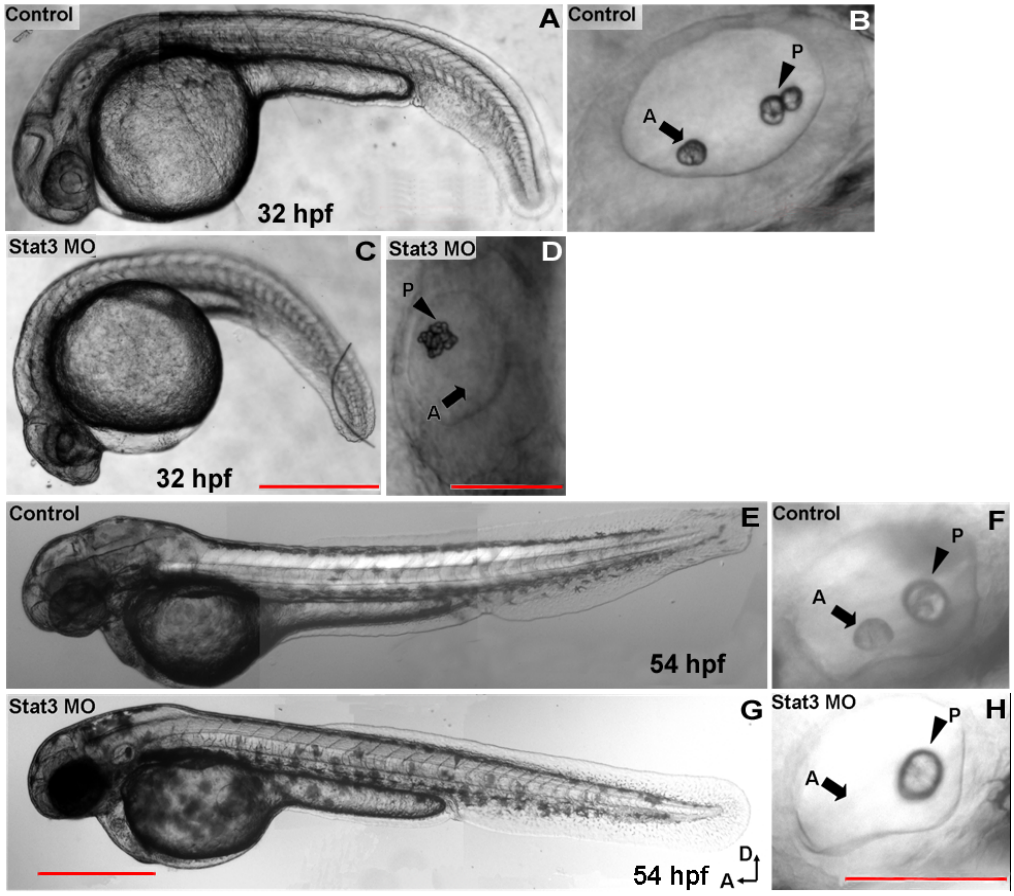
Control
A
32 hpf
Control
B
P
A
Stat3 MO
C
32 hpf
Stat3 MO
D
P
A
Control
E
54 hpf
Control
F
P
A
Stat3 MO
G
54 hpf
D
A
Stat3 MO
H
P
A

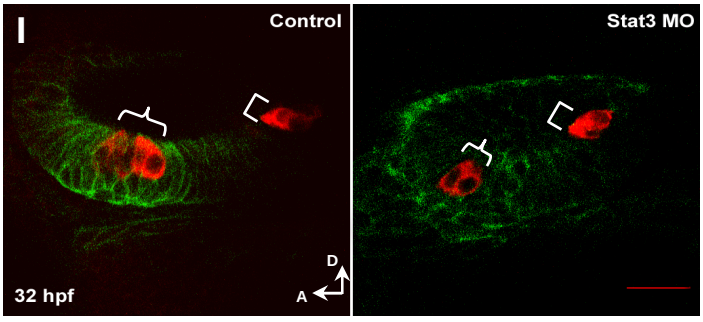
I
Control
Stat3 MO
32 hpf
D
A

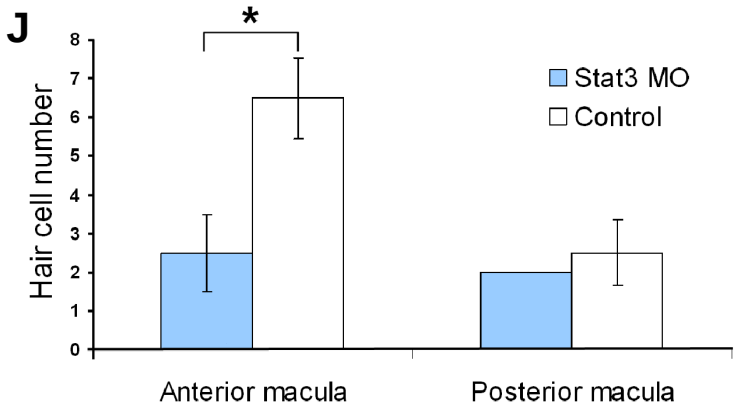
J
*
Hair cell number
0
1
2
3
4
5
6
7
8
Stat3 MO
Control
Anterior macula
Posterior macula

Figure 4.3. Stat3 knock-down resulted in abnormal development of the otic vesicles in zebrafish embryos. A)-H) Stat3 morphants showed deficiencies in otic vesicle development, typically completely missing the anterior otolith but leaving the posterior otolith spared. Arrows (A): anterior otolith; arrow heads (P): posterior otolith. Left scale bar = 500 µm; right scale bar = 100 µm. **I)** Accordingly, anti-myosin VI antibody staining (red) showed a reduction in the number of hair cells in the anterior macula (brace) but not in the posterior macula (bracket) at 32 hpf. GFP (green) labeling the outline of cells in otic vesicle in Tg(cldnb:GFP) embryos. Scale bar = 20 µm. **J)** The reduction in hair cell number is statistically significant (n = 6 (morphants) and 4 (control), one-tail t-test, *p < 0.01). MO: morpholino, D: dorsal, A: anterior, hpf: hour post fertilization.

4.4.4 pS-stat3 activity in developing neuromasts

Phosphorylation of S727 regulates human STAT3 activity (Decker & Kovarik, 2000). Because the corresponding amino acid (S751) and the flanking amino acid sequences are highly conserved in zebrafish stat3 compared to human, we first tracked the stat3 with the phosphorylated serine residue (pS-stat3) in the developing neuromasts using an antibody that recognizes phosphorylated S727 in human STAT3 ($STAT3^{pS727}$). In young neuromasts (3 dpf), we found that the majority of cells in the neuromasts showed homogenous $STAT3^{pS727}$ labeling in their nuclei but not in their cytoplasm (Figure 4.4A, upper panel). Double-labeling with scm1:GFP demonstrates that those cells are supporting cells and differentiating hair cells (Figure 4.4A, upper panel). In more mature hair cells, an intense but spotty labeling of $STAT3^{pS727}$

antibody was found in the cytoplasm, while nuclear labeling was much weaker compared to the cytoplasmic labeling (Figure 4.4A, close-ups in upper panel).

During the maturation of neuromasts, the overall number of cells with nuclear STAT3^{pS727} antibody labeling decreased (Figure 4.4A, lower panel). In neuromasts in 5-dpf larvae, the STAT3^{pS727} antibody labeling in the mature hair cells (Figure 4.4A, lower panel) resembled those in the young neuromasts (3 dpf; Figure 4.4A, upper panel) with strong cytoplasmic labeling and weak nuclear labeling. However, STAT3^{pS727} antibody labeling was no longer detectable in most of the non-sensory cells in the neuromast except for a small group of cells that were located several cell-layers away from the hair cells (Figure 4.4A, lower panel). Most of the labeled nuclei possessed an elongated oval shape (Figure 4.4A, arrowheads in lower panel). The immunohistological staining in transgenic ET20 larvae shows that most of those cells with nuclear labeling of STAT3^{pS727} antibody are mantle cells (Figure 4.4A, arrowheads in lower panel).

4.4.5 Nuclear import of pS-stat3 after CuSO4-induced hair cell death in lateral line neuromasts

We induced hair cell death in the lateral line neuromasts with $CuSO_4$, a protocol ensuring complete hair cell elimination within 2 h in 5-dpf larvae (Hernández et al., 2007) followed by regeneration to control level within 72 h (Behra et al., 2009). The experiment was done in Tg(scm1:GFP) larvae where the supporting cells in the neuromasts are labeled with GFP (Behra et al., 2009). We found a significant increase ($p < 0.01$) in the number of STAT3^{pS727}-positive nuclei in the neuromasts at 12 hours

post $CuSO_4$ treatment (hpt) in the $CuSO_4$-treated larvae relative to control (Figure 4.4B and C. Double-labeling with GFP in Tg(scm1:GFP) (Behra et al., 2009) demonstrates that cells with nuclear staining of $STAT3^{pS727}$ are mainly the supporting cells (Figure 4.4B).

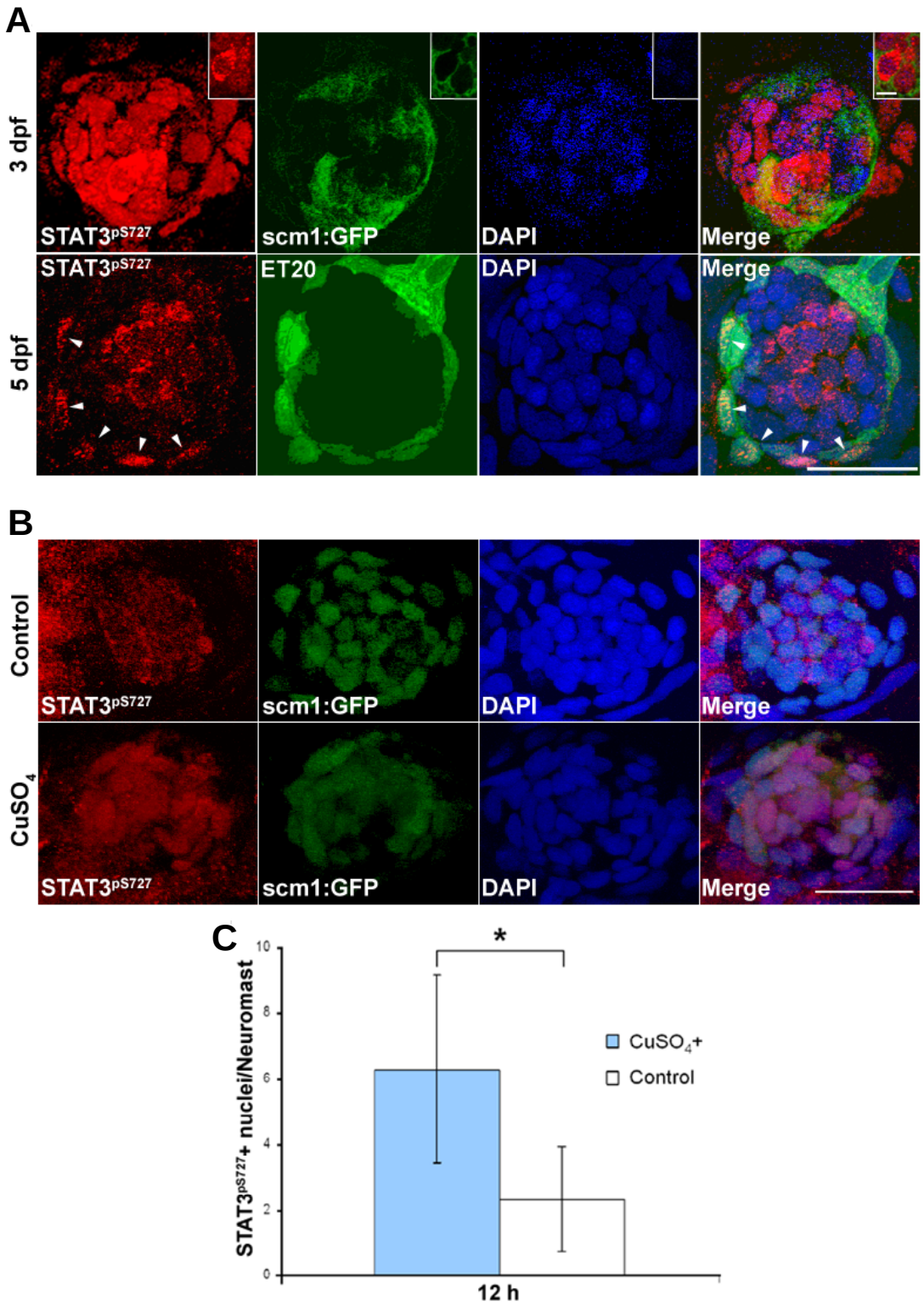

Figure 4.4. The phosphorylation and nuclear import of stat3 protein were detected after $CuSO_4$-induced hair cell death in lateral line neuromasts and

similar activation of stat3 was also observed during neuromast development. A) In 3-dpf (days post fertilization) larvae, a large number of the nuclei (blue) were homogenously labeled with $STAT3^{pS727}$ antibody (red), some of which were supporting cells with scm1:GFP-labeling (green) (upper panel). A small number of maturing hair cells showed decreased and spotty $STAT3^{pS727}$-labeling in the nuclei but elevated $STAT3^{pS727}$-labeling in the cytoplasm (close-ups in upper panel). Nuclear $STAT3^{pS727}$-labeling decreased dramatically in more mature neuromasts in 5-dpf larvae, except for a small group of cells in labeled with GFP in ET20 transgenic larvae (lower panel, arrowheads). Scale bar (close-ups) = 5 µm; scale bar (panel) = 20 µm. **B)** Co-staining of anti-$STAT3^{pS727}$ (red) with DAPI (blue) in Tg(scm1:GFP) larvae confirmed the increased anti-$STAT3^{pS727}$ labeling locates mainly in the nuclei of supporting cells (GFP-positive) (green) at 12 hours post copper treatment compared to untreated controls (scale bar = 20 µm). **C)** The increase in nuclear localized phospho-stat3 was statistically significant (n = 10 (treated) and 9 (control), one-tail t-test, *$p < 0.01$). S727 in human STAT3 corresponds to S751 in zebrafish stat3 by sequence alignment.

4.4.6 S3I-201 treatment promoted hair cell regeneration in zebrafish lateral line neuromasts

To further clarify the function of stat3, we compared the lateral line hair cell regeneration processes with and without the presence of a putative stat3 inhibitor, S3I-201. S3I-201 is a cell-permeable chemical that binds to the SH2-domain of mammalian stat3 protein and reportedly blocks the dimerization of phosphorylated (activated) stat3 molecules (Siddiquee et al., 2007). After exposing Tg(pou4f3:GFP)

larvae (Xiao et al., 2005) to $CuSO_4$, we quantified the regenerating hair cells and performed a bromodeoxyuridine (BrdU) incorporation assay. The S3I-201-treated larvae had more hair cells (GFP-positive) per neuromast at 48 hpt ($p < 0.01$), but not at 24 or 72 hpt (Figure 4.5A). Accordingly, the S3I-201-treated larvae showed a significant increase in BrdU incorporation in the neuromasts compared to DMSO-treated larvae (control) at 24 hpt, but not at 48 or 72 hpt (Figure 4.5A), which is consistent with an expected lag between supporting cell division and subsequent hair cell differentiation. In essence, the hair cells regenerated faster in the S3I-201 treated embryos than in controls. Similar results were observed when hair cell quantification was done by myosin VI antibody staining. S3I-201 did not have a significant impact on hair cell numbers in larvae that had not been treated with $CuSO_4$.

4.4.7 S3I-201 up-regulated of stat3/socs3 signaling in cultured zebrafish cells

The effect of S3I-201 on cell division and regeneration in zebrafish embryos was the opposite of what was predicted for an inhibitor of stat3 activation. In order to confirm S3I-201's inhibitory function, we compared the mRNA levels of four transcriptional targets of stat3 (stat3, socs3a, bcl6, and mmp9) in zebrafish Pac2 cells treated with or without S3I-201 using qRT-PCR. We detected a significant increase in the mRNA levels of all four genes after S3I-201 treatment for 2 h (Figure 4.5B), demonstrating that S3I-201 is in zebrafish, an activator of stat3 instead of the reported inhibitor.

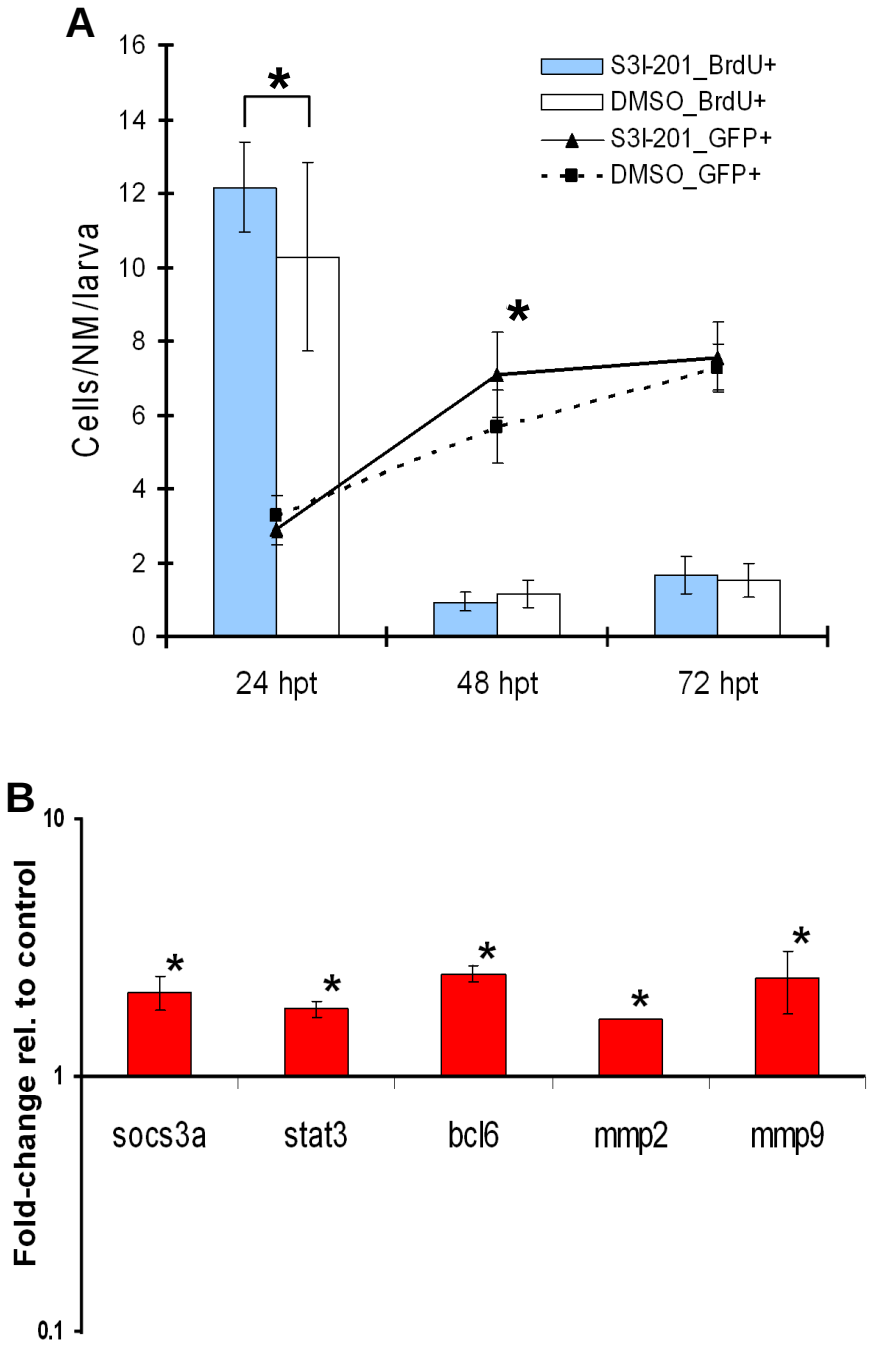

Figure 4.5. S3I-201 promoted lateral line hair cell regeneration by up-regulating stat3/socs3 signaling. A) After lateral line hair cell loss induced by $CuSO_4$ treatment, larvae incubated with S3I-201 had more hair cells (GFP-positive cells in Tg(pou4f3:GFP)) per neuromast (NM) at 48 h post $CuSO_4$ treatment (hpt) compared

to the control larvae incubated with DMSO (n = 12 (S3I-201-treated) and 9 (control), one-tail t-test, *p < 0.01), but not at 24 or 72 hpt (line graph). The BrdU incorporation assay showed a significantly higher number of BrdU-positive cells per neuromast in larvae incubated with S3I-201 at 24 hpt (n = 16 (S3I-201-treated) and 10 (control), one-tail t-test, *p < 0.01), but not at later time-points (bar graph). **B)** qRT-PCR results demonstrate that a 2 h-incubation of S3I-201 significantly up-regulated the mRNA levels of both stat3 and its downstream targets, including socs3a, bcl6, mmp2, and mmp9 (n = 3, one-tail t-test *p < 0.05). bactin1 was used as the reference gene.

4.5 Discussion

4.5.1 A negative feedback loop exists between zebrafish stat3 and socs3a

In mammals, stat3 activates the transcription of socs3, the protein of which inhibits stat3 activity (Gao & Ward, 2007). The qRT-PCR results from RNA extracted from MO-injected zebrafish embryos (Table 4.2) suggest that the negative feedback in stat3/socs3 pathway broadly studied in mammals is also conserved in zebrafish where stat3 initiates the transcription of both stat3 and socs3a while socs3a protein antagonizes the activation of stat3 signaling.

4.5.2 Stat3/socs3 signaling is required for normal hair cell/supporting cell production during zebrafish development

Down-regulation of stat3 reduced the number of hair cells in both the lateral line neuromasts (Figure 4.2) and the anterior macula of otic vesicle (Figure 4.3I and J), which suggests that stat3 is important for normal hair cell production during development. Accordingly, the sub-cellular staining pattern of $STAT3^{pS727}$ antibody

changed dramatically in the differentiating hair cells/supporting cells during the neuromast development (Figure 4.4A). However, when an up-regulation of stat3 expression was achieved by knocking-down socs3a expression (Table 4.2), there were still fewer hair cells produced in the neuromasts (Figure 4.2A), which suggests that the over-activation of stat3 in socs3a morphants impaired hair cell production. In addition, during hair cell/supporting cell differentiation in the lateral line neuromasts, nuclear labeling of $STAT3^{pS727}$ antibody was greatly reduced in differentiating hair cells/supporting cells (Figure 4.4A). The results from both the socs3a knockdown and the antibody staining indicate that a down-regulation in stat3 signaling is required for hair cell (and maybe supporting cell) differentiation. It seems that the stat3 signaling is required for establishing the group of prosensory cells in the neuromast. The cells with nuclear pS-stat3 activity in the young neuromasts may represent a group of cells temporarily maintaining self-renewal ability and actively dividing to generate enough prosensory cells for fully formed neuromasts. However, as the neuromast matures, stat3 signaling needs to be repressed to facilitate cell cycle exit and further cell differentiation. The normal inner ear hair cell production in socs3a morphants may be due to the absence of socs3a expression in the otic vesicle (Figure 4.1).

4.5.3 Stat3/socs3 signaling cross-talks with atoh1 in hair cell/supporting cell production during development

Atoh1a is the zebrafish homolog of atoh1, which is an essential gene required for hair cell fate commitment (Bermingham et al., 1999; Millimaki et al., 2007; Woods et al., 2004). Animals with atoh1 knockdown/knockout fail to produce hair cells during development while ectopic expression of atoh1 results in over-production of hair cells

(Bermingham et al., 1999; Millimaki et al., 2007; Woods et al., 2004). Zebrafish atoh1a also has functions similar to its mammalian homolog (Millimaki et al., 2007). Atoh1a expression was down-regulated in stat3 morphants and up-regulated in socs3a morphants (Table 4.2), suggesting a direct or indirect activation of atoh1a by stat3 signaling. Surprisingly, a decrease in the number of lateral line hair cells was found in socs3a morphants where the increase in atoh1a expression in the morphants was confirmed both by qRT-PCR (Table 4.2) and by *in situ* hybridization (Figure 4.2B). It has been shown that low level of atoh1 expression is required for the commitment of both hair cells and supporting cells in the prosensory area before it is up-regulated in hair cells and down-regulated in supporting cells in developing mouse cochlea (Woods et al., 2004). The atoh1 expression is later down-regulated as the hair cell matures (Lanford et al., 1999), the mechanism for which is unknown. Together with the discussion in Section 4.5.2, we propose that in stat3 morphants, an early and overall down-regulation of atoh1a expression leads to a reduction in the commitment of prosensory cells and thus fewer hair cells while in socs3a morphants, atoh1a expression is expanded as a result of stat3 hyper-activation, but prolonged stat3 actually activity hampers the terminal differentiation of hair cells and supporting cells. However, such cross-talk between stat3/socs3 and atoh1 has not been reported. One possible mechanism to mediate this cross-talk is through Hairy and Enhancer of Split proteins (HES), important effectors of the Delta/Notch signaling pathway which plays an essential role in the hair cell/supporting cell fate commitment in both development and regeneration (Reviewed in Section 2.2.4). For example, it inhibits the transcription of atoh1 in differentiating supporting cells during the development

of the mouse cochlea (Woods et al., 2004). In addition, HES1 also promotes both jak2-mediated (Kamakura et al., 2004) and src-mediated (Lee et al., 2009) activation of stat3 in mammalian cell lines. Because Hes1 has been detected as associating with the jak2/stat3 complex (Kamakura et al., 2004), it is possible that over-expression of stat3 exhausts the cytoplasmic HES and thus alleviates the inhibition of HES on atoh1a transcription in socs3 morphants, resulting in prolonged (and maybe ectopic) atoh1a expression and disrupted hair cell/supporting cell maturation. In addition, stat3 is also related to the expression of Inhibitors of DNA binding (Ids) (Belletti et al., 2002; Prisco, Peruzzi, Belletti, & Baserga, 2001) and SRY-box containing gene 2 (sox2), both of which regulate atoh1 expression during cochlea development (Dabdoub et al., 2008; Jones et al., 2006).

4.5.4 Nuclear-cytoplasmic shuttling of pS-stat3 in developing and regenerating neuromasts

The different sub-cellular localization of pS-stat3 in differentiating hair cells and supporting cells/progenitor cells in young neuromasts (in 3-dpf larvae, Figure 4.4A) suggests nuclear pS-stat3 activity is involved in cell fate commitment and/or supporting cell differentiation while reduced pS-stat3 signaling is preferred in differentiating/maturing hair cells. Immuno-staining of $STAT3^{pS727}$ in the neuromasts in 5-dpf larvae further confirms the decrease in nuclear pS-stat3 activity during hair cell maturation (Figure 4.4A), consistent with our hypothesis that a down-regulation of stat3 signaling is required for terminal hair cell differentiation (See Section 4.5.2 and 4.5.3). The changes in the sub-cellular localization of pS-stat3 during the maturation of hair cells and supporting cells suggest that transcriptional activity of

stat3 is needed during the cell fate commitment and maybe the early differentiation of hair cell/supporting cell progenitors, but needs to be tuned down for the late stage of hair cell/supporting cell differentiation and maturation. Another possible function of stat3 signaling in immature neuromasts is to promote cell division and generate enough prosensory cells. In addition, although the non-sensory cells were scm1:GFP-positive in both young and more matured neuromasts, those in the more matured neuromasts seem farther down the differentiation path because of the $STAT3^{pS727}$ staining was absent from their nuclei.

The pattern of $STAT3^{pS727}$-staining signals in hair cells was a surprise because as the hair cell differentiation proceeded, the staining not only weakened in the nuclei, but also greatly intensified in the cytoplasm (Figure 4.4A). Given the intensity of the staining, we believe that there is pS-stat3 retained in the cytoplasm, though it remains possible that the cytoplasmic staining is due to cross-reaction and/or some kind of artifact. Mitochondria have been shown to interact with stat3 as a regulator of metabolism (Gough et al., 2009; Wegrzyn et al., 2009). Another cytoplasmic structure that has been found associated with stat3 is the microtubules of the cytoskeleton (Ng et al., 2010; Ng et al., 2006; Verma et al., 2009). Here we used $STAT3^{pS727}$ antibody to track the serine-phosphorylated stat3 in the neuromasts. Immunohistochemical staining with neither the pan-stat3 antibodies nor the $STAT3^{pY705}$ antibodies (for unknown reasons) yielded convincing results. As a result, the behavior of unphosphorylated stat3 protein and tyrosine-phosphorylated stat3 protein in neuromasts is still unknown.

It is known that hair cell production during development and regeneration, to some extent, share similar genetic programs (Cafaro et al., 2007; Daudet et al., 2009; Ma et al., 2008; Stone & Rubel, 1999). The examination of stat3 activity in lateral line neuromasts during development and regeneration further confirms the similarity shared between the two processes. When hair cell death was triggered in 5-dpf larvae the stat3 protein was activated and imported into the nuclei of the supporting cells again (Figure 4.4B), recapitulating the generalized stat3 activation during neuromast development (Figure 4.4A).

4.5.5 Stat3 signaling is involved in hair cell regeneration in the lateral line neuromasts of zebrafish larvae

Nuclear import of pS-stat3 happened subsequent to $CuSO_4$-induced hair cell loss in lateral line neuromasts at 12 hpt (Figure 4.4B), the earliest time-point checked after $CuSO_4$ treatment. The BrdU incorporation peaked at 15 h subsequent to neomycin-induced lateral line hair cell elimination in 5-dpf old zebrafish (Ma et al., 2008). The regeneration of hair cells in $CuSO_4$-treated larvae is likely to be delayed compared to neomycin-treated larvae because the $CuSO_4$ treatment does result in additional damage to nonsensory cells in the neuromasts (Olivari, Hernández, & Allende, 2008). Nuclear import of pS-stat3 preceded the peak of BrdU incorporation, suggesting that stat3 signaling may promote cell-cycle progress in hair cell regeneration, as seen in other regenerative processes (Kassen et al., 2009; Li et al., 2002). A recent study further supports this idea as it reported leukemia inhibitory factor (LIF) promoted cell division in a cochlea-derived cell line, HEI-OC1, through the stat3/jak2 signaling pathway (Chen et al., 2010). In addition, a very small number of early-emerging hair

cells are not generated by cell division during lateral line hair cell regeneration (Ma et al., 2008). Those hair cells may originate from the differentiation/maturation of supporting cells or young hair cells that have survived the ototoxic treatment. Since pS-stat3 activity was also detected in the nuclei of differentiating hair cells/supporting cells during development (Figure 4.4A), some of the cells with $STAT3^{pS727}$-positive nuclei might be differentiating hair cells or transdifferentiating/differentiating supporting cells. The activation and the nuclear import of pS-stat3 in the supporting cells indicate the involvement of stat3 signaling during hair cell regeneration.

4.5.6 S3I-201 treatment positively regulated stat3 signaling and promoted hair cell regeneration in lateral line neuromasts of zebrafish larvae

S3I-201 treatment after CuSO4-induced hair cell death promoted hair cell regeneration in zebrafish lateral line by accelerating cell division (Figure 4.5A). Interestingly, the S3I-201 treatment only accelerated hair cell regeneration without producing supernumerary hair cells compared to the control larvae by 72 hpt (Figure 4.5A). A possible explanation is that pharmacological hyper-activation of stat3 was transient because of inhibition from the subsequent elevated level of socs3a through an intact stat3/socs3a self-restrictive loop.

S3I-201 was described as an antagonizer of stat3 activity by blocking the dimerization of phosphorylated (activated) stat3 proteins in mammalian cell lines (Siddiquee et al., 2007). However, S3I-201 treatment enhanced the mRNA level of four stat3 target genes in Pac2 cells (Figure 4.5B), demonstrating S3I-201 is an agonist of stat3 activity at least in zebrafish cells. First of all, the discrepancy in S3I-201 function between mammals and zebrafish may be the result of an organism-

specific response to the chemical. In addition, stat3 protein in zebrafish neuromasts is activated at least partially by serine phosphorylation (Figure 4.4). It is unclear whether S3I-201 has certain binding preference between pS-stat3 and pY-stat3. However, Lin et al. (2009) reported a more potent effect of S3I-201 on inhibiting cell proliferation in hepatocellular carcinoma cells with disrupted TGF-β signaling that resulted in a higher level of tyrosine phosphorylation but a lower level of serine phosphorylation of stat3. Another small-molecule inhibitor of stat3, stattic, targets the same binding region in the stat3 protein (SH2 domain) as S3I-201 and shows temperature-dependent inhibition efficiency: the efficiency decreases as the temperature gets lower (Schust, Sperl, Hollis, Mayer, & Berg, 2006). It is possible that S3I-201 acts differently in our experiment because the zebrafish and Pac2 cells were raised at temperatures (28ºC and 32ºC respectively) much lower than that in the published studies in cell lines (37ºC). Last but not least, previous studies on S3I-201 did not examine the effect of the chemical until after 24 h of treatment (Siddiquee et al., 2007) while we checked the mRNA level of the target genes of stat3 after 2 h of treatment in Pac2 cells. It is possible that prolonged-treatment of S3I-201 hyper-activated the negative feedback of socs3 and resulted in a delayed decrease in stat3 signaling.

Therefore stat3 signaling is directly involved in initiating cell division in the supporting cell population, in accordance with our observation of stat3 import into the nuclei of the supporting cells at a very early time-point (12 hpt) after the induction of hair cell death (Figure 4.4B), consistent with an activation of stat3 activity instead of inhibition. In addition, it is very likely that stat3 activity potentiated by S3I-201

promoted hair cell regeneration by regulating cell division based on the dramatic changes of pS-stat3 activity during neuromast development (Figure 4.4A) as well as the disrupted hair cell production (Figure 4.2A and 4.3) and atoh1a expression (Table 4.2 and Figure 4.2B) in stat3 and socs3a morphants. When both *in vivo* and *in vitro* results are taken into account, S3I-201 appeared to activate zebrafish stat3 signaling which accelerated hair cell regeneration.

4.5.7 Stat3 activity vs. the potential stem cell population in mature neuromasts

The nonsensory cells (usually addressed as "supporting cells" in general) in the neuromasts have been proposed as potential stem cells because of their ability to give rise to new sensory and nonsensory cells (Behra et al., 2009; Hernández et al., 2007; Ma et al., 2008). However, the nonsensory cells in the neuromasts are not a homogenous group of cells. Mantle cells are a subgroup of the nonsensory cells defined by their location: in the outer cell layers of a neuromasts and with no direct contact with hair cells (Hama & Yamada, 1977; Jones & Corwin, 1993). They are also characterized by the crescent-shaped cell body, elongated nucleus, and short, sparse microvilli at the apical surface (Hama & Yamada, 1977). In mature neuromasts, mantle cells are the only dividing cells in the neuromasts (Williams & Holder, 2000). When older zebrafish larvae (10 dpf) are given a pulse-treatment of BrdU and sacrificed at different time-points after the treatment, incorporation of BrdU is only detected in mantle cells at the earliest time-point examined followed by detection of BrdU in supporting cells in later time points (Williams & Holder, 2000). In addition, mantle cells divide and give rise to whole neuromasts when the neuromasts in the fin/tail are completely eliminated by amputation in zebrafish

(Dufourcq et al., 2006) and salamanders (Jones & Corwin, 1993). Taking all the evidence together, mantle cells act like a pool of multipotent stem cells in the neuromasts by going through cell division to renew themselves as well as give rise to new hair cells/supporting cells.

In the transgenic zebrafish line ET20, the outermost nonsensory cells in the neuromasts (possibly a subgroup of the mantle cells) are labeled with GFP (Choo et al., 2006). In our data, we showed that nuclear staining of $STAT3^{pS727}$ was only maintained in the GFP-positive cells in ET20 fish in more matured neuromasts (Figure 4.4A). Hence it is reasonable to propose pS-stat3 as a stem cell marker in lateral line neuromasts. As supporting evidence to the hypothesis, stat3 is known as required for the maintenance of pluripotency in mouse embryonic stem cells (Raz, Lee, Cannizzaro, d'Eustachio, & Levy, 1999). However, the effect of stat3 in the oligopotent neural progenitor cells (NPCs) seems controversial. On one hand, stat3 was reported as promoting the astrogliogenetic differentiation of NPCs (Cao, Hata, Zhu, Nakashiro, & Sakanaka, 2010; Nakashima et al., 1999; Taga & Fukuda, 2005). On the other hand, stat3 was found promoting the proliferation and inhibiting differentiation of NPCs (Wada et al., 2006). The difference may be due to the different stages of NPCs examined. For example, stat3-activating ligands induce astrocytic differentiation in late-staged (gliogenic) NPCs but fail to do so in early-staged (expansion and neurogenic) NPCs during the development of mouse forebrain (Hirabayashi & Gotoh, 2005). The suggestion is that stat3 acts as a stage-dependent, multifunctional regulator in neurogenesis.

An alternative function of the pS-stat3-positive mantle cells in mature and intact neuromasts may be a “stem cell niche.” They may regulate the adjacent stem cells through a non-autonomous mechanism similar to the role of stat92E in the Escort Stem Cells in the Drosophila ovary, which regulate germline stem cell division in a non-autonomous fashion (Decotto & Spradling, 2005). These pS-stat3-positive mantle cells would thus represent part of the niche environment necessary to promote normal cell turnover as well as tissue regeneration.

4.5.8 Development vs. regeneration: a working model of stat3 function in zebrafish lateral line neuromasts

In immature neuromasts, stat3 activity was detected in most of the cells (Figure 4.4A), suggesting the less differentiated status of those cells. Although not tested, it is possible that those cells are more stem cell-like and still capable of active division before they are further differentiated. During neuromast maturation, down-regulation in stat3 activity in the nuclei accompanies (and is probably required by) the differentiation of hair cells and supporting cells. Reduced stat3 activity in the nuclei of differentiated hair cells/supporting cells may partially account for their inability to move on with the cell cycle. In contrast, some mantle cells maintain the stat3 activity in their nuclei, either acting as or helping maintaining the multi-potent stem cells in the neuromasts.

While pS-stat3 was nearly absent from supporting cells in intact mature neuromasts (Figure 4.4A), it was detected again shortly after $CuSO_4$-induced hair cell death (Figure 4.4B). In lateral line hair cell regeneration in zebrafish larvae, the majority of new hair cells come from the cell division in supporting cells (and maybe

mantle cells as well) division (Ma et al., 2008). Based on the fact that supporting cell division is rare in intact zebrafish neuromasts (Williams & Holder, 2000), we propose supporting cells as uni-potent cells which hold the ability to terminally differentiate only into hair cells. Lateral inhibition possibly restricts the self-renewal ability of supporting cells and holds them at the post-mitotic stage. As a result, supporting cells have to rely on the division of the multi-potent stem cells, likely the mantle cells, for replenishment. Different from supporting cells, mantle cells divide on a regular basis, partially due to the autonomous or non-autonomous mitogenic activity of the stat3 signaling. When small numbers of the hair cells die as part of the regular turnover, the lateral inhibition on their surrounding supporting cells is partially alleviated, which enables them to completely differentiate into hair cells. During the differentiation, stat3 protein may be activated again, but is eventually restricted to the cytoplasm. When acute and disastrous hair cell death takes place (e.g. toxic chemical exposure), the supporting cells are totally free of lateral inhibition, resulting in the translocation of activated stat3 protein into the nuclei and subsequent cell cycle progression. When new hair cells differentiate, the lateral inhibition is re-established to turn off the stat3 signaling and hold the supporting cells at the post-mitotic stage again. During regeneration, mantle cells continue to divide (or to promote cell division), likely at an elevated rate.

It may seem reasonable to consider supporting cells and mantle cells as equivalent cells that behave differently in different contexts: supporting cells are mantle cells temporarily turned quiescent by hair cells or mantle cells are supporting cells free of lateral inhibition as a result of no direct contact with hair cells. However,

because the two groups of cells possess very distinct morphological and molecular features, this simple model seems unlikely and they should probably be considered as two different cell types, mantle cells as multi-potent stem cells and parent cells of supporting cells which are uni-potent cells.

4.5.9 Mammals vs. zebrafish: stat3 signaling in hair cell regeneration

It was also reported that stat3 showed a temporal expression pattern similar to gata2 and C/EBP during the *in vitro* differentiation of conditional cell lines derived from the mouse otocyst (Holley, Kneebone, & Milo, 2007). Very little is known about stat3 in the inner ear of mammals other than that the protein is detected only in the nuclei of outer hair cells but not in any supporting cells in embryonic or neonatal mice (Hertzano et al., 2004). However, stat3 remains active in a subgroup of nonsensory cells (GFP-positive cells in ET20 fish line) of mature neuromasts (Figure 4.4A), which may serve as a putative group of stem cells or "stem cell niche" (See Section 4.5.7). The numbers of stem cell-like cells decreased rapidly in the cochlea of mice after birth (Oshima et al., 2006) while those cells are still available in vestibular end organs of adult mice (Li, Liu, & Heller, 2003). The rapid decrease of stem cell-like cells in the cochlea may be due to the lack of a "stem cell niche" to maintain those cells. It is unclear that if stat3 contributes to the maintenance of the stem cell-like cells in the vestibular end organs.

Stat3 in outer hair cells may play a protective role against oxidative stress as a previous microarray study did show basal-level expression of stat3 in newborn rat cochlea that could be elevated by stress in explant cultures (Gross et al., 2008). However, if stat3 signaling remains absent in supporting cells after hair cell death in

mouse cochlea, it is not likely to be involved in hair cell regeneration. Therefore, the difference in hair cell regeneration ability between mice and zebrafish can be partially attributed to the mitogenic and differentiation roles of stat3 signaling. From a therapeutic standpoint, inducing stat3 activity in supporting cells may trigger cell cycle progression and hair cell regeneration in the mammalian ears.

4.5.10 The stat3/socs3 pathway may serve as a common initiator in a variety of regenerative processes

Previous publications have revealed the critical role of stat3 and socs3 in the regenerative processes of various tissues in both mammals and zebrafish (See Section 4.2.3). Taken together, all these data strengthen our hypothesis that stat3/socs3 is a central activating mechanism to activate adult stem cells in many if not all forms of regeneration.

The self-restricted signaling loop of stat3/socs3 makes it of special interest as a therapeutic target for regeneration. Under typical circumstances, an immediate and brief up-regulation of stat3 expression in response to tissue damage seems to be necessary to initiate regeneration. The tight temporal control of activation is achieved by the negative feedback from socs3. Prolonged stat3 signaling after injury can sometimes result in inflammation and disrupt regeneration. In addition, constitutive hyperactivation of stat3 is often observed in cancer cells where cell proliferation is out of control. Unregulated activation of stat3 would not be ideal in induced regenerative therapy. Pharmacologically up-regulating stat3 expression while allowing the normal socs3 feedback may help achieve the desirable regenerative effect of accelerating the wound healing response, but preventing over-production of

cells. Thus chemical activators of stat3 may represent a safely self-regulating therapy in a wide variety of injuries and therapies for tissue regeneration.

Chapter 5 Summary and Future Studies

5.1 High-throughput gene expression profiling with Digital Gene Expression

In this study, we used Digital Gene Expression (DGE/tag profiling) to generate in-depth gene expression profiles from inner ear tissue samples collected at different time-points during hair cell regeneration. The five expression profiles captured over 300,000 unique tag sequences with an accumulative count of more than 15 million tags (Table 3.3). Such data depth allows the identification of low-abundance transcripts and provides great statistical power for comparison. The clustering and pathway analyses strongly suggest that the DGE profiling properly reflected the biological changes during hair cell regeneration (Figure 3.4). By profile comparison, more than 2,000 candidate genes were identified (Supplemental file 3) and some of them were confirmed with qRT-PCR (Figure 3.3A). In summary, the DGE technique provided large-scale and in-depth profiling results that gave me a comprehensive overview of the regenerative process at the molecular level as well as identifying candidate genes in a high-throughput manner.

The DGE profiling experiments were carried out around the time when DGE was first introduced to the research community. Due to the lack of previous studies and the relatively high cost of the technique at that time, the application of DGE technique in this study has significant room for improvement. Starting with the experimental design, more biological and technical replicates should be included in future studies to improve the statistical power. Due to new amplification techniques

allowing for a decrease in the required minimum amount of starting materials, biological samples can be collected from conventional dissection as well as micro-dissection or Fluorescence Activated Cell Sorting (FACS) to examine the profiles of a more homogenous group of cells, which will provide expression profiles with even finer spatial resolution and a higher signal-to-noise ratio. To get a finer temporal resolution, more time-points of tissue sampling (especially between the onset of the noise exposure and 24 hpt in this study) are needed.

Some miRNA-encoding genes were identified as candidate genes in this study (See Section 3.4.10) as well as in other regenerative studies (Kren et al., 2009; Marquez et al., 2010; Yin et al., 2008). Since DGE is designed mainly for profiling protein-coding genes, other sequencing-based techniques designed for profiling small RNAs (and/or other non-coding RNAs) are needed to more accurately explore the function of small RNAs (and even non-coding RNAs) during hair cell regeneration.

5.2 Stat3/socs3 pathway in hair cell regeneration

The stat3/socs3 pathway was identified by comparing gene expression profiles collected at different time-points during hair cell regeneration. The expression level of both stat3 and socs3a were up-regulated at 0 hpe and returned to control levels by 24 hpe (Supplemental file 3). Both genes were involved in hair cell production during development and regeneration (Figure 4.2A, 4.3, and 4.4). These functions may be partially fulfilled by regulating atoh1a (Figure 4.2B and Table 4.2). More interestingly, pharmacological hyperactivation of stat3 signaling accelerated hair cell regeneration by promoting cell division in the supporting cells (Figure 4.5A).

This study provided a preliminary functional study of the stat3/socs3 pathway in hair cell regeneration, leaving many interesting questions to be answered. First, the role of the stat3/socs3 pathway needs to be directly examined in the inner ear during hair cell regeneration instead of using the lateral line as a proxy. In addition, it is also important to characterize the activity of stat3 signaling in the mammalian inner ear under normal conditions as well as after hair cell death. Second, the upstream genes activating stat3 signaling after hair cell death and the downstream effectors of stat3 are still unknown. Third, here only the activation of the stat3 protein by S727 (S751 in zebrafish) phosphorylation was characterized. Since stat3 protein can also be activated by the phosphorylation of Y705 (Y708 in zebrafish), it would be interesting to know how tyrosine phosphorylation is regulated in hair cell regeneration. Fourth, because the nucleus-cytoplasm trafficking of stat3 protein is closely related to the functions of the stat3 signaling pathway, a closer examination of the nuclear import and export of stat3 protein in both regeneration and development is needed for further understanding of the regulation of the stat3/socs3 pathway. In addition, the function of cytoplasmic stat3 proteins in the hair cells also remains intriguing. Fifth, examination of the interaction between stat3/socs3 and atoh1, a crucial factor for hair cell fate commitment, will give us a better understanding of the functions of the stat3/socs3 pathway during hair cell production as well as the regulatory mechanisms of atoh1. Finally, it is known that the stat3/socs3 pathway is also involved in immune responses and cell protection in injured tissues (See Section 4.2). It would be interesting to see if stat3/socs3 pathway is involved in the immune responses induced by hair cell death, which may have further impact on hair cell regeneration. Because

stat3 is known to be expressed in the outer hair cells in mouse cochlea (Hertzano et al., 2004), it would be interesting to see if the stat3 protein can provide protection to those hair cells against ototoxicity.

5.3 Zebrafish and hair cell regeneration

5.3.1 Zebrafish as a model system for hair cell regeneration studies

There are three main reasons for choosing zebrafish as a potential model system for hair cell regeneration studies. First, the conservation of the inner ear sensory epithelial structure through all vertebrates justifies the claim that our understanding of hair cell regeneration in nonmammalian vertebrates will potentially translate into strategies for inducing similar regeneration in the ears of mammals. Second, zebrafish studies are facilitated by the availability of well-annotated genome/transcriptome sequences, mutant/transgenic fish lines, and a series of cellular and molecular tools. Finally, the superficially located neuromasts in the lateral line offer a simple system for functional studies on genes of interest during regeneration (Behra et al., 2009; Harris et al., 2003; Hernández et al., 2007; Ma et al., 2008).

This study further justifies the choice of zebrafish as a model system for hair cell regeneration studies. Large-scale candidate gene screening would offer a comprehensive overview of the regenerative process. Such screening would be more difficult in organisms without a well-annotated genome/transcriptome, e.g. chicken or frog. The functional studies of the stat3/socs3 pathway in the lateral line system provide an example of how efficient follow-up studies can be performed after the

initial, large-scale screening, which is lacking in the hair cell regeneration studies in chickens (Hawkins et al., 2003, 2007).

In line with the regenerative studies, the lateral line neuromasts can also serve as a potential model system for studying somatic stem cells. It has been suggested that the supporting cells (or a subgroup of the supporting cells) in the inner ear serve as somatic stem cells (Parker & Cotanche, 2004). The supporting cells (or nonsensory neuromast cells) in the neuromasts are capable of self-renewal (Williams & Holder, 2000) as well as hair cell progenitor production (Ma et al., 2008), which is characteristic of somatic stem cells. In addition, the dynamic activity of stat3 protein during development and regeneration found in this study further suggests a possible "stem cell/niche" pattern in the neuromasts (See Section 4.4.4, 4.4.5, and 4.5.7). A better understanding of the somatic stem cells maintenance and their reaction triggered by damage in the neuromasts will help us understand not only how hair cells are regenerated but also how other regenerative processes are regulated.

5.3.2 The toolbox for future hair cell regeneration studies in zebrafish

One of the future research directions is to further establish zebrafish as a model system for hair cell regeneration studies. In order to accomplish that, new experimental tools are needed to help examine the regeneration in zebrafish. In addition to the molecular/cellular tools used in this study, there are several others that could be incorporated for future studies.

First, it will be helpful to incorporate different physical, chemical and biological tools in addition to acoustic over-exposure for inducing hair cell death. Those tools include laser ablation (Balak et al., 1990; Millimaki et al., 2010), ototoxic chemicals

(Harris et al., 2003; Hernández et al., 2007; Ou et al., 2007), and the nitroreductase (NTR) system (Pisharath et al., 2007). In addition to using these tools to efficiently eliminate hair cells/supporting cells, it will also be interesting to compare the effects of different ototoxic treatments on hair cell regeneration.

Second, the superficially located neuromasts provide an excellent system for live imaging. Using fluorescent protein-labeled transgenic zebrafish lines (e.g. pou4f3:GFP, scm1:GFP, and ET20), it is easy to track the behaviors of cells during hair cell regeneration in real-time. In addition, it is relatively easy to generate transgenic fish lines producing target proteins fused with a fluorescent protein so that the sub-cellular trafficking of the target proteins can be imaged in real-time. Such imaging will be particularly informative if the functions of the gene of interest are closely related to its sub-cellular localization, e.g. a transcription factor responsive to cell signaling.

Finally, the use of small molecule screening could help with our understanding of the mechanisms involved in hair cell regeneration. There are mainly two ways to incorporate the small molecules into regenerative studies: using chemicals to inhibit or stimulate candidate genes/pathways and using chemicals for gene function studies. The lateral line system has already been used for large-scale ototoxic chemical screening (Chiu, Cunningham, Raible, Rubel, & Ou, 2008). It could also be used for screening of small molecule chemicals that block or promote hair cell regeneration. Large-scale screening of chemicals could help us to identify the candidate pathways involved in the hair cell regeneration process. On the other hand, when testing a known gene or pathway, the chemical agonists/antagonists targeting the candidate can

be used for *in vivo* functional studies, a strategy that was utilized in this study to understand the functions of the stat3/socs3 pathway in hair cell regeneration. An advantage of incorporating small molecules into the regenerative studies is that if any regeneration-promoting chemical is identified, it could potentially have clinical application towards regenerative medicine. For decades, scientists have strived to induce hair cell regeneration in mammals. Such research has so far been focused on two strategies: gene therapy (Gubbels et al., 2008; Ryan, Mullen, & Doherty, 2009) and stem cell transplantation (Tateya et al., 2003; Kesser & Lalwani, 2009; Oshima et al., 2010). While progress has been made, it is still questionable if there will be a truly applicable clinical approach in the near future. Pharmacological strategies may have greater potential in hair cell regeneration induction for clinical practice.

Appendix

List of Supplemental Files

Supplemental file 1. Raw data of five expression profiles generated by DGE. It is a tab-delimited text file with six columns. The first column contains the sequences of the tags and the second to sixth columns contain the count of the corresponding tags in control, 0-hpe, 24-hpe, 48-hpe, and 96-hpe profiles respectively.

Supplemental file 2. UniGene clusters identified from unambiguously mapped tags. It is a tab-delimited text file with six columns. The first column contains the UniGene IDs. The second to sixth columns contain the count of the corresponding UniGene clusters in control, 0-hpe, 24-hpe, 48-hpe, and 96-hpe profiles respectively.

Supplemental file 3. Candidate genes identified by comparison of the expression profiles during regeneration to the control profiles. It is a tab-delimited text file with 19 columns. The contents in each column are specified in the header.

Supplemental file 4. A list of the candidate genes known to be expressed in the inner ear and/or the lateral line system during development. It is a tab-delimited text file with four columns which contain UniGene IDs, ZFIN IDs, Entrez Gene IDs, and gene symbols respectively.

Bibliography

Adams, M., Kelley, J., Gocayne, J., Dubnick, M., Polymeropoulos, M., Xiao, H., Merril, C., et al. (1991). Complementary DNA sequencing: expressed sequence tags and human genome project. *Science, 252*(5013), 1651-1656.

Adler, H. J., & Raphael, Y. (1996). New hair cells arise from supporting cell conversion in the acoustically damaged chick inner ear. *NeuroScienceLetters, 205*(1), 17-20.

Aggarwal, B. B., Kunnumakkara, A. B., Harikumar, K. B., Gupta, S. R., Tharakan, S. T., Koca, C., Dey, S., et al. (2009). Signal transducer and activator of transcription-3, inflammation, and cancer: How intimate is the relationship? *Annals of the New York Academy of Sciences, 1171*(1), 59-76.

Ahsan, H., Aziz, M. H., & Ahmad, N. (2005). Ultraviolet B exposure activates Stat3 signaling via phosphorylation at tyrosine705 in skin of SKH1 hairless mouse: A target for the management of skin cancer? *Biochemical and Biophysical Research Communications, 333*(1), 241-246.

Akira, S., Nishio, Y., Inoue, M., Wang, X., We, S., Matsusaka, T., Yoshida, K., et al. (1994). Molecular cloning of APRF, a novel IFN-stimulated gene factor 3 p91-related transcription factor involved in the gp130-mediated signaling pathway. *Cell, 77*(1), 63-71.

Amsterdam, A., Burgess, S., Golling, G., Chen, W., Sun, Z., Townsend, K., Farrington, S., et al. (1999). A large-scale insertional mutagenesis screen in zebrafish. *Genes & Development, 13*(20), 2713-2724.

Asmann, Y., Klee, E., Thompson, E. A., Perez, E., Middha, S., Oberg, A., Therneau, T., et al. (2009). 3' tag digital gene expression profiling of human brain and universal reference RNA using Illumina Genome Analyzer. *BMC Genomics, 10*(1), 531.

Auernhammer, C. J., Bousquet, C., & Melmed, S. (1999). Autoregulation of pituitary corticotroph SOCS-3 expression: Characterization of the murine SOCS-3 promoter. *Proceedings of the National Academy of Sciences of the United States of America, 96*(12), 6964 -6969.

Avallone, B., Fascio, U., Balsamo, G., & Marmo, F. (2008). Gentamicin ototoxicity in the saccule of the lizard Podarcis Sicula induces hair cell recovery and regeneration. *Hearing Research, 235*(1-2), 15-22.

Avallone, B., Porritiello, M., Esposito, D., Mutone, R., Balsamo, G., & Marmo, F. (2003). Evidence for hair cell regeneration in the crista ampullaris of the lizard Podarcis sicula. *Hearing Research, 178*(1-2), 79-88.

Aziz, M. H., Manoharan, H. T., Church, D. R., Dreckschmidt, N. E., Zhong, W., Oberley, T. D., Wilding, G., et al. (2007). Protein Kinase Cε interacts with Signal Transducers and Activators of Transcription 3 (Stat3), phosphorylates Stat3Ser727, and regulates its constitutive activation in prostate cancer.

Cancer Research, *67*(18), 8828 -8838.

Babon, J. J., McManus, E. J., Yao, S., DeSouza, D. P., Mielke, L. A., Sprigg, N. S., Willson, T. A., et al. (2006). The structure of SOCS3 reveals the basis of the extended SH2 domain function and identifies an unstructured insertion that regulates stability. *Molecular Cell*, *22*(2), 205-216.

Baird, R. A., Steyger, P. S., & Schuff, N. R. (1996). Mitotic and nonmitotic hair cell regeneration in the bullfrog vestibular otolith organs. *Annals of the New York Academy of Sciences*, *781*(1), 59-70.

Baird, R., Torres, M., & Schuff, N. (1993). Hair cell regeneration in the bullfrog vestibular otolith organs following aminoglycoside toxicity. *Hearing Research*, *65*(1-2), 164-174.

Baird, R. A., Burton, M. D., Fashena, D. S., & Naeger, R. A. (2000). Hair cell recovery in mitotically blocked cultures of the bullfrog saccule. *Proceedings of the National Academy of Sciences of the United States of America*, *97*(22), 11722 -11729.

Baker, K., Brough, D., & Staecker, H. (2009). Repair of the vestibular system via adenovector delivery of Atoh1: A potential treatment for balance disorders. *Advances in otorhinolaryngology*, *66*, 52-63.

Balak, K., Corwin, J., & Jones, J. (1990). Regenerated hair cells can originate from supporting cell progeny: evidence from phototoxicity and laser ablation experiments in the lateral line system. *The Journal of Neuroscience*, *10*(8), 2502-2512.

Baltayiannis, G., Baltayiannis, N., & Tsianos, E. V. (2008). Suppressors of cytokine signaling as tumor repressors. Silencing of SOCS3 facilitates tumor formation and growth in lung and liver. *Journal of B.U.ON.: Official Journal of the Balkan Union of Oncology*, *13*(2), 263-265.

Bang, P. I., Sewell, W. F., & Malicki, J. J. (2001). Morphology and cell type heterogeneities of the inner ear epithelia in adult and juvenile zebrafish (Danio rerio). *The Journal of Comparative Neurology*, *438*(2), 173-190.

Barbieri, I., Pensa, S., Pannellini, T., Quaglino, E., Maritano, D., Demaria, M., Voster, A., et al. (2010). Constitutively active Stat3 enhances Neu-mediated migration and metastasis in mammary tumors via upregulation of Cten. *Cancer Research*, *70*(6), 2558 -2567.

Becker, S., Groner, B., & Muller, C. W. (1998). Three-dimensional structure of the Stat3[beta] homodimer bound to DNA. *Nature*, *394*(6689), 145-151.

Begitt, A., Meyer, T., van Rossum, M., & Vinkemeier, U. (2000). Nucleocytoplasmic translocation of Stat1 is regulated by a leucine-rich export signal in the coiled-coil domain. *Proceedings of the National Academy of Sciences of the United States of America*, *97*(19), 10418 -10423.

Behra, M., Bradsher, J., Sougrat, R., Gallardo, V., Allende, M. L., & Burgess, S. M. (2009). Phoenix is required for mechanosensory hair cell regeneration in the

zebrafish lateral line. *PLoS Genetics*, *5*(4), e1000455.

Belletti, B., Drakas, R., Morrione, A., Tu, X., Prisco, M., Yuan, T., Casaburi, I., et al. (2002). Regulation of Id1 protein expression in mouse embryo fibroblasts by the type 1 insulin-like growth factor receptor. *Experimental Cell Researchearch*, *277*(1), 107-118.

Bennett, S. (2004). Solexa Ltd. *Pharmacogenomics*, *5*(4), 433-438.

Bennett, S. T., Barnes, C., Cox, A., Davies, L., & Brown, C. (2005). Toward the $1000 human genome. *Pharmacogenomics*, *6*(4), 373-382.

Bermingham, N. A., Hassan, B. A., Price, S. D., Vollrath, M. A., Ben-Arie, N., Eatock, R. A., Bellen, H. J., et al. (1999). Math1: an essential gene for the generation of inner ear hair cells. *Science*, *284*(5421), 1837-1841.

Bermingham-McDonogh, O., Stone, J. S., Reh, T. A., & Rubel, E. W. (2001). FGFR3 expression during development and regeneration of the chick inner ear sensory epithelia. *Developmental Biology*, *238*(2), 247-259.

Borowiak, M., Garratt, A. N., Wüstefeld, T., Strehle, M., Trautwein, C., & Birchmeier, C. (2004). Met provides essential signals for liver regeneration. *Proceedings of the National Academy of Sciences of the United States of America*, *101*(29), 10608 -10613.

Brand, S., Dambacher, J., Beigel, F., Zitzmann, K., Heeg, M. H. J., Weiss, T. S., Prufer, T., et al. (2007). IL-22-mediated liver cell regeneration is abrogated by SOCS-1/3 overexpression in vitro. *The American Journal of Physiology - Gastrointestinal and Liver Physiology*, *292*(4), G1019-1028.

Brenner, S., Johnson, M., Bridgham, J., Golda, G., Lloyd, D. H., Johnson, D., Luo, S., et al. (2000). Gene expression analysis by massively parallel signature sequencing (MPSS) on microbead arrays. *Nature Biotechnology*, *18*(6), 630-634.

Brent, M. R. (2008). Steady progress and recent breakthroughs in the accuracy of automated genome annotation. *Nature Reviews Genetics*, *9*(1), 62-73.

Cacalano, N. A., Sanden, D., & Johnston, J. A. (2001). Tyrosine-phosphorylated SOCS-3 inhibits STAT activation but binds to p120 RasGAP and activates Ras. *Nature Cell Biology*, *3*(5), 460-465.

Cafaro, J., Lee, G. S., & Stone, J. S. (2007). Atoh1 expression defines activated progenitors and differentiating hair cells during avian hair cell regeneration. *Developmental Dynamics*, *236*(1), 156-170.

Caldenhoven, E., van Dijk, T. B., Solari, R., Armstrong, J., Raaijmakers, J. A., Lammers, J. W., Koenderman, L., et al. (1996). STAT3beta, a splice variant of transcription factor STAT3, is a dominant negative regulator of transcription. *The Journal of Biological Chemistry*, *271*(22), 13221-13227.

Caldwell, R., Kierzek, A., Arakawa, H., Bezzubov, Y., Zaim, J., Fiedler, P., Kutter, S., et al. (2004). Full-length cDNAs from chicken bursal lymphocytes to facilitate gene function analysis. *Genome Biology*, *6*(1), R6.

Campbell, J. S., Prichard, L., Schaper, F., Schmitz, J., Stephenson-Famy, A., Rosenfeld, M. E., Argast, G. M., et al. (2001). Expression of suppressors of cytokine signaling during liver regeneration. *Journal of Clinical Investigation, 107*(10), 1285-1292.

Cao, F., Hata, R., Zhu, P., Nakashiro, K., & Sakanaka, M. (2010). Conditional deletion of Stat3 promotes neurogenesis and inhibits astrogliogenesis in neural stem cells. *Biochemical and Biophysical Research Communications, 394*(3), 843-847.

Catlett-Falcone, R., Landowski, T., Oshiro, M., Turkson, J., Levitzki, A., Savino, R., Ciliberto, G., et al. (1999). Constitutive activation of Stat3 signaling confers resistance to qpoptosis in human U266 myeloma dells. *Immunity, 10*(1), 105-115.

Chardin, S., & Romand, R. (1995). Regeneration and mammalian auditory hair cells. *Science, 267*(5198), 707-711.

Chen, H., Ma, H., Sytwu, H., Wang, H., Chen, C. V., Liu, S., Chen, C., et al. (2010). Neural stem cells secrete factors that promote auditory cell proliferation via a leukemia inhibitory factor signaling pathway. *Journal of NeuroScienceResearch, 88*(15), 3308-3318.

Chen, P., & Segil, N. (1999). p27(Kip1) links cell proliferation to morphogenesis in the developing organ of Corti. *Development, 126*(8), 1581 -1590.

Chen, P., Zindy, F., Abdala, C., Liu, F., Li, X., Roussel, M. F., & Segil, N. (2003). Progressive hearing loss in mice lacking the cyclin-dependent kinase inhibitor Ink4d. *Nature Cell Biology, 5*(5), 422-426.

Chen, Z., Laurence, A., Kanno, Y., Pacher-Zavisin, M., Zhu, B., Tato, C., Yoshimura, A., et al. (2006). Selective regulatory function of Socs3 in the formation of IL-17-secreting T cells. *Proceedings of the National Academy of Sciences of the United States of America, 103*(21), 8137 -8142.

Chiu, L. L., Cunningham, L. L., Raible, D. W., Rubel, E. W., & Ou, H. C. (2008). Using the zebrafish lateral line to screen for ototoxicity. *Journal of the Association for Research in Otolaryngology, 9*(2), 178-190.

Choo, B., Kondrichin, I., Parinov, S., Emelyanov, A., Go, W., Toh, W., & Korzh, V. (2006). Zebrafish transgenic Enhancer TRAP line database (ZETRAP). *BMC Developmental Biology, 6*(1), 5.

Chung, C. D., Liao, J., Liu, B., Rao, X., Jay, P., Berta, P., & Shuai, K. (1997). Specific inhibition of Stat3 signal transduction by PIAS3. *Science, 278*(5344), 1803-1805.

Chung, J., Uchida, E., Grammer, T., & Blenis, J. (1997). STAT3 serine phosphorylation by ERK-dependent and -independent pathways negatively modulates its tyrosine phosphorylation. *Molecular and Cellular Biology, 17*(11), 6508-6516.

Cloonan, N., Forrest, A. R. R., Kolle, G., Gardiner, B. B. A., Faulkner, G. J., Brown,

M. K., Taylor, D. F., et al. (2008). Stem cell transcriptome profiling via massive-scale mRNA sequencing. *Nature Methods*, *5*(7), 613-619.

Coffin, A. B., Dabdoub, A., Kelley, M. W., & Popper, A. N. (2007). Myosin VI and VIIa distribution among inner ear epithelia in diverse fishes. *Hearing Research*, *224*(1-2), 15-26.

Collum, R. G., Brutsaert, S., Lee, G., & Schindler, C. (2000). A Stat3-interacting protein (StIP1) regulates cytokine signal transduction. *Proceedings of the National Academy of Sciences of the United States of America*, *97*(18), 10120 -10125.

Corwin, J. T. (1981). Postembryonic production and aging of inner ear hair cells in sharks. *The Journal of Comparative Neurology*, *201*(4), 541-553.

Corwin, J., & Cotanche, D. (1988). Regeneration of sensory hair cells after acoustic trauma. *Science*, *240*(4860), 1772-1774.

Cotanche, D. A., Saunders, J. C., & Tilney, L. G. (1987). Hair cell damage produced by acoustic trauma in the chick cochlea. *Hearing Research*, *25*(2-3), 267-286.

Cressman, D. E., Greenbaum, L. E., DeAngelis, R. A., Ciliberto, G., Furth, E. E., Poli, V., & Taub, R. (1996). Liver failure and defective hepatocyte regeneration in Interleukin-6-deficient mice. *Science*, *274*(5291), 1379-1383.

Croker, B. A., Krebs, D. L., Zhang, J., Wormald, S., Willson, T. A., Stanley, E. G., Robb, L., et al. (2003). SOCS3 negatively regulates IL-6 signaling in vivo. *Nature Immunology*, *4*(6), 540-545.

Croker, B. A., Metcalf, D., Robb, L., Wei, W., Mifsud, S., DiRago, L., Cluse, L. A., et al. (2004). SOCS3 is a critical physiological negative regulator of G-CSF signaling and emergency granulopoiesis. *Immunity*, *20*(2), 153-165.

Croker, B. A., Kiu, H., & Nicholson, S. E. (2008). SOCS regulation of the JAK/STAT signalling pathway. *Seminars in Cell & Developmental Biology*, *19*(4), 414-422.

Cruz, R. M., Lambert, P. R., & Rubel, E. W. (1987). Light microscopic evidence of hair cell regeneration after gentamicin toxicity in chick cochlea. *Archives of Otolaryngology-Head & Neck Surgery*, *113*(10), 1058-1062.

Curado, S., Stainier, D. Y. R., & Anderson, R. M. (2008). Nitroreductase-mediated cell/tissue ablation in zebrafish: a spatially and temporally controlled ablation method with applications in developmental and regeneration studies. *Nature Protocols*, *3*(6), 948-954.

Dabdoub, A., Puligilla, C., Jones, J. M., Fritzsch, B., Cheah, K. S. E., Pevny, L. H., & Kelley, M. W. (2008). Sox2 signaling in prosensory domain specification and subsequent hair cell differentiation in the developing cochlea. *Proceedings of the National Academy of Sciences the United States of America*, *105*(47), 18396 -18401.

Darnowski, J. W., Goulette, F. A., Guan, Y., Chatterjee, D., Yang, Z., Cousens, L. P., & Chin, Y. E. (2006). Stat3 cleavage by caspases: impact on full-length Stat3

expression, fragment formation, and transcriptional activity. *Journal of Biological Chemistry*, *281*(26), 17707 -17717.

Daudet, N., Gibson, R., Shang, J., Bernard, A., Lewis, J., & Stone, J. (2009). Notch regulation of progenitor cell behavior in quiescent and regenerating auditory epithelium of mature birds. *Developmental Biology*, *326*(1), 86-100.

De Souza, D., Fabri, L. J., Nash, A., Hilton, D. J., Nicola, N. A., & Baca, M. (2002). SH2 domains from suppressor of cytokine signaling-3 and protein tyrosine phosphatase SHP-2 have similar binding specificities†. *Biochemistry*, *41*(29), 9229-9236.

Decker, T., & Kovarik, P. (2000). Serine phosphorylation of STATs. *Oncogene*, *19*(21), 2628-2637.

Decotto, E., & Spradling, A. C. (2005). The Drosophila ovarian and testis stem cell niches: similar somatic stem cells and signals. *Developmental Cell*, *9*(4), 501-510.

Demoulin, J., Uyttenhove, C., Van Roost, E., DeLestre, B., Donckers, D., Van Snick, J., & Renauld, J. (1996). A single tyrosine of the interleukin-9 (IL-9) receptor is required for STAT activation, antiapoptotic activity, and growth regulation by IL-9. *Molecular and Cellular Biology*, *16*(9), 4710-4716.

Doetzlhofer, A., Basch, M. L., Ohyama, T., Gessler, M., Groves, A. K., & Segil, N. (2009). Hey2 regulation by FGF provides a Notch-independent mechanism for maintaining pillar cell fate in the organ of Corti. *Developmental cell*, *16*(1), 58-69.

Dooling, R. J., Ryals, B. M., Dent, M. L., & Reid, T. L. (2006). Perception of complex sounds in budgerigars (Melopsittacus undulatus) with temporary hearing loss. *The Journal of the Acoustical Society of America*, *119*(4), 2524-2532.

Driver, E. C., & Kelley, M. W. (2009). Specification of cell fate in the mammalian cochlea. *Birth Defects Research Part C: Embryo Today: Reviews*, *87*(3), 212-221.

Dufourcq, P., Roussigné, M., Blader, P., Rosa, F., Peyrieras, N., & Vriz, S. (2006). Mechano-sensory organ regeneration in adults: The zebrafish lateral line as a model. *Molecular and Cellular Neuroscience*, *33*(2), 180-187.

Duggan, D. J., Bittner, M., Chen, Y., Meltzer, P., & Trent, J. M. (1999). Expression profiling using cDNA microarrays. *Nature Genetics*, *21*, 10-14.

Dye, B. J., Frank, T. C., Newlands, S. D., & Dickman, J. D. (1999). Distribution and time course of hair cell regeneration in the pigeon utricle. *Hearing Research*, *133*(1-2), 17-26.

Dziennis, S., & Alkayed, N. J. (2008). Role of Signal Transducer and Activator of Transcription 3 in Neuronal Survival and Regeneration. *Reviews in the neurosciences*, *19*(4-5), 341-361.

Eid, J., Fehr, A., Gray, J., Luong, K., Lyle, J., Otto, G., Peluso, P., et al. (2009). Real-

time DNA sequencing from single polymerase molecules. *Science*, *323*(5910), 133-138.

Ekelund, E., Saaf, A., Tengvall-Linder, M., Melen, E., Link, J., Barker, J., Reynolds, N. J., et al. (2006). Elevated expression and genetic association links the SOCS3 gene to atopic dermatitis. *American Journal of Human Genetics*, *78*(6), 1060-1065.

Ernst, M., Najdovska, M., Grail, D., Lundgren-May, T., Buchert, M., Tye, H., Matthews, V. B., et al. (2008). STAT3 and STAT1 mediate IL-11–dependent and inflammation-associated gastric tumorigenesis in gp130 receptor mutant mice. *The Journal of Clinical Investigation*, *118*(5), 1727-1738.

Fay, R. R. (1978). Phase-locking in goldfish saccular nerve fibres accounts for frequency discrimination capacities. *Nature*, *275*(5678), 320-322.

Feng, L., Liu, H., Liu, Y., Lu, Z., Guo, G., Guo, S., Zheng, H., et al. (2010). Power of deep aequencing and Agilent microarray for gene expression profiling study. *Molecular Biotechnology*, *45*(2), 101-110.

Fortini, M. E. (2009). Notch signaling: The core pathway and its posttranslational regulation. *Developmental Cell*, *16*(5), 633-647.

Friedman, L. M., Dror, A. A., Mor, E., Tenne, T., Toren, G., Satoh, T., Biesemeier, D. J., et al. (2009). MicroRNAs are essential for development and function of inner ear hair cells in vertebrates. *Proceedings of the National Academy of Sciences of the United States of America*, *106*(19), 7915 -7920.

Fritzsch, B., Beisel, K. W., Pauley, S., & Soukup, G. (2007). Molecular evolution of the vertebrate mechanosensory cell and ear. *The International Journal of Developmental Biology*, *51*(6-7), 663-678.

Fritzsch, B., Pauley, S., & Beisel, K. W. (2006). Cells, molecules and morphogenesis: the making of the vertebrate ear. *Brain Research*, *1091*(1), 151-171.

Fuchs, P. A., Glowatzki, E., & Moser, T. (2003). The afferent synapse of cochlear hair cells. *Current Opinion in Neurobiology*, *13*(4), 452-458. Gaemers, I. C., Vos, H. L., Volders, H. H., van der Valk, S. W., & Hilkens, J. (2001). A STAT-responsive element in the promoter of the episialin/MUC1 gene is involved in Its overexpression in carcinoma cells. *Journal of Biological Chemistry*, *276*(9), 6191 -6199.

Gale, J. E., Meyers, J. R., Periasamy, A., & Corwin, T. (2002). Survival of bundleless hair cells and subsequent bundle replacement in the bullfrog's saccule. *Journal of Neurobiology*, *50*(2), 81-92.

Gao, H., & Ward, P. A. (2007). STAT3 and suppressor of cytokine signaling 3: potential targets in lung inflammatory responses. *Expert Opinion on Therapeutic Targets*, *11*(7), 869-880.

Garcia, R., Yu, C., Hudnall, A., Catlett, R., Nelson, K., Smithgall, T., Fujita, D., et al. (1997). Constitutive activation of Stat3 in fibroblasts transformed by diverse oncoproteins and in breast carcinoma cells. *Cell Growth & Differentiation*,

8(12), 1267-1276.

Gartsbein, M., Alt, A., Hashimoto, K., Nakajima, K., Kuroki, T., & Tennenbaum, T. (2006). The role of protein kinase C delta activation and STAT3 Ser727 phosphorylation in insulin-induced keratinocyte proliferation. *Journal of Cell Science*, *119*(3), 470-481.

Gatsios, P., Terstegen, L., Schliess, F., Häussinger, D., Kerr, I. M., Heinrich, P. C., & Graeve, L. (1998). Activation of the Janus kinase/signal transducer and activator of transcription pathway by osmotic shock. *Journal of Biological Chemistry*, *273*(36), 22962 -22968.

Ge, X., Jung, Y., Wu, Q., Kibbe, W. A., & Wang, S. M. (2006). Annotating nonspecific SAGE tags with microarray data. *Genomics*, *87*(1), 173-180.

Gillespie, P. G., & Walker, R. G. (2001). Molecular basis of mechanosensory transduction. *Nature*, *413*(6852), 194-202.

Girod, D. A., Tucci, D. L., & Rubel, E. W. (1991). Anatomical correlates of functional recovery in the avian inner ear following aminoglycoside ototoxicity. *The Laryngoscope*, *101*(11), 1139-1149.

Goodyear, R., Killick, R., Legan, P. K., & Richardson, G. P. (1996). Distribution of beta-tectorin mRNA in the early posthatch and developing avian inner ear. *Hearing Research*, *96*(1-2), 167-178.

Gordon, W. R., Arnett, K. L., & Blacklow, S. C. (2008). The molecular logic of Notch signaling - a structural and biochemical perspective. *Journal of Cell Science*, *121*(19), 3109-3119.

Goren, I., Linke, A., Muller, E., Pfeilschifter, J., & Frank, S. (2005). The suppressor of cytokine signaling-3 Is upregulated in impaired skin repair: implications for keratinocyte proliferation. *The Journal of Investigative Dermatology* , *126*(2), 477-485.

Gough, D. J., Corlett, A., Schlessinger, K., Wegrzyn, J., Larner, A. C., & Levy, D. E. (2009). Mitochondrial STAT3 supports Ras-dependent oncogenic transformation. *Science*, *324*(5935), 1713-1716.

Gritsko, T., Williams, A., Turkson, J., Kaneko, S., Bowman, T., Huang, M., Nam, S., et al. (2006). Persistent activation of Stat3 signaling induces Survivin gene expression and confers resistance to apoptosis in human breast cancer cells. *Clinical Cancer Research*, *12*(1), 11 -19.

Gross, J., Machulik, A., Gross, J., Machulik, A., Moller, R., Gross, J., Machulik, A., et al. (2008). mRNA expression of members of the IGF system in the organ of Corti, the modiolus and the stria vascularis of newborn rats. *Growth Factors*, *26*(4), 180-191.

Gubbels, S. P., Woessner, D. W., Mitchell, J. C., Ricci, A. J., & Brigande, J. V. (2008). Functional auditory hair cells produced in the mammalian cochlea by in utero gene transfer. *Nature*, *455*(7212), 537-541.

Guo, L., Lobenhofer, E. K., Wang, C., Shippy, R., Harris, S. C., Zhang, L., Mei, N.,

et al. (2006). Rat toxicogenomic study reveals analytical consistency across microarray platforms. *Nature Biotechnology*, *24*(9), 1162-1169.

Guttman, M., Garber, M., Levin, J. Z., Donaghey, J., Robinson, J., Adiconis, X., Fan, L., et al. (2010). Ab initio reconstruction of cell type-specific transcriptomes in mouse reveals the conserved multi-exonic structure of lincRNAs. *Nature Biotechnology*, *28*(5), 503-510.

Haan, S., Ferguson, P., Sommer, U., Hiremath, M., McVicar, D. W., Heinrich, P. C., Johnston, J. A., et al. (2003). Tyrosine phosphorylation disrupts elongin interaction and accelerates SOCS3 degradation. *Journal of Biological Chemistry*, *278*(34), 31972 -31979.

Haas, P., & Gilmour, D. (2006). Chemokine signaling mediates self-organizing tissue migration in the zebrafish lateral line. *Developmental Cell*, *10*(5), 673-680.

Haddon, C., Jiang, Y., Smithers, L., & Lewis, J. (1998). Delta-Notch signalling and the patterning of sensory cell differentiation in the zebrafish ear: evidence from the mind bomb mutant. *Development*, *125*(23), 4637 -4644.

Haddon, C., Mowbray, C., Whitfield, T., Jones, D., Gschmeissner, S., & Lewis, J. (1999). Hair cells without supporting cells: further studies in the ear of the zebrafish mind bomb mutant. *Journal of Neurocytology*, *28*(10), 837-850.

Haga, S., Terui, K., Zhang, H. Q., Enosawa, S., Ogawa, W., Inoue, H., Okuyama, T., et al. (2003). Stat3 protects against Fas-induced liver injury by redox-dependent and -independent mechanisms. *The Journal of Clinical Investigation*, *112*(7), 989-998.

Halgren, R. G., Fielden, M. R., Fong, C. J., & Zacharewski, T. R. (2001). Assessment of clone identity and sequence fidelity for 1189 IMAGE cDNA clones. *Nucleic Acids Research*, *29*(2), 582 -588.

Hama, K., & Yamada, Y. (1977). Fine structure of the ordinary lateral line organ. II. The lateral line canal organ of spotted shark, Mustelus manazo. *Cell and Tissue Research*, *176*(1), 23-36.

Han, Z., Yang, J., Chi, F., Cong, N., Huang, Y., Gao, Z., & Li, W. (2010). Survival and fate of transplanted embryonic neural stem cells by Atoh1 gene transfer in guinea pigs cochlea. *NeuroReport*, *21*(7), 490-496.

Harbig, J., Sprinkle, R., & Enkemann, S. A. (2005). A sequence-based identification of the genes detected by probesets on the Affymetrix U133 plus 2.0 array. *Nucleic Acids Research*, *33*(3), e31.

Harris, J. A., Cheng, A. G., Cunningham, L. L., MacDonald, G., Raible, D. W., & Rubel, E. W. (2003). Neomycin-induced hair cell death and rapid regeneration in the lateral line of zebrafish (Danio rerio). *Journal of the Association for Research in Otolaryngology*, *4*(2), 219-234.

Hawkins, R. D., Bashiardes, S., Helms, C. A., Hu, L., Saccone, N. L., Warchol, M. E., & Lovett, M. (2003). Gene expression differences in quiescent versus regenerating hair cells of avian sensory epithelia: implications for human

hearing and balance disorders. *Human Molecular Genetics*, *12*(11), 1261 - 1272.

Hawkins, R. D., Bashiardes, S., Powder, K. E., Sajan, S. A., Bhonagiri, V., Alvarado, D. M., Speck, J., et al. (2007). Large scale gene expression profiles of regenerating inner ear sensory epithelia. *PLoS ONE*, *2*(6), e525.

Hazan-Halevy, I., Harris, D., Liu, Z., Liu, J., Li, P., Chen, X., Shanker, S., et al. (2010). STAT3 is constitutively phosphorylated on serine 727 residues, binds DNA, and activates transcription in CLL cells. *Blood*, *115*(14), 2852-2863.

He, B., You, L., Uematsu, K., Zang, K., Xu, Z., Lee, A. Y., Costello, J. F., et al. (2003). SOCS-3 is frequently silenced by hypermethylation and suppresses cell growth in human lung cancer. *Proceedings of the National Academy of Sciences of the United States of America*, *100*(24), 14133 -14138.

Hegedűs, Z., Zakrzewska, A., Ágoston, V. C., Ordas, A., Rácz, P., Mink, M., Spaink, H. P., et al. (2009). Deep sequencing of the zebrafish transcriptome response to mycobacterium infection. *Molecular Immunology*, *46*(15), 2918-2930.

Heim, M., Kerr, I., Stark, G., & Darnell, J. (1995). Contribution of STAT SH2 groups to specific interferon signaling by the Jak-STAT pathway. *Science*, *267*(5202), 1347-1349.

Hernández, P. P., Olivari, F. A., Sarrazin, A. F., Sandoval, P. C., & Allende, M. L. (2007). Regeneration in zebrafish lateral line neuromasts: Expression of the neural progenitor cell marker sox2 and proliferation-dependent and-independent mechanisms of hair cell renewal. *Developmental Neurobiology*, *67*(5), 637-654.

Hertzano, R., Montcouquiol, M., Rashi-Elkeles, S., Elkon, R., Yücel, R., Frankel, W. N., Rechavi, G., et al. (2004). Transcription profiling of inner ears from Pou4f3ddl/ddl identifies Gfi1 as a target of the Pou4f3 deafness gene. *Human Molecular Genetics*, *13*(18), 2143 -2153.

Hevehan, D. L., Miller, W. M., & Papoutsakis, E. T. (2002). Differential expression and phosphorylation of distinct STAT3 proteins during granulocytic differentiation. *Blood*, *99*(5), 1627-1637.

Higgs, D. M., Souza, M. J., Wilkins, H. R., Presson, J. C., & Popper, A. N. (2002). Age- and size-related changes in the inner ear and hearing ability of the adult zebrafish (Danio rerio). *Journal of the Association for Research in Otolaryngology*, *3*(2), 174-184.

Hirabayashi, Y., & Gotoh, Y. (2005). Stage-dependent fate determination of neural precursor cells in mouse forebrain. *NeuroScienceResearch*, *51*(4), 331-336.

't Hoen, P. A. C., Ariyurek, Y., Thygesen, H. H., Vreugdenhil, E., Vossen, R. H. A. M., de Menezes, R. X., Boer, J. M., et al. (2008). Deep sequencing-based expression analysis shows major advances in robustness, resolution and inter-lab portability over five microarray platforms. *Nucleic Acids Research*, *36*(21), e141.

Holley, M., Kneebone, A., & Milo, M. (2007). Information for gene networks in inner ear development: A study centered on the transcription factor gata2. *Hearing Research*, *227*(1-2), 32-40.

Hordichok, A. J., & Steyger, P. S. (2007). Closure of supporting cell scar formations requires dynamic actin mechanisms. *Hearing Research*, *232*(1-2), 1-19.

Hsu, C., Hou, M., Hong, J., Wu, J., & Her, G. M. (2009). Inducible male infertility by targeted cell ablation in zebrafish testis. *Marine Biotechnology*, *12*(4), 466-478.

Hu, S., Lin, P., Liao, C., Gong, H., Lin, G., Kawakami, K., & Wu, J. (2009). Nitroreductase-mediated gonadal dysgenesis for infertility control of genetically modified zebrafish. *Marine Biotechnology*, *12*(5), 569-578.

Hudspeth, A. J. (1997). How hearing happens. *Neuron*, *19*(5), 947-950.

Hughes, T. R., & Shoemaker, D. D. (2001). DNA microarrays for expression profiling. *Current Opinion in Chemical Biology*, *5*(1), 21-25.

Inoue, M., Minami, M., Matsumoto, M., Kishimoto, T., & Akira, S. (1997). The amino acid residues immediately carboxyl-terminal to the tyrosine phosphorylation site contribute to Interleukin 6-specific activation of Signal Transducer and Activator of Transcription 3. *Journal of Biological Chemistry*, *272*(14), 9550 -9555.

Izumikawa, M., Batts, S. A., Miyazawa, T., Swiderski, D. L., & Raphael, Y. (2008). Response of the flat cochlear epithelium to forced expression of Atoh1. *Hearing Research*, *240*(1-2), 52-56.

Izumikawa, M., Minoda, R., Kawamoto, K., Abrashkin, K. A., Swiderski, D. L., Dolan, D. F., Brough, D. E., et al. (2005). Auditory hair cell replacement and hearing improvement by Atoh1 gene therapy in deaf mammals. *Nature Medicine*, *11*(3), 271-276.

Jacobson, N. G., Szabo, S. J., Weber-Nordt, R. M., Zhong, Z., Schreiber, R. D., Darnell, J. E., & Murphy, K. M. (1995). Interleukin 12 signaling in T helper type 1 (Th1) cells involves tyrosine phosphorylation of signal transducer and activator of transcription (Stat)3 and Stat4. *The Journal of Experimental Medicine*, *181*(5), 1755-1762.

Jacques, B. E., Montcouquiol, M. E., Layman, E. M., Lewandoski, M., & Kelley, M. W. (2007). Fgf8 induces pillar cell fate and regulates cellular patterning in the mammalian cochlea. *Development*, *134*(16), 3021 -3029.

Jain, N., Zhang, T., Fong, S. L., Lim, C. P., & Cao, X. (1998). Repression of Stat3 activity by activation of mitogen-activated protein kinase (MAPK). *Oncogene*, *17*(24), 3157-3167.

Jain, N., Zhang, T., Kee, W. H., Li, W., & Cao, X. (1999). Protein kinase C δ associates with and phosphorylates Stat3 in an Interleukin-6-dependent manner. *Journal of Biological Chemistry*, *274*(34), 24392 -24400.

Järvinen, A., Hautaniemi, S., Edgren, H., Auvinen, P., Saarela, J., Kallioniemi, O., &

Monni, O. (2004). Are data from different gene expression microarray platforms comparable? *Genomics*, *83*(6), 1164-1168.

Ji, J., Elyaman, W., Yip, H. K., Lee, V. W. H., Yick, L., Hugon, J., & So, K. (2004). CNTF promotes survival of retinal ganglion cells after induction of ocular hypertension in rats: the possible involvement of STAT3 pathway. *European Journal of Neuroscience*, *19*(2), 265-272.

Jiang, H., Patel, P. H., Kohlmaier, A., Grenley, M. O., McEwen, D. G., & Edgar, B. A. (2009). Cytokine/Jak/Stat signaling mediates regeneration and homeostasis in the Drosophila midgut. *Cell*, *137*(7), 1343-1355.

Jones, J., & Corwin, J. (1993). Replacement of lateral line sensory organs during tail regeneration in salamanders: identification of progenitor cells and analysis of leukocyte activity. *The Journal of Neuroscience*, *13*(3), 1022-1034.

Jones, J. M., Montcouquiol, M., Dabdoub, A., Woods, C., & Kelley, M. W. (2006). Inhibitors of differentiation and DNA binding (Ids) regulate Math1 and hair cell formation during the development of the organ of Corti. *The Journal of Neuroscience*, *26*(2), 550-558.

Jørgensen, J. M., & Mathiesen, C. (1988). The avian inner ear. *Naturwissenschaften*, *75*(6), 319-320.

Kamakura, S., Oishi, K., Yoshimatsu, T., Nakafuku, M., Masuyama, N., & Gotoh, Y. (2004). Hes binding to STAT3 mediates crosstalk between Notch and JAK-STAT signalling. *Nature Cell Biology*, *6*(6), 547-554.

Kassen, S. C., Thummel, R., Campochiaro, L. A., Harding, M. J., Bennett, N. A., & Hyde, D. R. (2009). CNTF induces photoreceptor neuroprotection and Müller glial cell proliferation through two different signaling pathways in the adult zebrafish retina. *Experimental Eye Research*, *88*(6), 1051-1064.

Kawasaki, E. S. (2006). The end of the microarray Tower of Babel: Will universal standards lead the way? *Journal of Biomolecular Techniques*, *17*(3), 200-206.

Kelley, M. W. (2007). Cellular commitment and differentiation in the organ of Corti. *The International Journal of Developmental Biology*, *51*(6-7), 571-583.

Kesser, B. W., & Lalwani, A. K. (2009). Gene therapy and stem cell transplantation: strategies for hearing restoration. *Advances in Oto-Rhino-Laryngology*, *66*, 64-86.

Kida, H., Mucenski, M. L., Thitoff, A. R., Le Cras, T. D., Park, K., Ikegami, M., Muller, W., et al. (2008). GP130-STAT3 regulates epithelial cell migration and is required for repair of the bronchiolar epithelium. *The American Journal of Pathology*, *172*(6), 1542-1554.

Kidder, B. L., Yang, J., & Palmer, S. (2008). Stat3 and c-Myc genome-wide promoter occupancy in embryonic stem cells. *PLoS ONE*, *3*(12), e3932.

Kiernan, A. E., Xu, J., & Gridley, T. (2006). The Notch ligand JAG1 is required for sensory progenitor development in the mammalian inner ear. *PLoS Genetics*, *2*(1), e4.

Kil, J., Warchol, M., & Corwin, J. (1997). Cell death, cell proliferation, and estimates of hair cell life spans in the vestibular organs of chicks. *Hearing Research*, *114*(1-2), 117-126.

Kim, J., Yoon, M., & Chen, J. (2009). Signal Transducer and Activator of Transcription 3 (STAT3) mediates amino acid inhibition of insulin signaling through Serine 727 phosphorylation. *Journal of Biological Chemistry*, *284*(51), 35425 -35432.

Kira, M., Sano, S., Takagi, S., Yoshikawa, K., Takeda, J., & Itami, S. (2002). STAT3 deficiency in keratinocytes leads to compromised cell migration through hyperphosphorylation of p130cas. *Journal of Biological Chemistry*, *277*(15), 12931 -12936.

Kirjavainen, A., Sulg, M., Heyd, F., Alitalo, K., Ylä-Herttuala, S., Möröy, T., Petrova, T. V., et al. (2008). Prox1 interacts with Atoh1 and Gfi1, and regulates cellular differentiation in the inner ear sensory epithelia. *Developmental Biology*, *322*(1), 33-45.

Kiuchi, N., Nakajima, K., Ichiba, M., Fukada, T., Narimatsu, M., Mizuno, K., Hibi, M., et al. (1999). STAT3 Is required for the gp130-mediated full activation of the c-myc gene. *The Journal of Experimental Medicine*, *189*(1), 63-73.

Kordula, T., Bugno, M., Goldstein, J., & Travis, J. (1995). Activation of Signal Transducer and Activator of Transcription-3 (STAT3) expression by Interferon-[gamma] and Interleukin-6 in hepatoma cells. *Biochemical and Biophysical Research Communications*, *216*(3), 999-1005.

Kothapalli, R., Yoder, S., Mane, S., & Loughran, T. (2002). Microarray results: how accurate are they? *BMC Bioinformatics*, *3*(1), 22.

Kren, B. T., Wong, P. Y., Shiota, A., Zhang, X., Zeng, Y., & Steer, C. J. (2009). Polysome trafficking of transcripts and microRNAs in regenerating liver after partial hepatectomy. *The American Journal of Physiology - Gastrointestinal and Liver Physiology*, *297*(6), G1181-1192.

Kuliyev, E., Doherty, J. R., & Mead, P. E. (2005). Expression of Xenopus suppressor of cytokine signaling 3 (xSOCS3) is induced by epithelial wounding. *Developmental Dynamics*, *233*(3), 1123-1130.

Kuntz, A., & Oesterle, E. (1998). Transforming growth factor α with insulin stimulates cell proliferation in vivo in adult rat vestibular sensory epithelium. *The Journal of Comparative Neurology*, *399*(3), 413-423.

Kuo, W. P., Jenssen, T., Butte, A. J., Ohno-Machado, L., & Kohane, I. S. (2002). Analysis of matched mRNA measurements from two different microarray technologies. *Bioinformatics*, *18*(3), 405 -412.

Laine, H., Doetzlhofer, A., Mantela, J., Ylikoski, J., Laiho, M., Roussel, M. F., Segil, N., et al. (2007). p19Ink4d and p21Cip1 collaborate to maintain the postmitotic state of auditory hair cells, their codeletion leading to DNA damage and p53-mediated apoptosis. *The Journal of Neuroscience*, *27*(6), 1434-1444.

Laine, H., Sulg, M., Kirjavainen, A., & Pirvola, U. (2010). Cell cycle regulation in the inner ear sensory epithelia: Role of cyclin D1 and cyclin-dependent kinase inhibitors. *Developmental Biology*, *337*(1), 134-146.

Lambert, P. R. (1994). Inner ear hair cell regeneration in a mammal: Identification of a triggering factor. *The Laryngoscope*, *104*(6), 701-718.

Lanford, P. J., Lan, Y., Jiang, R., Lindsell, C., Weinmaster, G., Gridley, T., & Kelley, M. W. (1999). Notch signalling pathway mediates hair cell development in mammalian cochlea. *Nature Genetics*, *21*(3), 289-292.

Lang, R. (2005). Tuning of macrophage responses by Stat3-inducing cytokines: molecular mechanisms and consequences in infection. *Immunobiology*, *210*(2-4), 63-76.

Lee, J. H., Suk, J., Park, J., Kim, S. B., Kwak, S. S., Kim, J. W., Lee, C. H., et al. (2009). Notch signal activates hypoxia pathway through HES1-dependent SRC/signal transducers and activators of transcription 3 pathway. *Molecular Cancer Research*, *7*(10), 1663 -1671.

Lee, J., Wang, M., & Chen, J. (2009). Acetylation and activation of STAT3 mediated by nuclear translocation of CD44. *The Journal of Cell Biology*, *185*(6), 949-957.

Lee, K. H., & Cotanche, D. A. (1996). Potential role of BFGF and retinoic acid in the regeneration of chicken cochlear hair cells. *Hearing Research*, *94*(1-2), 1-13.

Lee, N., Neitzel, K. L., Devlin, B. K., & MacLennan, A. J. (2004). STAT3 phosphorylation in injured axons before sensory and motor neuron nuclei: Potential role for STAT3 as a retrograde signaling transcription factor. *The Journal of Comparative Neurology*, *474*(4), 535-545.

Levic, S., Nie, L., Tuteja, D., Harvey, M., Sokolowski, B. H. A., & Yamoah, E. N. (2007). Development and regeneration of hair cells share common functional features. *Proceedings of the National Academy of Sciences of the United States of America*, *104*(48), 19108 -19113.

Li, H., Kloosterman, W., & Fekete, D. M. (2010). MicroRNA-183 family members regulate sensorineural fates in the inner ear. *The Journal of Neuroscience*, *30*(9), 3254-3263.

Li, H., Liu, H., & Heller, S. (2003). Pluripotent stem cells from the adult mouse inner ear. *Nature Medicine*, *9*(10), 1293-1299.

Li, J., Pankratz, M., & Johnson, J. A. (2002). Differential gene expression patterns revealed by oligonucleotide versus long cDNA arrays. *Toxicological Sciences*, *69*(2), 383 -390.

Li, W., Liang, X., Kellendonk, C., Poli, V., & Taub, R. (2002). STAT3 contributes to the mitogenic response of hepatocytes during iver regeneration. *Journal of Biological Chemistry*, *277*(32), 28411 -28417.

Liang, J., & Burgess, S. M. (2009). Gross and fine dissection of inner ear sensory epithelia in adult zebrafish (Danio rerio). *Journal of Visualized Experiments*,

(27).

Lim, C. P., & Cao, X. (2006). Structure, function, and regulation of STAT proteins. *Molecular BioSystems*, *2*(11), 536.

Lim, D. J. (1976). Ultrastructural cochlear changes following acoustic hyperstimulation and ototoxicity. *The Annals of Otology, Rhinology, and Laryngology*, *85*(6 PT. 1), 740-751.

Lin, L., Amin, R., Gallicano, G. I., Glasgow, E., Jogunoori, W., Jessup, J. M., Zasloff, M., et al. (2009). The STAT3 inhibitor NSC 74859 is effective in hepatocellular cancers with disrupted TGF-beta signaling. *Oncogene*, *28*(7), 961-972.

Lin, S., Gaiano, N., Culp, P., Burns, J., Friedmann, T., Yee, J., & Hopkins, N. (1994). Integration and germ-line transmission of a pseudotyped retroviral vector in zebrafish. *Science*, *265*(5172), 666-669.

Liu, J., Shin, J. H., Hyrc, K. L., Liu, S., Lei, D., Holley, M. C., & Bao, J. (2006). Stem cell therapy for hearing loss: Math1 overexpression in VOT-E36 cells. *Otology and Neurotology*, *27*(3), 414-421.

Liu, L., McBride, K. M., & Reich, N. C. (2005). STAT3 nuclear import is independent of tyrosine phosphorylation and mediated by importin-α3. *Proceedings of the National Academy of Sciences of the United States of America*, *102*(23), 8150 -8155.

Loffler, D., Brocke-Heidrich, K., Pfeifer, G., Stocsits, C., Hackermuller, J., Kretzschmar, A. K., Burger, R., et al. (2007). Interleukin-6 dependent survival of multiple myeloma cells involves the Stat3-mediated induction of microRNA-21 through a highly conserved enhancer. *Blood*, *110*(4), 1330-1333.

Lombarte, A., Yan, H. Y., Popper, A. N., Chang, J. S., & Platt, C. (1993). Damage and regeneration of hair cell ciliary bundles in a fish ear following treatment with gentamicin. *Hearing Research*, *64*(2), 166-174.

Löwenheim, H., Furness, D. N., Kil, J., Zinn, C., Gültig, K., Fero, M. L., Frost, D., et al. (1999). Gene disruption of p27Kip1 allows cell proliferation in the postnatal and adult organ of Corti. *Proceedings of the National Academy of Sciences of the United States of America*, *96*(7), 4084 -4088.

Lufei, C., Ma, J., Huang, G., Zhang, T., Novotny-Diermayr, V., Ong, C. T., & Cao, X. (2003). GRIM-19, a death-regulatory gene product, suppresses Stat3 activity via functional interaction. *EMBO J*, *22*(6), 1325-1335.

Lütticken, C., Wegenka, U. M., Yuan, J., Buschmann, J., Schindler, C., Ziemiecki, A., Harpur, A. G., et al. (1994). Association of transcription factor APRF and protein kinase Jak1 with the interleukin-6 signal transducer gp130. *Science*, *263*(5143), 89-92.

Ma, E. Y., Rubel, E. W., & Raible, D. W. (2008). Notch signaling regulates the extent of hair cell regeneration in the zebrafish lateral line. *The Journal of*

Neuroscience, *28*(9), 2261-2273.

Ma, J., & Cao, X. (2006). Regulation of Stat3 nuclear import by importin [alpha]5 and importin [alpha]7 via two different functional sequence elements. *Cellular Signalling*, *18*(8), 1117-1126.

Ma, J., Zhang, T., Novotny-Diermayr, V., Tan, A. L. C., & Cao, X. (2003). A novel sequence in the coiled-coil domain of Stat3 essential for its nuclear translocation. *Journal of Biological Chemistry*, *278*(31), 29252 -29260.

Mahboubi, K., Li, F., Plescia, J., Kirkiles-Smith, N. C., Mesri, M., Du, Y., Carroll, J. M., et al. (2001). Interleukin-11 up-regulates survivin expression in endothelial cells through a signal transducer and activator of transcription-3 pathway. *Laboratory Investigation; a Journal of Technical Methods and Pathology*, *81*(3), 327-334.

Malig, R., Varela, C., Agosin, E., & Melo, F. (2006). Accurate and unambiguous tag-to-gene mapping in serial analysis of gene expression. *BMC Bioinformatics*, *7*(1), 487.

Mantela, J., Jiang, Z., Ylikoski, J., Fritzsch, B., Zacksenhaus, E., & Pirvola, U. (2005). The retinoblastoma gene pathway regulates the postmitotic state of hair cells of the mouse inner ear. *Development*, *132*(10), 2377 -2388.

MAQC Consortium. (2006). The MicroArray Quality Control (MAQC) project shows inter- and intraplatform reproducibility of gene expression measurements. *Nature Biotechnology*, *24*(9), 1151-1161.

Margulies, M., Egholm, M., Altman, W. E., Attiya, S., Bader, J. S., Bemben, L. A., Berka, J., et al. (2005). Genome sequencing in microfabricated high-density picolitre reactors. *Nature*, *437*(7057), 376-380.

Marine, J. C., McKay, C., Wang, D., Topham, D. J., Parganas, E., Nakajima, H., Pendeville, H., et al. (1999). SOCS3 is essential in the regulation of fetal liver erythropoiesis. *Cell*, *98*(5), 617-627.

Marioni, J. C., Mason, C. E., Mane, S. M., Stephens, M., & Gilad, Y. (2008). RNA-seq: An assessment of technical reproducibility and comparison with gene expression arrays. *Genome Research*, *18*(9), 1509 -1517.

Maritano, D., Sugrue, M. L., Tininini, S., Dewilde, S., Strobl, B., Fu, X., Murray-Tait, V., et al. (2004). The STAT3 isoforms alpha and beta have unique and specific functions. *Nature Immunology*, *5*(4), 401-409.

Marquez, R. T., Wendlandt, E., Galle, C. S., Keck, K., & McCaffrey, A. P. (2010). MicroRNA-21 is upregulated during the proliferative phase of liver regeneration, targets Pellino-1, and inhibits NF-{kappa}B signaling. *The American Journal of Physiology - Gastrointestinal and Liver Physiology*, *298*(4), G535-541.

Martini, M., Pallini, R., Luongo, G., Cenci, T., Lucantoni, C., & Larocca, L. M. (2008). Prognostic relevance of SOCS3 hypermethylation in patients with glioblastoma multiforme. *International Journal of Cancer*, *123*(12), 2955-

2960.

Masuda, M., Suzui, M., Yasumatu, R., Nakashima, T., Kuratomi, Y., Azuma, K., Tomita, K., et al. (2002). Constitutive activation of signal transducers and activators of transcription 3 correlates with cyclin D1 overexpression and may provide a novel prognostic marker in head and neck squamous cell carcinoma. *Cancer Research*, *62*(12), 3351 -3355.

McDermott Jr., B. M., Asai, Y., Baucom, J. M., Jani, S. D., Castellanos, Y., Gomez, G., McClintock, J. M., et al. (2010). Transgenic labeling of hair cells in the zebrafish acousticolateralis system. *Gene Expression Patterns*, *10*(2-3), 113-118.

Mcgill, T. J. I., & Schuknecht, H. F. (1976). Human cochlear changes in noise induced hearing loss. *The Laryngoscope*, *86*(9), 1293-1302.

McHenry, M., Feitl, K., Strother, J., & Van Trump, W. (2009). Larval zebrafish rapidly sense the water flow of a predator's strike. *Biology Letters*, *5*(4), 477 - 479.

Melton, C., Judson, R. L., & Blelloch, R. (2010). Opposing microRNA families regulate self-renewal in mouse embryonic stem cells. *Nature*, *463*(7281), 621-626.

Miao, T., Wu, D., Zhang, Y., Bo, X., Subang, M. C., Wang, P., & Richardson, P. M. (2006). Suppressor of cytokine signaling-3 suppresses the ability of activated signal transducer and activator of transcription-3 to stimulate neurite growth in rat primary sensory neurons. *The Journal of Neuroscience*, *26*(37), 9512-9519.

Millimaki, B. B., Sweet, E. M., Dhason, M. S., & Riley, B. B. (2007). Zebrafish atoh1 genes: classic proneural activity in the inner ear and regulation by Fgf and Notch. *Development*, *134*(2), 295 -305.

Millimaki, B. B., Sweet, E. M., & Riley, B. B. (2010). Sox2 is required for maintenance and regeneration, but not initial development, of hair cells in the zebrafish inner ear. *Developmental Biology*, *338*(2), 262-269.

Minamoto, S., Ikegame, K., Ueno, K., Narazaki, M., Naka, T., Yamamoto, H., Matsumoto, T., et al. (1997). Cloning and functional analysis of new members of STAT Induced STAT Inhibitor (SSI) family: SSI-2 and SSI-3. *Biochemical and Biophysical Research Communications*, *237*(1), 79-83.

Minegishi, Y., Saito, M., Tsuchiya, S., Tsuge, I., Takada, H., Hara, T., Kawamura, N., et al. (2007). Dominant-negative mutations in the DNA-binding domain of STAT3 cause hyper-IgE syndrome. *Nature*, *448*(7157), 1058-1062.

Montgomery, J., Carton, G., Voigt, R., Baker, C., & Diebel, C. (2000). Sensory processing of water currents by fishes. *Philosophical Transactions of the Royal Society B: Biological Sciences*, *355*(1401), 1325-1327.

Montgomery, J. E., Parsons, M. J., & Hyde, D. R. (2010). A novel model of retinal ablation demonstrates that the extent of rod cell death regulates the origin of

the regenerated zebrafish rod photoreceptors. *The Journal of Comparative Neurology*, *518*(6), 800-814.

Morest, D. K., & Cotanche, D. A. (2004). Regeneration of the inner ear as a model of neural plasticity. *Journal of NeuroScienceResearch*, *78*(4), 455-460.

Mori, H., Hanada, R., Hanada, T., Aki, D., Mashima, R., Nishinakamura, H., Torisu, T., et al. (2004). Socs3 deficiency in the brain elevates leptin sensitivity and confers resistance to diet-induced obesity. *Nature Medicine*, *10*(7), 739-743.

Morrissy, A. S., Morin, R. D., Delaney, A., Zeng, T., McDonald, H., Jones, S., Zhao, Y., et al. (2009). Next-generation tag sequencing for cancer gene expression profiling. *Genome Research*, *19*(10), 1825 -1835.

Mortazavi, A., Williams, B. A., McCue, K., Schaeffer, L., & Wold, B. (2008). Mapping and quantifying mammalian transcriptomes by RNA-Seq. *Nature Methods*, *5*(7), 621-628.

Mueller, K. L., Jacques, B. E., & Kelley, M. W. (2002). Fibroblast growth factor signaling regulates pillar cell development in the organ of Corti. *The Journal of Neuroscience*, *22*(21), 9368-9377.

Müller, A., Hauk, T. G., Leibinger, M., Marienfeld, R., & Fischer, D. (2009). Exogenous CNTF stimulates axon regeneration of retinal ganglion cells partially via endogenous CNTF. *Molecular and Cellular Neuroscience*, *41*(2), 233-246.

Müller, M., Smolders, J. W. T., Ding-Pfennigdorff, D., & Klinke, R. (1996). Regeneration after tall hair cell damage following severe acoustic trauma in adult pigeons: correlation between cochlear morphology, compound action potential responses and single fiber properties in single animals. *Hearing Research*, *102*(1-2), 133-154.

Murray, P. J. (2007). The JAK-STAT signaling pathway: input and output integration. *The Journal of Immunology*, *178*(5), 2623-2629.

Nagalakshmi, U., Wang, Z., Waern, K., Shou, C., Raha, D., Gerstein, M., & Snyder, M. (2008). The transcriptional landscape of the yeast genome defined by RNA sequencing. *Science*, *320*(5881), 1344-1349.

Naka, T., Narazaki, M., Hirata, M., Matsumoto, T., Minamoto, S., Aono, A., Nishimoto, N., et al. (1997). Structure and function of a new STAT-induced STAT inhibitor. *Nature*, *387*(6636), 924-929.

Nakashima, K., Yanagisawa, M., Arakawa, H., Kimura, N., Hisatsune, T., Kawabata, M., Miyazono, K., et al. (1999). Synergistic signaling in fetal brain by STAT3-Smad1 complex bridged by p300. *Science*, *284*(5413), 479-482.

Natarajan, A., Wagner, B., & Sibilia, M. (2007). The EGF receptor is required for efficient liver regeneration. *Proceedings of the National Academy of Sciences of the United States of America*, *104*(43), 17081 -17086.

Ng, D. C. H., Lim, C. P., Lin, B. H., Zhang, T., & Cao, X. (2010). SCG10-like protein (SCLIP) is a STAT3-interacting protein involved in maintaining

epithelial morphology in MCF-7 breast cancer cells. *The Biochemical Journal*, *425*(1), 95-105.

Ng, D. C. H., Lin, B. H., Lim, C. P., Huang, G., Zhang, T., Poli, V., & Cao, X. (2006). Stat3 regulates microtubules by antagonizing the depolymerization activity of stathmin. *The Journal of Cell Biology*, *172*(2), 245-257.

Ng, J., & Cantrell, D. (1997). STAT3 is a serine kinase target in T lymphocytes: Interleukin 2 and T cell antigen receptor signals converge upon serine 727. *Journal of Biological Chemistry*, *272*(39), 24542 -24549.

Nicholson, S. E., De Souza, D., Fabri, L. J., Corbin, J., Willson, T. A., Zhang, J., Silva, A., et al. (2000). Suppressor of cytokine signaling-3 preferentially binds to the SHP-2-binding site on the shared cytokine receptor subunit gp130. *Proceedings of the National Academy of Sciences of the United States of America*, *97*(12), 6493 -6498.

Nicolson, T. (2005). The genetics of hearing and balance in zebrafish. *Annual Review of Genetics*, *39*(1), 9-22.

Nielsen, K. L., Høgh, A. L., & Emmersen, J. (2006). DeepSAGE—digital transcriptomics with high sensitivity, simple experimental protocol and multiplexing of samples. *Nucleic Acids Research*, *34*(19), e133.

Nishiki, S., Hato, F., Kamata, N., Sakamoto, E., Hasegawa, T., Kimura-Eto, A., Hino, M., et al. (2004). Selective activation of STAT3 in human monocytes stimulated by G-CSF: implication in inhibition of LPS-induced TNF-alpha production. *The American Journal of Physiology*, *286*(6), C1302-1311.

Nishinakamura, R., Matsumoto, Y., Matsuda, T., Ariizumi, T., Heike, T., Asashima, M., & Yokota, T. (1999). Activation of stat3 by cytokine receptor gp130 ventralizes Xenopus embryos independent of BMP-4. *Developmental Biology*, *216*(2), 481-490.

Oates, A. C., Wollberg, P., Pratt, S. J., Paw, B. H., Johnson, S. L., Ho, R. K., Postlethwait, J. H., et al. (1999). Zebrafish stat3 is expressed in restricted tissues during embryogenesis and stat1 rescues cytokine signaling in a STAT1-deficient human cell line. *Developmental Dynamics*, *215*(4), 352-370.

Oesterle, E. C., Bhave, S. A., & Coltrera, M. D. (2000). Basic fibroblast growth factor inhibits cell proliferation in cultured avian inner ear sensory epithelia. *The Journal of Comparative Neurology*, *424*(2), 307-326.

Oesterle, E. C., Tsue, T. T., & Rubel, E. W. (1997). Induction of cell proliferation in avian inner ear sensory epithelia by insulin-like growth factor-I and insulin. *The Journal of Comparative Neurology*, *380*(2), 262-274.

Okada, S., Nakamura, M., Katoh, H., Miyao, T., Shimazaki, T., Ishii, K., Yamane, J., et al. (2006). Conditional ablation of Stat3 or Socs3 discloses a dual role for reactive astrocytes after spinal cord injury. *Nature Medicine*, *12*(7), 829-834.

Olivari, F. A., Hernández, P. P., & Allende, M. L. (2008). Acute copper exposure induces oxidative stress and cell death in lateral line hair cells of zebrafish

larvae. *Brain Research*, *1244*, 1-12.

Ono, K., Nakagawa, T., Kojima, K., Matsumoto, M., Kawauchi, T., Hoshino, M., & Ito, J. (2009). Silencing p27 reverses post-mitotic state of supporting cells in neonatal mouse cochleae. *Molecular and Cellular Neuroscience*, *42*(4), 391-398.

Oshima, K., Grimm, C. M., Corrales, C. E., Senn, P., Martinez Monedero, R., Géléoc, G. S. G., Edge, A., et al. (2006). Differential distribution of stem cells in the auditory and vestibular organs of the inner ear. *Journal of the Association for Research in Otolaryngology*, *8*(1), 18-31.

Oshima, K., Shin, K., Diensthuber, M., Peng, A. W., Ricci, A. J., & Heller, S. (2010). Mechanosensitive hair cell-like cells from embryonic and induced pluripotent stem cells. *Cell*, *141*(4), 704-716.

Ou, H. C., Raible, D. W., & Rubel, E. W. (2007). Cisplatin-induced hair cell loss in zebrafish (Danio rerio) lateral line. *Hearing Research*, *233*(1-2), 46-53.

Oxtoby, E., & Jowett, T. (1993). Cloning of the zebrafish krox-20 gene (krx-20) and its expression during hindbrain development. *Nucleic Acids Research*, *21*(5), 1087 -1095.

Park, K., Luo, J., Hisheh, S., Harvey, A. R., & Cui, Q. (2004). Cellular mechanisms associated with spontaneous and ciliary neurotrophic factor-cAMP-induced survival and axonal regeneration of adult retinal ganglion cells. *The Journal of Neuroscience*, *24*(48), 10806-10815.

Parker, M., & Cotanche, D. (2004). The potential use of stem cells for cochlear repair. *Audiology and Neurotology*, *9*(2), 72-80.

Peraldi, P., Filloux, C., Emanuelli, B., Hilton, D. J., & Van Obberghen, E. (2001). Insulin induces suppressor of cytokine signaling-3 tyrosine phosphorylation through Janus-activated kinase. *Journal of Biological Chemistry*, *276*(27), 24614 -24620.

Picardi, E., Horner, D. S., Chiara, M., Schiavon, R., Valle, G., & Pesole, G. (2010). Large-scale detection and analysis of RNA editing in grape mtDNA by RNA deep-sequencing. *Nucleic Acids Research*, *38*(14), 4755 -4767.

Pickert, G., Neufert, C., Leppkes, M., Zheng, Y., Wittkopf, N., Warntjen, M., Lehr, H., et al. (2009). STAT3 links IL-22 signaling in intestinal epithelial cells to mucosal wound healing. *The Journal of Experimental Medicine*, *206*(7), 1465-1472.

Pickles, J., & van Heumen, W. (1997). The expression of messenger RNAs coding for growth factors, their receptors, and eph-class receptor tyrosine kinases in normal and ototoxically damaged chick cochleae. *Developmental Neuroscience*, *19*(6), 476-487.

Piessevaux, J., Lavens, D., Peelman, F., & Tavernier, J. (2008). The many faces of the SOCS box. *Cytokine & Growth Factor Reviews*, *19*(5-6), 371-381.

Pisharath, H., Rhee, J. M., Swanson, M. A., Leach, S. D., & Parsons, M. J. (2007).

Targeted ablation of beta cells in the embryonic zebrafish pancreas using E. coli nitroreductase. *Mechanisms of Development*, *124*(3), 218-229.

Platt, C. (1993). Zebrafish inner ear sensory surfaces are similar to those in goldfish. *Hearing Research*, *65*(1-2), 133-140.

Plaza-Menacho, I., van der Sluis, T., Hollema, H., Gimm, O., Buys, C. H. C. M., Magee, A. I., Isacke, C. M., et al. (2007). Ras/ERK1/2-mediated STAT3 Ser727 phosphorylation by familial medullary thyroid carcinoma-associated RET mutants induces full activation of STAT3 and is required for c-fos promoter activation, cell mitogenicity, and transformation. *Journal of Biological Chemistry*, *282*(9), 6415 -6424.

Popper, A. N., & Hoxter, B. (1984). Growth of a fish ear: 1. Quantitative analysis of hair cell and ganglion cell proliferation. *Hearing Research*, *15*(2), 133-142.

Presson, J. C., & Popper, A. N. (1990). Possible precursors to new hair cells, support cells, and Schwann cells in the ear of a post-embryonic fish. *Hearing Research*, *46*(1-2), 9-21.

Prisco, M., Peruzzi, F., Belletti, B., & Baserga, R. (2001). Regulation of Id gene expression by Type I insulin-Like growth factor: roles of STAT3 and the Tyrosine 950 residue of the receptor. *Molecular and Cellular Biology*, *21*(16), 5447-5458.

Puligilla, C., Feng, F., Ishikawa, K., Bertuzzi, S., Dabdoub, A., Griffith, A. J., Fritzsch, B., et al. (2007). Disruption of fibroblast growth factor receptor 3 signaling results in defects in cellular differentiation, neuronal patterning, and hearing impairment. *Developmental Dynamics*, *236*(7), 1905-1917.

Puligilla, C., & Kelley, M. W. (2009). Building the world's best hearing aid; regulation of cell fate in the cochlea. *Current Opinion in Genetics & Development*, *19*(4), 368-373.

Puthier, D., Derenne, S., Barillé, S., Moreau, P., Harousseau, J., Bataille, R., & Amiot, M. (1999). Mcl-1 and Bcl-xL are co-regulated by IL-6 in human myeloma cells. *British Journal of Haematology*, *107*(2), 392-395.

Qin, H. R., Kim, H., Kim, J., Hurt, E. M., Klarmann, G. J., Kawasaki, B. T., Duhagon Serrat, M. A., et al. (2008). Activation of signal transducer and activator of transcription 3 through a phosphomimetic Serine 727 promotes prostate tumorigenesis independent of Tyrosine 705 phosphorylation. *Cancer Research*, *68*(19), 7736 -7741.

Qin, Z., Barthel, L. K., & Raymond, P. A. (2009). Genetic evidence for shared mechanisms of epimorphic regeneration in zebrafish. *Proceedings of the National Academy of Sciences of United States of America*, *106*(23), 9310 - 9315.

Qiu, J., Cafferty, W. B. J., McMahon, S. B., & Thompson, S. W. N. (2005). Conditioning injury-induced spinal axon regeneration requires signal transducer and activator of transcription 3 activation. *The Journal of Neuroscience*, *25*(7), 1645-1653.

Radaeva, S., Sun, R., Pan, H., Hong, F., & Gao, B. (2004). Interleukin 22 (IL-22) plays a protective role in T cell-mediated murine hepatitis: IL-22 is a survival factor for hepatocytes via STAT3 activation. *Hepatology*, *39*(5), 1332-1342.

Raphael, Y. (1992). Evidence for supporting cell mitosis in response to acoustic trauma in the avian inner ear. *Journal of Neurocytology*, *21*(9), 663-671.

Raz, R., Lee, C., Cannizzaro, L. A., d'Eustachio, P., & Levy, D. E. (1999). Essential role of STAT3 for embryonic stem cell pluripotency. *Proceedings of the National Academy of Sciences of the United States of America*, *96*(6), 2846 - 2851.

Rebay, I., Fleming, R. J., Fehon, R. G., Cherbas, L., Cherbas, P., & Artavanis-Tsakonas, S. (1991). Specific EGF repeats of Notch mediate interactions with Delta and serrate: Implications for notch as a multifunctional receptor. *Cell*, *67*(4), 687-699.

Reinartz, J., Bruyns, E., Lin, J., Burcham, T., Brenner, S., Bowen, B., Kramer, M., et al. (2002). Massively parallel signature sequencing (MPSS) as a tool for in-depth quantitative gene expression profiling in all organisms. *Briefings in Functional Genomics & Proteomics*, *1*(1), 95 -104.

Riehle, K. J., Campbell, J. S., McMahan, R. S., Johnson, M. M., Beyer, R. P., Bammler, T. K., & Fausto, N. (2008). Regulation of liver regeneration and hepatocarcinogenesis by suppressor of cytokine signaling 3. *The Journal of Experimental Medicine*, *205*(1), 91-103.

Robb, L., Boyle, K., Rakar, S., Hartley, L., Lochland, J., Roberts, A. W., Alexander, W. S., et al. (2005). Genetic reduction of embryonic leukemia-inhibitory factor production rescues placentation in SOCS3-null embryos but does not prevent inflammatory disease. *Proceedings of the National Academy of Sciences of the United States of America*, *102*(45), 16333 -16338.

Roberson, D. W., & Rubel, E. W. (1994). Cell division in the gerbil cochlea after acoustic trauma. *The American Journal of Otology*, *15*(1), 28-34.

Roberson, D. W., Alosi, J. A., & Cotanche, D. A. (2004). Direct transdifferentiation gives rise to the earliest new hair cells in regenerating avian auditory epithelium. *Journal of NeuroScienceResearch*, *78*(4), 461-471.

Roberson, D. W., Alosi, J. A., Mercola, M., & Cotanche, D. A. (2002). REST mRNA expression in normal and regenerating avian auditory epithelium. *Hearing Research*, *172*(1-2), 62-72.

Roberts, A. W., Robb, L., Rakar, S., Hartley, L., Cluse, L., Nicola, N. A., Metcalf, D., et al. (2001). Placental defects and embryonic lethality in mice lacking suppressor of cytokine signaling 3. *Proceedings of the National Academy of Sciences of the United States of America*, *98*(16), 9324 -9329.

Rubel, E. W., Dew, L. A., & Roberson, D. W. (1995). Mammalian vestibular hair cell regeneration. *Science*, *267*(5198), 701-707.

Ruben, R. J. (1967). Development of the inner ear of the mouse: a radioautographic

study of terminal mitoses. *Acta Oto-Laryngologica*, Suppl 220:1-44.

Ruff-Jamison, S., Zhong, Z., Wen, Z., Chen, K., Darnell, J. E., & Cohen, S. (1994). Epidermal growth factor and lipopolysaccharide activate Stat3 transcription factor in mouse liver. *Journal of Biological Chemistry*, *269*(35), 21933 - 21935.

Ryals, B., & Rubel, E. (1988). Hair cell regeneration after acoustic trauma in adult Coturnix quail. *Science*, *240*(4860), 1774-1776.

Ryan, A. F., Mullen, L. M., & Doherty, J. K. (2009). Cellular targeting for cochlear gene therapy. *Advances in Oto-Rhino-Laryngology*, *66*, 99-115.

Sadowski, H. B., & Gilman, M. Z. (1993). Cell-free activation of a DNA-binding protein by epidermal growth factor. *Nature*, *362*(6415), 79-83.

Sage, C., Huang, M., Karimi, K., Gutierrez, G., Vollrath, M. A., Zhang, D., Garcia-Anoveros, J., et al. (2005). Proliferation of functional hair cells in vivo in the absence of the retinoblastoma protein. *Science*, *307*(5712), 1114-1118.

Saha, S., Sparks, A. B., Rago, C., Akmaev, V., Wang, C. J., Vogelstein, B., Kinzler, K. W., et al. (2002). Using the transcriptome to annotate the genome. *Nature Biotechnology*, *20*(5), 508-512.

Salazar-Montes, A., Ruiz-Corro, L., Sandoval-Rodriguez, A., Lopez-Reyes, A., & Armendariz-Borunda, J. (2006). Increased DNA binding activity of NF-kappaB, STAT-3, SMAD3 and AP-1 in acutely damaged liver. *World Journal of Gastroenterology*, *12*(37), 5995-6001.

Sano, S., Chan, K. S., & DiGiovanni, J. (2008). Impact of Stat3 activation upon skin biology: A dichotomy of its role between homeostasis and diseases. *Journal of Dermatological Science*, *50*(1), 1-14.

Sano, S., Itami, S., Takeda, K., Tarutani, M., Yamaguchi, Y., Miura, H., Yoshikawa, K., et al. (1999). Keratinocyte-specific ablation of Stat3 exhibits impaired skin remodeling, but does not affect skin morphogenesis. *EMBO J*, *18*(17), 4657-4668.

Sasaki, A., Yasukawa, H., Suzuki, A., Kamizono, S., Syoda, T., Kinjyo, I., Sasaki, M., et al. (1999). Cytokine-inducible SH2 protein-3 (CIS3/SOCS3) inhibits Janus tyrosine kinase by binding through the N-terminal kinase inhibitory region as well as SH2 domain. *Genes to Cells*, *4*(6), 339-351.

Sasse, J., Hemmann, U., Schwartz, C., Schniertshauer, U., Heesel, B., Landgraf, C., Schneider-Mergener, J., et al. (1997). Mutational analysis of acute-phase response factor/Stat3 activation and dimerization. *Molecular and Cellular Biology*, *17*(8), 4677-4686.

Sato, N., Tsuruma, R., Imoto, S., Sekine, Y., Muromoto, R., Sugiyama, K., & Matsuda, T. (2005). Nuclear retention of STAT3 through the coiled-coil domain regulates its activity. *Biochemical and Biophysical Research Communications*, *336*(2), 617-624.

Schaper, F., Siewert, E., Gómez-Lechón, M. J., Gatsios, P., Sachs, M., Birchmeier,

W., Heinrich, P. C., et al. (1997). Hepatocyte growth factor/scatter factor (HGF/SF) signals via the STAT3/APRF transcription factor in human hepatoma cells and hepatocytes. *FEBS Letters, 405*(1), 99-103.

Schebesta, M., Lien, C., Engel, F. B., & Keating, M. T. (2006). Transcriptional profiling of caudal fin regeneration in zebrafish. *The Scientific World JOURNAL, 6*, 38-54.

Schena, M., Shalon, D., Heller, R., Chai, A., Brown, P. O., & Davis, R. W. (1996). Parallel human genome analysis: microarray-based expression monitoring of 1000 genes. *Proceedings of the National Academy of Sciences of the United States of America, 93*(20), 10614 -10619.

Schena, M., Shalon, D., Davis, R. W., & Brown, P. O. (1995). Quantitative monitoring of gene expression patterns with a complementary DNA microarray. *Science, 270*(5235), 467-470.

Schuck, J. B., & Smith, M. E. (2009). Cell proliferation follows acoustically-induced hair cell bundle loss in the zebrafish saccule. *Hearing Research, 253*(1-2), 67-76.

Schust, J., Sperl, B., Hollis, A., Mayer, T. U., & Berg, T. (2006). Stattic: a small-molecule inhibitor of STAT3 activation and dimerization. *Chemistry & Biology, 13*(11), 1235-1242.

Seki, E., Kondo, Y., Iimuro, Y., Naka, T., Son, G., Kishimoto, T., Fujimoto, J., et al. (2008). Demonstration of cooperative contribution of MET- and EGFR-mediated STAT3 phosphorylation to liver regeneration by exogenous suppressor of cytokine signalings. *Journal of Hepatology, 48*(2), 237-245.

Sengupta, T. K., Talbot, E. S., Scherle, P. A., & Ivashkiv, L. B. (1998). Rapid inhibition of interleukin-6 signaling and Stat3 activation mediated by mitogen-activated protein kinases. *Proceedings of the National Academy of Sciences of the United States of America, 95*(19), 11107 -11112.

Severgnini, M., Bicciato, S., Mangano, E., Scarlatti, F., Mezzelani, A., Mattioli, M., Ghidoni, R., et al. (2006). Strategies for comparing gene expression profiles from different microarray platforms: Application to a case-control experiment. *Analytical Biochemistry, 353*(1), 43-56.

Shendure, J. (2008). The beginning of the end for microarrays? *Nature Methods, 5*(7), 585-587.

Shendure, J., Porreca, G. J., Reppas, N. B., Lin, X., McCutcheon, J. P., Rosenbaum, A. M., Wang, M. D., et al. (2005). Accurate multiplex polony sequencing of an evolved bacterial genome. *Science, 309*(5741), 1728-1732.

Shi, L., Tong, W., Fang, H., Scherf, U., Han, J., Puri, R., Frueh, F., et al. (2005). Cross-platform comparability of microarray technology: Intra-platform consistency and appropriate data analysis procedures are essential. *BMC Bioinformatics, 6*(Suppl 2), S12.

Shi, S., Calhoun, H. C., Xia, F., Li, J., Le, L., & Li, W. X. (2006). JAK signaling

globally counteracts heterochromatic gene silencing. *Nature Genetics*, *38*(9), 1071-1076.

Shi, S., Larson, K., Guo, D., Lim, S. J., Dutta, P., Yan, S., & Li, W. X. (2008). Drosophila STAT is required for directly maintaining HP1 localization and heterochromatin stability. *Nature Cell Biology*, *10*(4), 489-496.

Shim, K., Minowada, G., Coling, D. E., & Martin, G. R. (2005). Sprouty2, a mouse deafness gene, regulates cell fate decisions in the auditory sensory epithelium by antagonizing FGF signaling. *Developmental Cell*, *8*(4), 553-564.

Shirogane, T., Fukada, T., Muller, J. M., Shima, D. T., Hibi, M., & Hirano, T. (1999). Synergistic roles for Pim-1 and c-Myc in STAT3-mediated cell cycle progression and antiapoptosis. *Immunity*, *11*(6), 709-719.

Shouda, T., Yoshida, T., Hanada, T., Wakioka, T., Oishi, M., Miyoshi, K., Komiya, S., et al. (2001). Induction of the cytokine signal regulator SOCS3/CIS3 as a therapeutic strategy for treating inflammatory arthritis. *Journal of Clinical Investigation*, *108*(12), 1781-1788.

Shuai, K., Horvath, C. M., Huang, L. H. T., Qureshi, S. A., Cowburn, D., & Darnell, J. E. (1994). Interferon activation of the transcription factor Stat91 involves dimerization through SH2-phosphotyrosyl peptide interactions. *Cell*, *76*(5), 821-828.

Siddiquee, K., Zhang, S., Guida, W. C., Blaskovich, M. A., Greedy, B., Lawrence, H. R., Yip, M. L. R., et al. (2007). Selective chemical probe inhibitor of Stat3, identified through structure-based virtual screening, induces antitumor activity. *Proceedings of the National Academy of Sciences of the United States of America*, *104*(18), 7391 -7396.

Skeath, J., & Carroll, S. (1992). Regulation of proneural gene expression and cell fate during neuroblast segregation in the Drosophila embryo. *Development*, *114*(4), 939 -946.

Slattery, E. L., Speck, J. D., & Warchol, M. E. (2009). Epigenetic influences on sensory regeneration: Histone deacetylases regulate supporting cell proliferation in the avian utricle. *Journal of the Association for Research in Otolaryngology*, *10*(3), 341-353.

Smith, M. E., Coffin, A. B., Miller, D. L., & Popper, A. N. (2006). Anatomical and functional recovery of the goldfish (Carassius auratus) ear following noise exposure. *The Journal of Experimental Biology*, *209*(21), 4193-4202.

Smith, P. D., Sun, F., Park, K. K., Cai, B., Wang, C., Kuwako, K., Martinez-Carrasco, I., et al. (2009). SOCS3 deletion promotes optic nerve regeneration in vivo. *Neuron*, *64*(5), 617-623.

Sommer, U., Schmid, C., Sobota, R. M., Lehmann, U., Stevenson, N. J., Johnston, J. A., Schaper, F., et al. (2005). Mechanisms of SOCS3 phosphorylation upon Interleukin-6 stimulation. *Journal of Biological Chemistry*, *280*(36), 31478 - 31488.

Song, J., Yan, H. Y., & Popper, A. N. (1995). Damage and recovery of hair cells in fish canal (but not superficial) neuromasts after gentamicin exposure. *Hearing Research*, *91*(1-2), 63-71.

Soucek, S., Michaels, L., & Frohlich, A. (1986). Evidence for hair cell degeneration as the primary lesion in hearing loss of the elderly. *The Journal of Otolaryngology*, *15*(3), 175-183.

Stahl, N., Farrugella, T. J., Boulton, T. G., Zhong, Z., Jr., J. E. D., & Yancopoulos, G. D. (1995). Choice of STATs and other substrates specified by modular tyrosine-based motifs in cytokine receptors. *Science*, *267*(5202), 1349-1353.

Starr, R., Willson, T. A., Viney, E. M., Murray, L. J. L., Rayner, J. R., Jenkins, B. J., Gonda, T. J., et al. (1997). A family of cytokine-inducible inhibitors of signalling. *Nature*, *387*(6636), 917-921.

Stone, J. S., & Cotanche, D. A. (1994). Identification of the timing of S phase and the patterns of cell proliferation during hair cell regeneration in the chick cochlea. *The Journal of Comparative Neurology*, *341*(1), 50-67.

Stone, J. S., Shang, J. L., & Tomarev, S. (2004). cProx1 immunoreactivity distinguishes progenitor cells and predicts hair cell fate during avian hair cell regeneration. *Developmental Dynamics*, *230*(4), 597-614.

Stone, J., & Rubel, E. (1999). Delta1 expression during avian hair cell regeneration. *Development*, *126*(5), 961 -973.

Stone, J. S., & Cotanche, D. A. (2007). Hair cell regeneration in the avian auditory epithelium. *The International Journal of Developmental Biology*, *51*(6-7), 633-647.

Stout, B. A., Bates, M. E., Liu, L. Y., Farrington, N. N., & Bertics, P. J. (2004). IL-5 and Granulocyte-Macrophage Colony-Stimulating Factor activate STAT3 and STAT5 and promote Pim-1 and Cyclin D3 protein expression in human eosinophils. *The Journal of Immunology*, *173*(10), 6409-6417.

Studzinski, A. L. M., Almeida, D. V., Lanes, C. F. C., Figueiredo, M. D. A., & Marins, L. F. (2009). SOCS1 and SOCS3 are the main negative modulators of the somatotrophic axis in liver of homozygous GH-transgenic zebrafish (Danio rerio). *General and Comparative Endocrinology*, *161*(1), 67-72.

Sultan, M., Schulz, M. H., Richard, H., Magen, A., Klingenhoff, A., Scherf, M., Seifert, M., et al. (2008). A global view of gene activity and alternative splicing by deep sequencing of the human transcriptome. *Science*, *321*(5891), 956-960.

Taft, A. S., Vermeire, J. J., Bernier, J., Birkeland, S. R., Cipriano, M. J., Papa, A. R., McArthur, A. G., et al. (2009). Transcriptome analysis of Schistosoma mansoni larval development using Serial Analysis of Gene Expression (SAGE). *Parasitology*, *136*(05), 469-485.

Taga, T., & Fukuda, S. (2005). Role of IL-6 in the neural stem cell differentiation. *Clinical Reviews in Allergy & Immunology*, *28*(3), 249-256.

Takeda, T., Kurachi, H., Yamamoto, T., Homma, H., Morishige, K., Miyake, A., & Murata, Y. (1997). Participation of JAK, STAT and unknown proteins in human placental lactogen-induced signaling: a unique signaling pathway different from prolactin and growth hormone. *Journal of Endocrinology, 153*(1), R1-3.

Tan, P. K., Downey, T. J., Spitznagel Jr, E. L., Xu, P., Fu, D., Dimitrov, D. S., Lempicki, R. A., et al. (2003). Evaluation of gene expression measurements from commercial microarray platforms. *Nucleic Acids Research, 31*(19), 5676 -5684.

Tanaka, K., & Smith, C. A. (1978). Structure of the chicken's inner ear: SEM and TEM study. *The American Journal of Anatomy, 153*(2), 251-271.

Tarnawski, A. S., & Jones, M. K. (1998). The role of epidermal growth factor (EGF) and its receptor in mucosal protection, adaptation to injury, and ulcer healing: involvement of EGF-R signal transduction pathways. *Journal of Clinical Gastroenterology, 27 Suppl 1*, S12-20.

Tateya, I., Nakagawa, T., Iguchi, F., Soo Kim, T., Endo, T., Yamada, S., Kageyama, R., et al. (2003). Fate of neural stem cells grafted into injured inner ears of mice. *NeuroReport, 14*(13), 1677-1681.

Taub, R. (2004). Liver regeneration: from myth to mechanism. *Nature Reviews Molecular Cell Biology, 5*(10), 836-847.

Taub, R., Greenbaum, L. E., & Peng, Y. (1999). Transcriptional Regulatory Signals Define Cytokine-Dependent and -Independent Pathways in Liver Regeneration. *Semin Liver Dis, 19*(02), 117,127.

Taylor, R. R., & Forge, A. (2005). Hair cell regeneration in sensory epithelia from the inner ear of a urodele amphibian. *The Journal of Comparative Neurology, 484*(1), 105-120.

Ter Haar, G., De Groot, J., Venker-van Haagen, A., Van Sluijs, F., & Smoorenburg, G. (2009). Effects of aging on inner ear morphology in dogs in relation to brainstem responses to toneburst auditory stimuli. *Journal of Veterinary Internal Medicine, 23*(3), 536-543.

Thalmann, R., Ignatova, E., Kachar, B., Ornitz, D. M., & Thalmann, I. (2001). Development and maintenance of otoconia. *Annals of the New York Academy of Sciences, 942*(1), 162-178.

Thisse, B., & Thisse, C. (2004). Fast release clones: a high throughput expression analysis. *ZFIN Direct Data Submission (http://zfin.org).*

Tokumaru, S., Sayama, K., Shirakata, Y., et al. (2005). Induction of keratinocyte migration via transactivation of the epidermal growth factor receptor by the antimicrobial peptide LL-37. *The Journal of Immunology, 175*(7), 4662-4668.

Tokumaru, S., Sayama, K., Yamasaki, K., et al. (2005). SOCS3/CIS3 negative regulation of STAT3 in HGF-induced keratinocyte migration. *Biochemical and Biophysical Research Communications, 327*(1), 100-105.

Toth, C., Martinez, J., Liu, W., Diggle, J., Guo, G., Ramji, N., Mi, R., et al. (2008). Local erythropoietin signaling enhances regeneration in peripheral axons. *The Journal of Neuroscience, 154*(2), 767-783.

Trapnell, C., Williams, B. A., Pertea, G., Mortazavi, A., Kwan, G., van Baren, M. J., Salzberg, S. L., et al. (2010). Transcript assembly and quantification by RNA-Seq reveals unannotated transcripts and isoform switching during cell differentiation. *Nature Biotechnology, 28*(5), 511-515.

Tsuyama, N., Danjoh, I., Otsuyama, K., Obata, M., Tahara, H., Ohta, T., & Ishikawa, H. (2005). IL-6-induced Bcl6 variant 2 supports IL-6-dependent myeloma cell proliferation and survival through STAT3. *Biochemical and Biophysical Research Communications, 337*(1), 201-208.

Umemoto, M., Sakagami, M., Fukazawa, K., Ashida, K., Kubo, T., Senda, T., & Yoneda, Y. (1995). Hair cell regeneration in the chick inner ear following acoustic trauma: ultrastructural and immunohistochemical studies. *Cell & Tissue Research, 281*(3), 435-443.

Ushijima, R., Sakaguchi, N., Kano, A., Maruyama, A., Miyamoto, Y., Sekimoto, T., Yoneda, Y., et al. (2005). Extracellular signal-dependent nuclear import of STAT3 is mediated by various importin alphas. *Biochemical and Biophysical Research Communications, 330*(3), 880-886.

Veeriah, S., Brennan, C., Meng, S., Singh, B., Fagin, J. A., Solit, D. B., Paty, P. B., et al. (2009). The tyrosine phosphatase PTPRD is a tumor suppressor that is frequently inactivated and mutated in glioblastoma and other human cancers. *Proceedings of the National Academy of Sciences of the United States of America, 106*(23), 9435 -9440.

Velculescu, V. E., Zhang, L., Vogelstein, B., & Kinzler, K. W. (1995). Serial analysis of gene expression. *Science, 270*(5235), 484-487.

Vera, J. C., Wheat, C. W., Fescemyer, H. W., Frilander, M. J., Crawford, D. L., Hanski, I., & Marden, J. H. (2008). Rapid transcriptome characterization for a nonmodel organism using 454 pyrosequencing. *Molecular Ecology, 17*(7), 1636-1647.

Verma, N. K., Dourlat, J., Davies, A. M., Long, A., Liu, W., Garbay, C., Kelleher, D., et al. (2009). STAT3-Stathmin interactions control microtubule dynamics in migrating T-cells. *Journal of Biological Chemistry, 284*(18), 12349 -12362.

Vignais, M., & Gilman, M. (1999). Distinct mechanisms of activation of Stat1 and Stat3 by platelet-derived growth factor receptor in a cell-free system. *Molecular and Cellular Biology, 19*(5), 3727-3735.

Vignais, M., Sadowski, H., Watling, D., Rogers, N., & Gilman, M. (1996). Platelet-derived growth factor induces phosphorylation of multiple JAK family kinases and STAT proteins. *Molecular and Cellular Biology, 16*(4), 1759-1769.

Vollrath, M. A., Kwan, K. Y., & Corey, D. P. (2007). The micromachinery of mechanotransduction in hair cells. *Annual Review of Neuroscience, 30*(1),

339-365.

Wada, K., Nakajima, A., Katayama, K., Kudo, C., Shibuya, A., Kubota, N., Terauchi, Y., et al. (2006). Peroxisome proliferator-activated receptor γ-mediated regulation of neural stem cell proliferation and differentiation. *Journal of Biological Chemistry*, *281*(18), 12673 -12681.

Wang, X., Luan, J., Li, J., Bao, Y., Zhang, C., & Liu, S. (2010). De novo characterization of a whitefly transcriptome and analysis of its gene expression during development. *BMC Genomics*, *11*(1), 400.

Wang, Z., Gerstein, M., & Snyder, M. (2009). RNA-Seq: a revolutionary tool for transcriptomics. *Nature Reviews Genetics*, *10*(1), 57-63.

Wangemann, P. (2006). Supporting sensory transduction: cochlear fluid homeostasis and the endocochlear potential. *The Journal of Physiology*, *576*(1), 11 -21.

Warchol, M. E. (1999). Immune cytokines and dexamethasone influence sensory regeneration in the avian vestibular periphery. *Journal of Neurocytology*, *28*(10), 889-900.

Warchol, M. E. (2002). Cell density and N-cadherin interactions regulate cell proliferation in the sensory epithelia of the inner ear. *The Journal of Neuroscience*, *22*(7), 2607-2616.

Warchol, M. E., & Corwin, J. T. (1996). Regenerative proliferation in organ cultures of the avian cochlea: Identification of the initial progenitors and determination of the latency of the proliferative response. *The Journal of Neuroscience*, *16*(17), 5466-5477.

Warchol, M., Lambert, P., Goldstein, B., Forge, A., & Corwin, J. (1993). Regenerative proliferation in inner ear sensory epithelia from adult guinea pigs and humans. *Science*, *259*(5101), 1619-1622.

Weber, T., Corbett, M. K., Chow, L. M. L., Valentine, M. B., Baker, S. J., & Zuo, J. (2008). Rapid cell-cycle reentry and cell death after acute inactivation of the retinoblastoma gene product in postnatal cochlear hair cells. *Proceedings of the National Academy of Sciences of the United States of America*, *105*(2), 781 -785.

Wegenka, U. M., Buschmann, J., Lutticken, C., Heinrich, P. C., & Horn, F. (1993). Acute-phase response factor, a nuclear factor binding to acute-phase response elements, is rapidly activated by interleukin-6 at the posttranslational level. *Molecular and Cellular Biology*, *13*(1), 276-288.

Wegrzyn, J., Potla, R., Chwae, Y., Sepuri, N. B. V., Zhang, Q., Koeck, T., Derecka, M., et al. (2009). Function of mitochondrial stat3 in cellular respiration. *Science*, *323*(5915), 793-797.

Wei, L., Laurence, A., Elias, K. M., & O'Shea, J. J. (2007). IL-21 is produced by Th17 cells and drives IL-17 production in a STAT3-dependent manner. *Journal of Biological Chemistry*, *282*(48), 34605 -34610.

Wen, Z., Zhong, Z., & Darnell, J. E. (1995). Maximal activation of transcription by

statl and stat3 requires both tyrosine and serine phosphorylation. *Cell*, *82*(2), 241-250.

Weston, M. D., Pierce, M. L., Rocha-Sanchez, S., Beisel, K. W., & Soukup, G. A. (2006). MicroRNA gene expression in the mouse inner ear. *Brain Research, 1111*(1), 95-104.

Wharton, K. A., Johansen, K. M., Xu, T., & Artavanis-Tsakonas, S. (1985). Nucleotide sequence from the neurogenic locus Notch implies a gene product that shares homology with proteins containing EGF-like repeats. *Cell*, *43*(3, Part 2), 567-581.

White, P. M., Doetzlhofer, A., Lee, Y. S., Groves, A. K., & Segil, N. (2006). Mammalian cochlear supporting cells can divide and trans-differentiate into hair cells. *Nature*, *441*(7096), 984-987.

Wienholds, E., Kloosterman, W. P., Miska, E., Alvarez-Saavedra, E., Berezikov, E., de Bruijn, E., Horvitz, H. R., et al. (2005). MicroRNA expression in zebrafish embryonic development. *Science, 309*(5732), 310-311.

Wilhelm, B. T., Marguerat, S., Goodhead, I., & Bahler, J. (2010). Defining transcribed regions using RNA-seq. *Nature Protocols*, *5*(2), 255-266.

Wilhelm, B. T., & Landry, J. (2009). RNA-Seq--quantitative measurement of expression through massively parallel RNA-sequencing. *Methods*, *48*(3), 249-257.

Wilhelm, B. T., Marguerat, S., Watt, S., Schubert, F., Wood, V., Goodhead, I., Penkett, C. J., et al. (2008). Dynamic repertoire of a eukaryotic transcriptome surveyed at single-nucleotide resolution. *Nature*, *453*(7199), 1239-1243.

Wilkins, H. R., Presson, J. C., & Popper, A. N. (1999). Proliferation of vertebrate inner ear supporting cells. *Journal of Neurobiology, 39*(4), 527-535.

Williams, J. A., & Holder, N. (2000). Cell turnover in neuromasts of zebrafish larvae. *Hearing Research*, *143*(1-2), 171-181.

Williams, L., Bradley, L., Smith, A., & Foxwell, B. (2004). Signal transducer and activator of transcription 3 Is the dominant mediator of the anti-inflammatory effects of IL-10 in human macrophages. *The Journal of Immunology, 172*(1), 567-576.

Witte, M. C., Montcouquiol, M., & Corwin, J. T. (2001). Regeneration in avian hair cell epithelia: identification of intracellular signals required for S-phase entry. *European Journal of Neuroscience, 14*(5), 829-838.

Woetmann, A., Nielsen, M., Christensen, S. T., Brockdorff, J., Kaltoft, K., Engel, A., Skov, S., et al. (1999). Inhibition of protein phosphatase 2A induces serine/threonine phosphorylation, subcellular redistribution, and functional inhibition of STAT3. *Proceedings of the National Academy of Sciences of the United States of America, 96*(19), 10620 -10625.

Wold, B., & Myers, R. M. (2008). Sequence census methods for functional genomics. *Nature Methods*, *5*(1), 19-21.

Wong, M., & Fish, E. N. (1998). RANTES and MIP-1α Activate Stats in T cells. *Journal of Biological Chemistry*, *273*(1), 309 -314.

Woods, C., Montcouquiol, M., & Kelley, M. W. (2004). Math1 regulates development of the sensory epithelium in the mammalian cochlea. *Nature Neuroscience*, *7*(12), 1310-1318.

Woolley, S. M. N., Wissman, A. M., & Rubel, E. W. (2001). Hair cell regeneration and recovery of auditory thresholds following aminoglycoside ototoxicity in Bengalese finches. *Hearing Research*, *153*(1-2), 181-195.

Wüstefeld, T., Rakemann, T., Kubicka, S., Manns, M. P., & Trautwein, C. (2000). Hyperstimulation with interleukin 6 inhibits cell cycle progression after hepatectomy in mice. *Hepatology*, *32*(3), 514-522.

Wüstefeld, T., Klein, C., Streetz, K. L., Betz, U., Lauber, J., Buer, J., Manns, M. P., et al. (2003). Interleukin-6/Glycoprotein 130-dependent pathways are protective during liver regeneration. *Journal of Biological Chemistry*, *278*(13), 11281 -11288.

Xia, Z., Salzler, R. R., Kunz, D. P., Baer, M. R., Kazim, L., Baumann, H., & Wetzler, M. (2001). A novel serine-dependent proteolytic activity is responsible for truncated signal transducer and activator of transcription proteins in acute myeloid leukemia blasts. *Cancer Research*, *61*(4), 1747 -1753.

Xiao, T., Roeser, T., Staub, W., & Baier, H. (2005). A GFP-based genetic screen reveals mutations that disrupt the architecture of the zebrafish retinotectal projection. *Development*, *132*(13), 2955 -2967.

Xie, T., Wei, D., Liu, M., Gao, A. C., Ali-Osman, F., Sawaya, R., & Huang, S. (2004). Stat3 activation regulates the expression of matrix metalloproteinase-2 and tumor invasion and metastasis. *Oncogene*, *23*(20), 3550-3560.

Xu, J., Sylvester, R., Tighe, A. P., Chen, S., & Gudas, L. J. (2008). Transcriptional activation of the Suppressor of Cytokine Signaling-3 (SOCS-3) gene via STAT3 is increased in F9 REX1 (ZFP-42) knockout teratocarcinoma stem cells relative to wild-type cells. *Journal of Molecular Biology*, *377*(1), 28-46.

Yamashita, S., Miyagi, C., Carmany-Rampey, A., Shimizu, T., Fujii, R., Schier, A. F., & Hirano, T. (2002). Stat3 controls cell movements during zebrafish gastrulation. *Developmental Cell*, *2*(3), 363-375.

Yamashita, S., Miyagi, C., Fukada, T., Kagara, N., Che, Y., & Hirano, T. (2004). Zinc transporter LIVI controls epithelial-mesenchymal transition in zebrafish gastrula organizer. *Nature*, *429*(6989), 298-302.

Yamauchi, K., Osuka, K., Takayasu, M., Usuda, N., Nakazawa, A., Nakahara, N., Yoshida, M., et al. (2006). Activation of JAK/STAT signalling in neurons following spinal cord injury in mice. *Journal of Neurochemistry*, *96*(4), 1060-1070.

Yanagisawa, M., Nakashima, K., Arakawa, H., Ikenaka, K., Yoshida, K., Kishimoto, T., Hisatsune, T., et al. (2000). Astrocyte differentiation of fetal

neuroepithelial cells by Interleukin-11 via activation of a common cytokine signal transducer, gp130, and a transcription factor, STAT3. *Journal of Neurochemistry*, *74*(4), 1498-1504.

Yang, J., Chatterjee-Kishore, M., Staugaitis, S. M., Nguyen, H., Schlessinger, K., Levy, D. E., & Stark, G. R. (2005). Novel roles of unphosphorylated STAT3 in oncogenesis and transcriptional regulation. *Cancer Research*, *65*(3), 939 - 947.

Yang, J., Liao, X., Agarwal, M. K., Barnes, L., Auron, P. E., & Stark, G. R. (2007). Unphosphorylated STAT3 accumulates in response to IL-6 and activates transcription by binding to NFκB. *Genes & Development*, *21*(11), 1396-1408.

Yang, J., & Stark, G. R. (2008). Roles of unphosphorylated STATs in signaling. *Cell Research*, *18*(4), 443-451.

Yasukawa, H., Ohishi, M., Mori, H., Murakami, M., Chinen, T., Aki, D., Hanada, T., et al. (2003). IL-6 induces an anti-inflammatory response in the absence of SOCS3 in macrophages. *Nature Immunology*, *4*(6), 551-556.

Yauk, C. L., & Berndt, M. L. (2007). Review of the literature examining the correlation among DNA microarray technologies. *Environmental and Molecular Mutagenesis*, *48*(5), 380-394.

Yin, V. P., Thomson, J. M., Thummel, R., Hyde, D. R., Hammond, S. M., & Poss, K. D. (2008). Fgf-dependent depletion of microRNA-133 promotes appendage regeneration in zebrafish. *Genes & Development*, *22*(6), 728-733.

Yokogami, K., Wakisaka, S., Avruch, J., & Reeves, S. A. (2000). Serine phosphorylation and maximal activation of STAT3 during CNTF signaling is mediated by the rapamycin target mTOR. *Current Biology*, *10*(1), 47-50.

Yu, C. L., Meyer, D. J., Campbell, G. S., Larner, A. C., Carter-Su, C., Schwartz, J., & Jove, R. (1995). Enhanced DNA-binding activity of a Stat3-related protein in cells transformed by the Src oncoprotein. *Science*, *269*(5220), 81-83.

Yu, Z., Bai, L., Qian, P., Xiao, Y., Wang, G., Qian, G., Bai, C., et al. (2009). Restoration of SOCS3 suppresses human lung adenocarcinoma cell growth by downregulating activation of Erk1/2, Akt apart from STAT3. *Cell Biology International*, *33*(9), 995-1001.

Yuan, Z., Guan, Y., Chatterjee, D., & Chin, Y. E. (2005). Stat3 dimerization regulated by reversible acetylation of a single lysine residue. *Science*, *307*(5707), 269-273.

Zauberman, A., Zipori, D., Krupsky, M., & Ben-Levy, R. (1999). Stress activated protein kinase p38 is involved in IL-6 induced transcriptional activation of STAT3. *Oncogene*, *18*(26), 3886-3893.

Zhang, T., Kee, W. H., Seow, K. T., Fung, W., & Cao, X. (2000). The coiled-coil domain of stat3 is essential for its SH2 domain-mediated receptor binding and subsequent activation induced by Epidermal Growth Factor and Interleukin-6. *Molecular and Cellular Biology*, *20*(19), 7132-7139.

Zhang, X., Blenis, J., Li, H. C., Schindler, C., & Chen-Kiang, S. (1995). Requirement of serine phosphorylation for formation of STAT-promoter complexes. *Science, 267*(5206), 1990-1994.

Zhang, X., Guo, A., Yu, J., Possemato, A., Chen, Y., Zheng, W., Polakiewicz, R. D., et al. (2007). Identification of STAT3 as a substrate of receptor protein tyrosine phosphatase T. *Proceedings of the National Academy of Sciences of the United States of America, 104*(10), 4060 -4064.

Zhang, X., Wrzeszczynska, M. H., Horvath, C. M., & Darnell, J. E. (1999). Interacting regions in stat3 and c-Jun that participate in cooperative transcriptional activation. *Molecular and Cellular Biology, 19*(10), 7138-7146.

Zheng, J. L., & Gao, W. (2000). Overexpression of Math1 induces robust production of extra hair cells in postnatal rat inner ears. *Nature Neuroscience, 3*(6), 580-586.

Zhong, Z., Wen, Z., & Darnell, J. E. (1994). Stat3: a STAT family member activated by tyrosine phosphorylation in response to epidermal growth factor and interleukin-6. *Science, 264*(5155), 95-98.

Zhu, B., Ishida, Y., Robinson, G. W., Pacher-Zavisin, M., Yoshimura, A., Murphy, P. M., & Hennighausen, L. (2008). SOCS3 negatively regulates the gp130-STAT3 pathway in mouse skin wound healing. *The Journal of Investigative Dermatology, 128*(7), 1821-1829.

Zine, A., Van De Water, T., & de Ribaupierre, F. (2000). Notch signaling regulates the pattern of auditory hair cell differentiation in mammals. *Development, 127*(15), 3373 -3383.

Zushi, S., Shinomura, Y., Kiyohara, T., Miyazaki, Y., Kondo, S., Sugimachi, M., Higashimoto, Y., et al. (1998). STAT3 mediates the survival signal in oncogenic ras-transfected intestinal epithelial cells. *International Journal of Cancer, 78*(3), 326-330.